Misregulation of the tumour suppressor gene *CYLD* drives hyperactivation of T cells leading to intestinal pathology

Dissertation

Zur Erlangung des Grades

Doktor der Naturwissenschaft

Am Fachbereich Biologie

Der Johannes Gutenberg-Universität Mainz

vorgelegt von

Sonja Reißig

geb. am 17. Januar 1980 in Unna, Deutschland

Mainz, 2011

Berichterstatter 1:

Berichterstatter 2:

Tag der mündlichen Prüfung: Juli 2011

1 INTRODUCTION 1

1.1 T CELLS 1

1.1.1 T cell development 1

1.1.2 T cell receptor signaling 3

1.1.3 T helper cell lineages 5

1.1.3.1 Regulatory T cells 6

1.2 NF-κB SIGNALING 7

1.2.1 The canonical NF-κB pathway 8

1.2.2 The noncanonical NF-κB pathway 10

1.3 CYLD 10

1.3.1 Familial Cylindromatosis 10

1.3.2 The function of the CYLD protein 11

1.3.3 The role of CYLD in NF-κB signaling 12

1.3.4 The role of CYLD in thymocyte development 13

1.4 INFLAMMATORY BOWEL DISEASE 14

1.5 EXPERIMENTAL AUTOIMMUNE ENCEPHALOMYELITIS 16

1.6 OBJECTIVES 17

2 MATERIALS AND METHODS 18

2.1 CHEMICALS AND BIOLOGICAL MATERIAL 18

2.2 MOLECULAR BIOLOGY 20

2.2.1 Preparation of genomic DNA 20

2.2.2 Polymerase chain reaction (PCR) 20

2.2.3 RNA isolation and Quantitative Real Time PCR 21

2.2.4 Agarose Gel Electrophoresis and DNA Gel Extraction 22

2.2.5 Quantification of DNA and RNA 22

2.3 CELL BIOLOGY 22

2.3.1 Preparation of single cell suspensions from lymphoid organs 22

2.3.2 Cell counting 23

2.3.3 Flow cytometry 23

2.3.4 Magnetic cell sorting and FACS sorting 24

2.3.5 CFSE labeling 25

2.3.6 Culture of ex vivo Splenocytes and Lymphocytes 25

2.3.7 T cell activation 25

2.3.8 Flow Cytomix 26

2.3.9 Treg Suppression Assay in vitro 26

2.4 HISTOLOGICAL ANALYSIS AND IMMUNOHISTOCHEMESTRY 26

2.5 BIOCHEMISTRY 27
2.5.1 Protein extract preparations *27*
2.5.2 Western Blot *27*
2.6 MOUSE EXPERIMENTS 28
2.6.1 Mice *28*
2.6.2 Adoptive Cell Transfer *29*
2.6.3 Induction and assessment of EAE *29*
2.6.4 Adoptive Transfer Colitis *29*
2.6.5 Treg suppression assay in vivo *30*
2.6.6 In vivo high resolution mini-endoscopy analysis of the colon *30*
2.6.7 Statistics *30*

3 RESULTS 31

3.1 OVEREXPRESSION OF SHORT CYLD LEADS TO A STRONG REDUCTION OF THE T CELL COMPARTMENT IN CYLD$^{EX7/8}$ MICE 31
3.2 IMPAIRED TCR SIGNALING IN CYLD$^{EX7/8}$ THYMOCYTES 34
3.3 IMPAIRED THYMIC SELECTION IN CYLD$^{EX7/8}$ THYMOCYTES ON HY TCR TRANSGENIC BACKGROUND 35
3.4 DEMINISHED DEVELOPMENT OF MTECS IN CYLD$^{EX7/8}$ THYMI 38
3.5 HYPERRESPONSIVENESS OF CYLD$^{EX7/8}$ T CELLS 40
3.6 CONSTITUTIVE ACTIVATION OF THE NONCANONICAL NF-KB PATHWAY 44
3.7 REGULATORY T CELLS OF CYLD$^{EX7/8}$ MICE DISPLAY REDUCED SUPPRESSIVE CAPACITIES 45
3.8 SPONTANEOUS COLITIS IN CYLD$^{EX7/8}$ MICE 49
3.9 NAIVE T CELLS OVEREXPRESSING SHORT CYLD FAIL TO INDUCE COLITIS 56
3.10 SPONTANEOUS COLITIS IN RAG1$^{-/-}$CYLD$^{EX7/8}$ MICE 62
3.11 GENERATION OF AUTOANTIBODIES IN TCR TRANSGENIC CYLD$^{EX7/8}$ MICE 68
3.12 CYLD$^{EX7/8}$ MICE ARE HYPERSUSCEPTIBLE TO EAE 69

4 DISCUSSION 72

4.1 SCYLD POSITIVELY REGULATES TCR SIGNALING IN THYMOCYTES 72
4.2 THE IMPACT OF SCYLD IN THE DEVELOPMENT OF MEDULLARY THYMIC EPITHELIAL CELLS 74
4.3 CYLD$^{EX7/8}$ T CELLS DISPLAY A HYPERACTIVATED PHENOTYPE 75
4.4 SCYLD OVEREXPRESSION DISTURBS THE SUPPRESSIVE FUNCTION OF REGULATORY T CELLS 76
4.5 SCYLD DRIVES THE DEVELOPMENT OF SPONTANEOUS INTESTINAL INFLAMMATION 77
4.6 T CELL-INDEPENDENT COLITIS IN RAG1$^{-/-}$ CYLD$^{EX7/8}$ MICE 80
4.7 INCREASED PRODUCTION OF NUCLEAR AUTOANTIBODIES IN TCR TRANSGENIC CYLD$^{EX7/8}$ MICE 81
4.8 CYLD$^{EX7/8}$ MICE ARE MORE SUSCEPTIBLE TO EAE 82

5 SUMMARY 84

6 ZUSAMMENFASSUNG 85

7 REFERENCES 87

8 ACKNOWLEDGEMENTS 103

9 VERSICHERUNG 104

10 LEBENSLAUF 105

PUBLIKATIONEN: 106

Abbreviations

Ab	antibody
AICD	activation induced cell death
ANA	anti-nuclear autoantibody
APC	antigen presenting cell
approx.	approximately
BBB	blood brain barrier
Bcl-3	B cell lymphoma 3
BCR	B cell receptor
Bio	biotinylated
BMDC	bone marrow derived dendritic cells
β-ME	β-mercaptoethanol
bp	base pair
BSA	bovine serum albumin
°C	temperature in degrees celsius
CD	Crohne's disease
CFA	Complete Freund's Adjuvant
cDNA	complementary DNA
CBA	Cytometric Bead Array
CFSE	carboxyfluorescein diacetate succinimidyl ester
CNS	central nervous system
Cre	site-specific recombinase (causes recombination)
Cyc	cychrome
CYLD	cylindromatosis protein
d	day/s
DC	dendritic cell
DMEM	Dulbecco's modified Eagle medium
DNA	desoxyribonucleic acid
dNTP	desoxynucleotide triphosphate

DP	double positive
DTT	dithiothritole
Dtx	Diphteria toxin
DUB	deubiquitinating enzyme
e.g.	exempli gratia (for instance)
EAE	experimental autoimmune encephalomyelitis
EDTA	ethylene-diaminetetraacetic acid
ELISA	enzyme-linked immuno-sorbent assay
ERK	extracellular signal regulated kinase
EtOH	ethanol
FACS	fluorescence activated cell sorting
FCS	fetal calf serum
Fig.	Figure
FITC	fluorescein isothiocyanate
FL-CYLD	full length CYLD
Foxp3	forkhead box protein 3
g	gramm
GITR	glucocorticoid-induced TNFR-related gene
h	hour/s
HEPES	N-2-hydroxyethylpiperazine-N´-2-ethansulfonic acid
IBD	inflammatory bowel disease
i.e.	id est (that is)
i.p.	intraperitoneally
i.v.	intravenously
IFN-γ	interferon-γ
Ig	immunoglobulin
IKB	I kappa B
IKK	I kappa kinase
IL	interleukin

K^{48}	lysine 48
K^{63}	lysine 63
kb	kilobase pair
ko	knockout
l	liter
LN	lymph node/s
loxp	recognition sequence for Cre (locus of X-ing over of phage P1)
LPS	lipopolysaccharide
Ly6C	lymphocyte antigen 6 complex, locus C
M	molar
MACS	magnetic activated cell sorter
MFI	mean fluorescence intensity
$MgCl_2$	magnesium chloride
MHC	major histocompatibility complex
min	minute
ml	milliliter
mM	millimolar
MOG	myelin oligodendrocyte glycoprotein
mRNA	messenger RNA
MS	multiple sclerosis
NaCl	sodium chloride
n	nano
NaOH	sodium hydroxide
NEMO, IKK-γ	NF-kappaB essential modulator
o/n	over night
OD	optical density
PBS	phosphate buffered saline
PCR	polymerase chain reaction
PE	phycoerythrine

Ptx	Pertussis toxin
RAG	recombinase activating gene
RNA	ribonucleic acid
rpm	revolutions per minute
RT	room temperature
RT PCR	realtime polymerase chain reaction
sCYLD	short CYLD
sec	seconds
SA	streptavidine
s.c.	subcutaneously
sc	spinal cord
SDS	sodium dodecyl sulfate
SN	supernatant
SP	single positive
SSC	sodium chloride/sodium citrate buffer
TAB1/2	transforming growth factor β activated protein kinase 1/2 binding protein
TAK1	transforming growth factor β activated kinase 1
TAE	Tris acetic acid-EDTA buffer
Taq	polymerase from *Thermus aquaticus*
TCR	T cell receptor
TE	Tris-EDTA buffer
TEC	thymic epithelial cell
tg	transgenic
TGF-β	transforming growth factor-β
TLR	toll-like receptor
TNF	tumour necrosis factor
TRAF	tumour necrosis receptor associated factor
Tregs	regulatory T cells
Tris	2-amino-2-(hydroxymethyl-)1,3-propandiole

U	units
Ub	ubiquitin
UC	ulcerative colitis
UV	ultraviolett
V	volts
vs	versus
v/v	volume per volume
w/v	weight per volume
WT	wild type
µl	microliter
µM	micromolar
3’	three prime end of DNA sequences
5’	five prime end of DNA sequences

1 Introduction

1.1 T cells

T cells play a central role in the cellular immune response. Their development takes place in the thymus and as mature T cells they leave the thymus and circulate through the periphery. There are two main subsets of T cells that differ in their effector function, MHC restriction and accessory molecule usage. First, cytotoxic T cells (CD8), which kill target cells that display peptide fragments of cytosolic pathogens, most notably viruses, bound to MHC class I. Second, T helper cells (CD4), recognizing fragments of antigens degraded within intracellular vesicles presented by MHC class II. These cells are characterized by their activity in supporting humoral and cell-mediated immune responses.

1.1.1 T cell development

T cells arise from hematopoietic stem cells in the bone marrow and migrate via the blood as T cell precursors into the thymus. The thymus is responsible for the development, selection and output of mature naive T lymphocytes into the periphery in a process called thymopoiesis (Taub and Longo 2005). T cell development is not cell autonomous, but requires signals from nonhematopoietic stromal cells such as thymic epithelial cells (TECs) and mesenchymal fibroblasts. These cells are located in distinct anatomical locations in the thymus (Anderson and Jenkinson 2001; Taub and Longo 2005). Movement of the T cell precursors between these distinct locations is critical for the perception of the different signals. In the earliest stage of thymocyte development, the immature thymocyte progenitors are negative for CD4 and CD8 cell surface expression and are termed double-negative (DN) cells. Their further maturation can be distinguished by their differential expression of the adhesion molecule pgp1 (CD44) and the IL-2 receptor α chain (CD25) (Germain 2002; Taub and Longo 2005). After entering the thymus, the thymocyte precursors start to express CD44 (DN1: $CD44^+$, $CD25^-$) followed by an upregulation of CD25 (DN2: $CD44^+$, $CD25^+$) and a subsequent down-regulation of CD44 (DN3: $CD44^-$, $CD25^+$). The DN3 stage is accompanied by an up-regulation of RAG1 and RAG2 gene expression which are essential to start rearrangement of the TCR γ, δ and β loci (Pearse, Gallagher et al. 1988; Pearse, Wu et al. 1989; Taub and Longo 2005). The two lineages of α/β- and γ/δ- T cells diverge at this stage (MacDonald et al. 2001; Taub and Longo 2005). Successful rearrangement of a γ and a δ gene leads to the expression of a functional γ/δ T cell receptor that signals the cell to differentiate along the γ:δ lineage. Cells that have successfully rearranged a β-chain gene, produce a functional TCRβ-chain that pairs with

the invariant pre-TCRα-chain to create a pre-T cell receptor (Groettrup and Boehmer 1993; Taub and Longo 2005), which results in downregulation of CD25 (DN4: $CD44^-$, $CD25^-$). In addition, transcription of the RAG enzymes is terminated to ensure allelic exclusion (Alt, Rosenberg et al. 1981; Aifantis, Buer et al. 1997). Successfully rearranged cells proliferate extensively (Falk, Biro et al. 1996) and start to express CD4 and CD8 which mark the double-positive (DP) stage of development (Fehling, Krotkova et al. 1995). In the DP stage, the transcription of RAG1 and RAG2 is upregulated for the second time and the rearrangement of the α-chain takes place (Mombaerts, Clarke et al. 1992; Wilson, Held et al. 1994) resulting in expression of a complete αβ TCR on the cell surface. The TCRα and TCRβ subunits are produced by programmed rearrangement of variable (V), diversity (D) and joining (J) gene segments. The extremely high number of possible combinations of these gene segments enables the formation of a diverse TCR repertoire necessary for the recognition of a variety of foreign antigens (Sommers, Samelson et al. 2004) and the ligand specificity of the receptor dictates the cell fate.

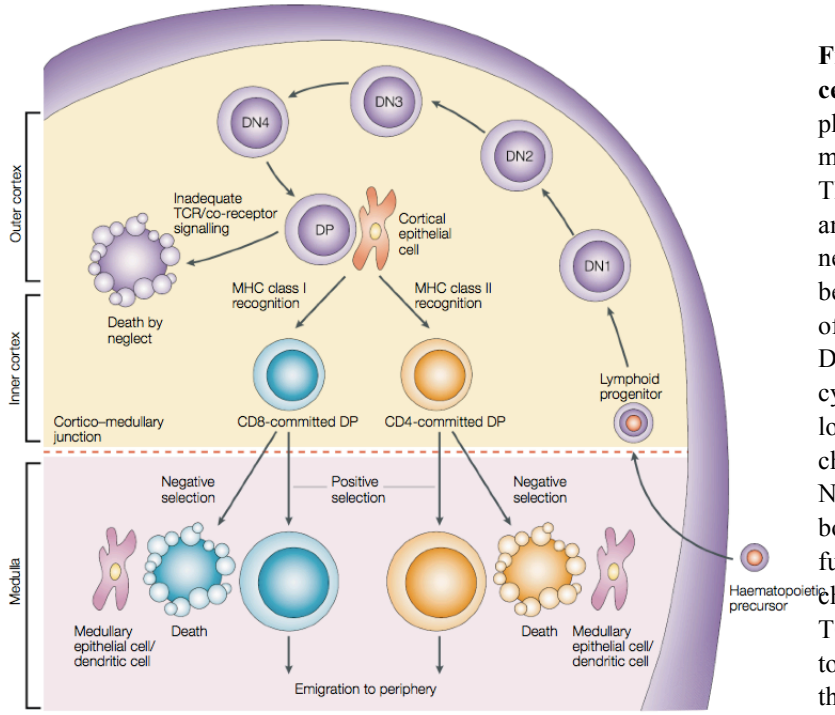

Figure 1: Traffic of thymocytes for T cell development and selection. Lymphoid progenitors arise in the bone marrow and migrate into the thymus. They lack the expression of TCR, CD4 and CD8 and are termed double-negative (DN) thymocytes, which can be further subdivided into four stages of differentiation (DN1; DN2; DN3; DN4). During DN2 to DN4, thymocytes rearrange the TCRβ-chain, followed by coupling with the pre-TCRα-chain to form the pre-TCR complex. Next, cells rapidly proliferate, express both CD4 and CD8 co-receptors, and functionally rearrange their TCRα-chain. Thymocytes expressing mature TCR and CD4 and CD8 surface receptors are termed double-positive (DP) thymocytes.

DP thymocytes interact with thymic epithelial cells and begin the process of positive and negative selection, resulting either to death via apoptosis or survival and subsequent maturation into CD4 single positive (SP) or CD8 SP thymocytes. These cells are then ready for export from the medulla to peripheral sites. Picture was taken from (Ronald N.Germain, 2002).

Once the mature TCR is expressed, DP thymocytes undergo two selection steps termed positive and negative selection. The positive selection is initiated by TCR recognition of peptide/MHC complexes at low avidity interactions on cortical thymic epithelial cells (cTECs)

and dendritic cells, resulting in survival and further differentiation into single positive (SP) thymocytes. The process of negative selection deletes via apoptosis thymocytes with high affinity for self-peptides presented by medullary thymic epithilial cells (mTECs). This process contributes to the deletion of self-reactive T cells, thereby ensuring self-tolerance and avoiding autoimmunity. In addition to TCR ligation, negative selection appears to require secondary signals delivered through contact with co-stimulatory molecules on antigen presenting cells (APCs). This selection process ensures that only cells with functional TCRs that recognize self-MHC but no self-peptides migrate into the periphery. The negative selection process results in a loss of nearly 95% of developing thymocytes. The surviving thymocytes down-regulate one of the co-receptors, becoming either CD4 SP or CD8 SP, and leave the thymus to circulate in the periphery as mature T cells.

1.1.2 T cell receptor signaling

The TCR is a multimeric complex composed of a receptor module associated with various signaling proteins (CD3γ, δ, ε and TCRζ chains). Stimulation of the TCR triggers signaling cascades required for T cell differentiation and proliferation. Signal transduction from the TCR is initiated by sequential activation of protein tyrosine kinases (PTKs) Lck/Fyn and Zap70/Syk (Guy and Vignali 2009). Lck is constitutively associated with the cytoplasmic domain of the co-receptors CD4 and CD8 whereas Fyn physically associates with the cytoplasmic domains of the CD3 chain from the TCR complex. After engagement of the TCR by self-peptide-MHC complexes, the CD8 or CD4 co-receptor deliver Lck to the TCRζ chain to phosphorylate the immunoreceptor tyrosine based activation motifs (ITAMs). Phosphorylation of the ζ chains enables them to bind Zap70 and bring it in close proximity to Lck. Then, Lck activates and phosphorylates Zap70, which subsequently phosphorylates the adaptor proteins LAT and SLP-76 (Wang, Kadlecek et al. 2010). These proximal signaling events lead to the activation of PLCγ-1 (Smith-Garvin, Koretzky et al. 2009), which in turn hydrolyzes phosphatidylinositol 4,5-biphosphate (PIP2) to generate two important second messengers, diacylglycerol (DAG) and inositol 1,4,5-triphosphates (IP3) (Imboden and Stobo 1985).

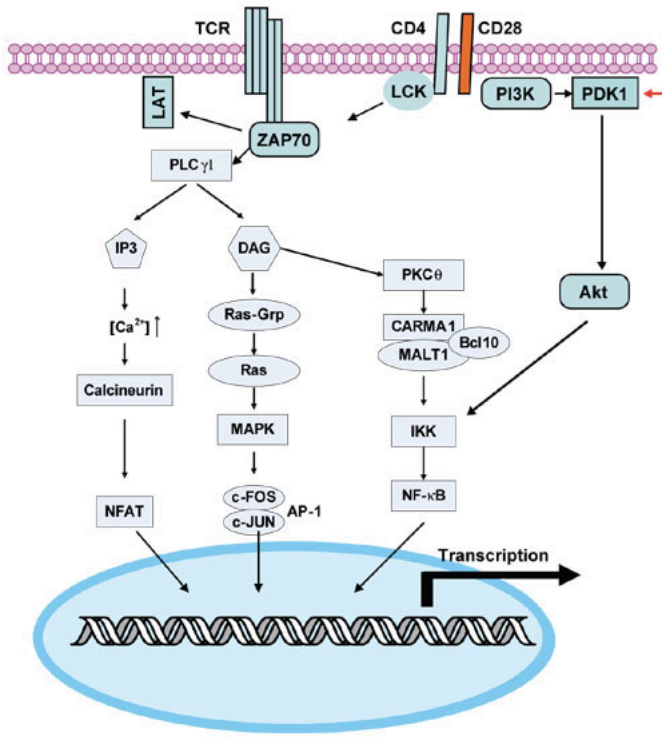

Figure 2: Schematic illustration of TCR signaling pathways. Upon TCR stimulation, PLC-γ1 is activated generating inositol triphosphate (IP3) and diacylglycerol (DAG). IP3 induces calcium release, thus activating the NFAT pathway, and DAG phosphorylates PKCθ, thus activating the NF-κB pathway. In addition, DAG triggers Ras-Grp resulting in the activation of the Ras-Mek1/2-Erk1/2-AP1 pathway. Picture was taken from (Hayashi, Mo et al. 2007).

IP3 binds to its receptor in the endoplasmic reticulum (ER) to trigger the release of Ca^{2+} to the cytosol. Ca^{2+} is required to activate the serine/threonine phosphatase calcineurin, which dephosphorylates the transcription factor NFAT. Then, dephosphorylated NFAT translocates into the nucleus to induce the transcription of genes essential for T cell activation and T cell tolerance. The second messenger DAG binds to PKCθ to induce its rapid translocation to the immunological synapse and its activation (Isakov and Altman 2002). Next, PKCθ phosphorylates Carma1 leading to the recruitment of Bcl10 and Malt1 to the lipid raft. PKCθ as well as the Carma1/Bcl10/Malt1 complex associate with the IKK complex and induce its activation (Lee, D'Acquisto et al. 2005). The activated IKK complex in turn phosphorylates IκB, which subsequently become ubiquitinated and then fully degraded through the proteasome. Thus, NF-κB complexes are freed and translocate into the nucleus to activate the expression of their target genes (Vallabhapurapu and Karin 2009). In addition, DAG associates and activates Ras-GRP1, which further induces the activation of the Ras-Mek1/2-Erk1/2-AP1 pathway (Roose, Mollenauer et al. 2005). Altogether, the activation of the TCR promotes a number of signaling cascades resulting in the activation of the transcription factors NF-κB, NFAT and AP-1. Activation of these molecules initiates new gene transcription that results in the differentiation, proliferation and effector actions of T cells.

1.1.3 T helper cell lineages

$CD4^+$ T helper cells (T_H) are important mediators of humoral and cell immune responses (Cantor and Boyse 1975). Following activation, naive T_H cells can differentiate into two functionally different lineages of T_H cells (Mosmann and Coffman 1989). Each subset produces mostly mutually exclusive panels of cytokines, which defines their distinct functions in immunity. First, the T_H1 cell subset, which is characterized by their capacity to produce the cytokines IFNγ and IL-2 and differentiate from naive T_H0 precursors under the influence of IL-12, IFNγ and the transcription factors STAT-1, STAT-4 and T-bet (Szabo, Kim et al. 2000). Second, the T_H2 cell subset, which produce the cytokines IL-4, IL-5, IL-6, IL-10 and IL-13. The development of T_H2 cells from naive T_H0 precursors is driven by IL-4 and the transcription factors STAT-6 and GATA-3 (Zheng and Flavell 1997). T_H1 cell cytokines drive cell-mediated responses, activating mononuclear phagocytes, natural killer (NK) cells and cytotoxic T cells to kill intracellular microbes and virally infected targets. T_H2 cell cytokines are important for the host defense against extracellular pathogens and enhance the antibody production by B cells. The initial source of the differentiation factors for both T_H1 and T_H2 cells are cells of the innate immune system responding to microbal anigens, parasitic antigens or allergens.

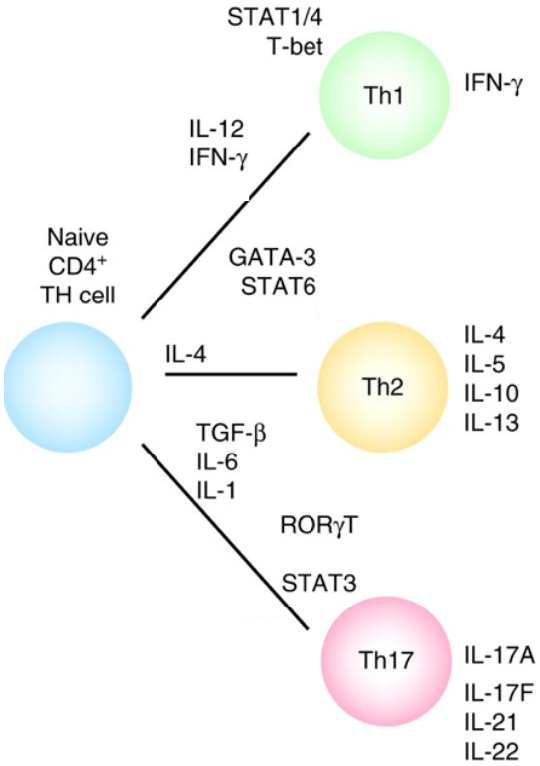

Figure 3: Development of T helper subsets from naive $CD4^+$ T cells. Cytokines and transcription factors inducing the development of T_H1, T_H2 and T_H17 cells are shown. On the right, the main effector cytokines produced by T_H1, T_H2 and T_H17 cell lines are indicated. Picture was taken from (Andreotti, Schwartzberg et al. 2010).

Recently, a third subset of effector T_H cells distinct from T_H1 or T_H2 cells has been identified known as T_H17 cells, which play an important role in host defence against specific pathogens and are potent inducers of autoimmunity and tissue inflammation (Harrington 2005; Langrish 2005; Park 2005). T_H17 cells are characterized by the production of IL-17A, IL-17F and IL-22, which are potent pro-inflammatory cytokines capable of inducing IL-6 and TNF production as well as driving granulocyte recruitment and tissue damage. T_H17 cells also secrete IL-21 to communicate with cells of the immune system. The differentiation of T_H17 cells from naive $CD4^+$ T cells is regulated by the cytokines TGFβ and IL-6 and the transcription factors STAT-3, RORγt and RORα (Veldhoen 2006).

1.1.3.1 Regulatory T cells

Regulatory T cells (Tregs) play an important role in the maintenance of immunological homeostasis and self-tolerance by suppressing the proliferation or function of autoreactive T cells (Thompson and Powrie 2004). They have been shown in several murine *in vivo* models to prevent the induction of autoimmune and inflammatory disease (Asano, Toda et al. 1996; Read, Malmstrom et al. 2000; Read, Malmström et al. 2000; Salomon, Lenschow et al. 2000; De Camargo Furtado, Olivares-Villagómez et al. 2001). There are two types of $CD4^+$ Tregs: natural Tregs (nTregs), which develop in the thymus during the course of positive and negative selection, and induced Tregs (iTregs), which are derived from naive conventional $CD4^+$ T cells in the periphery following antigenic stimulation under a variety of conditions. In naive mice, the nTreg cell population comprises 5-10% of all peripheral $CD4^+$ T cells (Sakaguchi 2004). The first identified cell surface marker which is preferentially expressed on nTregs was the high affinity IL-2 receptor α chain CD25 (Sakaguchi, Sakaguchi et al. 1995). However, CD25 expression is not unique to nTregs, since conventional T cells upregulate CD25 expression upon activation. The most specific marker of nTregs is the unique winged-helix/forkhead transcription factor Foxp3 (also called scurfin), that is required for their development, maintenance and function (Fontenot, Gavin et al. 2003; Hori, Nomura et al. 2003). Foxp3 is expressed exclusively in thymus-derived nTregs (Rudensky 2005) and also certain peripheral iTreg populations that have suppressive capabilities (Chen, Jin et al. 2003; Fantini, Becker et al. 2004). Genetic mutations in the gene encoding Foxp3 are fatal for both, mice and humans: Mice (called scurfy mice) and humans (IPEX syndrome: Immune dysregulation Polyendocrinopathy Enteropathy X-linked syndrome) develop a profound autoimmune-like lymphoproliferative disease displaying the importance of Tregs in the maintenance of peripheral tolerance (Bennett 2001; Brunkow 2001; Wildin 2001).

While nTregs develop in response to self-antigen or strongly ligating peptides in the thymus, iTregs develop in response to weaker, suboptimal TCR stimulation and exogenous antigens in the periphery (Apostolou and von Boehmer 2004; Kretschmer, Apostolou et al. 2005). There are two main subsets of iTregs generated in the periphery, which have been described based on the cytokines causing their induction. First, the type 1 regulatory T cells (Tr1), which are induced by IL-10 (Groux, O'Garra et al. 1997; Vieira, Christensen et al. 2004), and second, the T helper 3 (T_H3) cells, which are induced by TGFβ (Weiner 2001). Both subsets exert their suppressive activity primarily via soluble factors. Upon TCR triggering, Tr1 cells mediate suppression by producing IL-10, whereas T_H3 cells secrete the cytokine TGFβ (Chen, Kuchroo et al. 1994; Chen 2003; Fantini, Becker et al. 2004). In addition to the concept of soluble factor-mediated Treg suppression also other mechanisms of Treg suppression were described. Tregs can induce cytolysis of target cells by perforin, granzyme A in humans and granzyme B in mice (Gondek, Lu et al. 2005; Cao 2007). Recently, in several studies it was shown, that Tregs mediate suppression of conventional T cells via metabolic disruption by IL-2 deprivation which results in apoptosis, cAMP inhibition or by CD39/CD73-generated A2A-mediated immunosuppression (Sojka, Huang et al. 2008; Tang and Bluestone 2008; Vignali, Collison et al. 2008). Finally, Tregs can suppress target cells by modulating DC maturation or function via CD80/CD86 and CTLA-4 interaction or through the lymphocyte activation gene 3 (LAG-3) and MHC class II interaction (Sojka, Huang et al. 2008; Tang and Bluestone 2008; Vignali, Collison et al. 2008). This interaction results in the reduced ability of DCs to activate conventional T cells. In addition, they can induce the upregulation of the immunoregulatory enzyme indoleamine 2,3-dioxygenase (IDO) in DCs (Mellor and Munn 2004). Altogether, these mechanisms of Treg suppression provide a potent arsenal to maintain peripheral tolerance and preventing autoimmunity.

1.2 NF-κB signaling

Nuclear factor-κB (NF-κB) plays a central role in the regulation of diverse biological processes, including inflammation, immunity and cell survival (Karin and Ben-Neriah 2000; Li and Verma 2002). It comprises a family of transcription factors, which regulate numerous genes that are involved in the innate and adaptive immune responses. In mammalian, the NF-κB family consists of five inducible dimeric transcription factors belonging to the Rel familiy: c-Rel, RelA (p65), RelB, NF-κB1 (p50/p105) and NF-κB2 (p52/p100), which function as

homo- and heterodimers (Gilmore and Herscovitch 2000). All five contain a Rel-homology domain (RHD) that is responsible for DNA binding, dimerization, nuclear translocation and interaction with the inhibitory IκB proteins (Ghosh, May et al. 1998; Ghosh and Karin 2002). In unstimulated cells, NF-κB proteins are sequestered inactive in the cytoplasm bound to ankyrin-rich regions of inhibitor of NF-κB (IκB) inhibitory proteins (IκBα, IκBβ, and IκBε) or the precursor proteins of NF-κB1 and NF-κB2, p105 and p100, respectively (Ghosh, May et al. 1998). This binding serves to retain the dimers in the cytoplasm, therefore inhibiting the transcription of target genes. In response to stimulation, IκBs are rapidly degraded by the ubiquitin-proteasome pathway. The process of ubiquitination is an important signaling mechanism involved in NF-κB activation. Thereby, linkage through lysine 48 (K^{48}) targets substrates to the proteasome while lysine 63 (K^{63}) linkages seem to play important roles in directing cellular signaling events. Degradation of the inhibitor IκB allows NF-κB dimers to enter the nucleus and turn on a large number of target genes, particularly those involved in the immune system and defense against pathogens, but also genes relating to inflammation, injury, stress, and the acute phase response (Li and Verma 2002). The activation of the NF-κB transcription factors is controlled by two signaling cascades, each activated by a set of signal ligands: the canonical (also called classical) pathway and the noncanonical (also called alternatively) pathway.

1.2.1 The canonical NF-κB pathway

The canonical pathway of NF-κB activation is important at multiple stages of normal development and function of the immune system, whereas a dysregulation may result in the initiation and progression of autoimmune pathologies. A large variety of stimuli like mitogens, cytokines, microbal components and DNA damage can rapidly activate the canonical pathway (Pahl 1999) through a variety of cell membrane receptors such as tumour necrosis factor receptor (TNFR), IL-1 receptor and Toll like receptor (TLR), which results in phosphorylation, ubiquitination and proteasomal degradation of the IκBs. Upon stimulation, specific membrane receptors engage and trigger K^{63} polyubiquitination and activation of TRAF (TNF receptor-associated factor) ubiquitin ligases TRAF2, TRAF6 as well as RIP and NEMO (IKKγ) (Sun, Deng et al. 2004). TRAF ubiquitin ligases function together with a dimeric ubiquitin-conjugated enzyme (Ubc; also known as E2) complex Ubc13-Uev1A to catalyze the synthesis of a unique polyubiquitin chain linked through K^{63} of ubiquitin (Xia and Chen, 2005). The polyubiquitin chains bind to a specialized Ub-binding domain on TAB2 and TAB3 (Kanayama, Seth et al. 2004), resulting in the recruitment and activation of the TAK1 com-

plex. Activated TAK1 phosphorylates and activates the IκB kinase (IKK) complex, which is composed of two catalytic subunits, IKKα and IKKβ, and an essential regulatory subunit, NEMO (Xia and Chen, 2005).

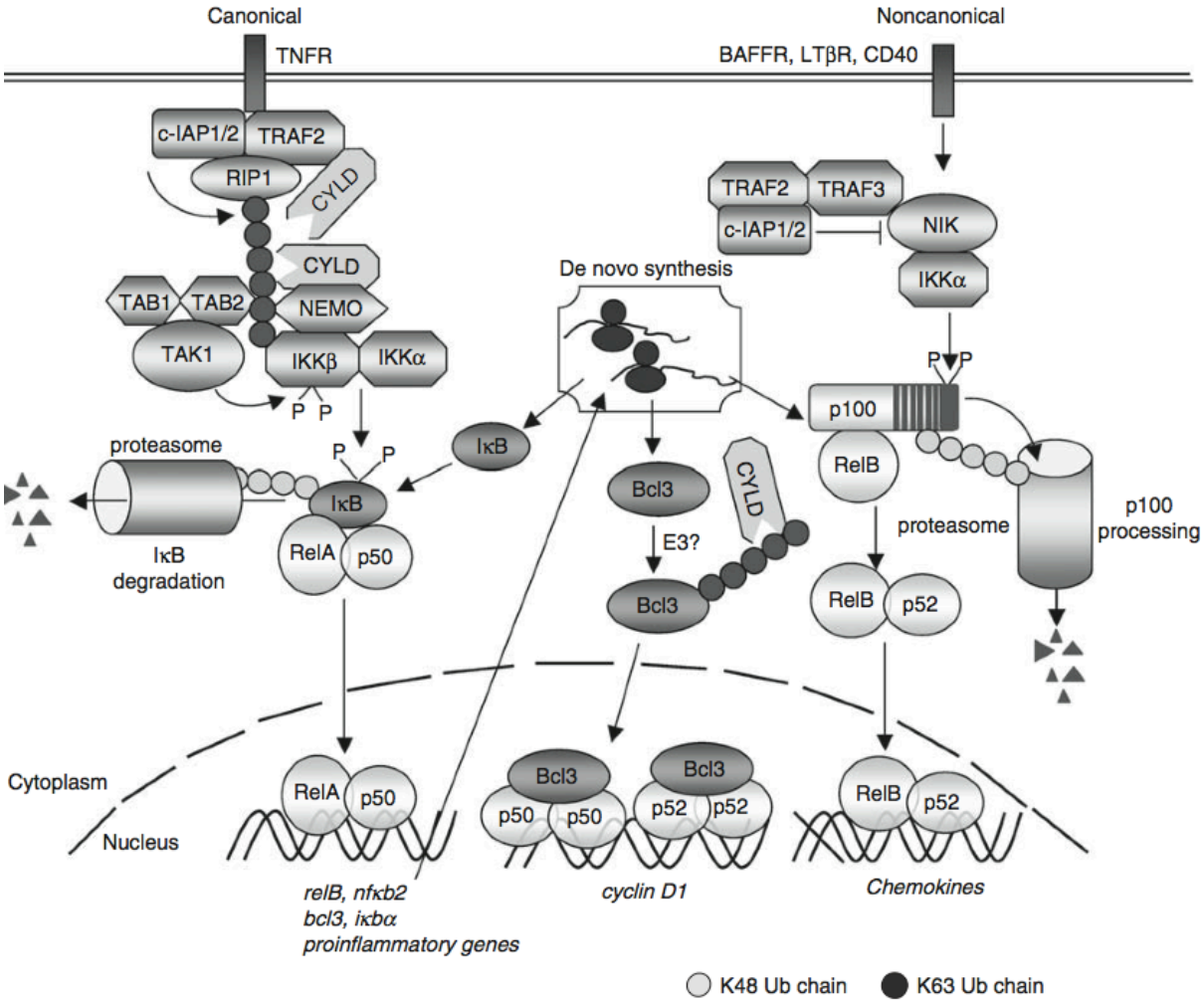

Figure 4: Regulation of the canonical and noncanonical pathways of NF-κB activation. NF-κB can be activated by canonical and noncanonical pathways, which rely on IκB degradation and p100 processing, respectively. Noncanonical NF-κB signaling involves receptor-mediated degradation of negative regulatory ubiquitin ligase complex, c-IAP/TRAF2/TRAF3, and accumulation of NIK. The canonical pathway involves K^{63} ubiquitination of several signaling components, such as RIP1, which is required for the recruitment and activation of IKK and its activating kinase, Tak1. The different NF-κB complexes regulate distinct target genes, although they may function cooperatively in many cases. Picture was taken from (Sun 2009).

Next, IKKβ phosphorylates IκB bound to cytosolic NF-κB, which subsequently triggers bTrCP E3 ubiquitin ligase-mediated K48 polyubiquitination and proteosomal degradation of IκB (Karin and Ben Neriah 2000; Verma et al. 1995). Degradation of IκB releases NF-κB heterodimers p50/RelA, which translocate into the nucleus to activate transcription of NF-κB

target genes, including genes encoding pro-inflammatory cytokines and chemokines, cell-adhesion molecules and anti-apoptotic proteins (Karin and Ben Neriah 2000). The deubiquitinases CYLD and A20 may block NF-κB activation by removal of K^{63} chains from activated TRAFs, RIP and NEMO. Additionally, CYLD may also indirectly inhibit the atypical NF-κB pathways, as the inducible expression of noncanonical NF-κB members, RelB and NF-κB2 (p100) depending on the canonical NF-κB activation.

1.2.2 The noncanonical NF-κB pathway

The noncanonical pathway is usually triggered by non-inflammatory stimuli, such as lymphotoxin-β receptor signaling (LTβR), LTαR, CD40L, RANK, and BAFFR. Activation of the noncanonical NF-κB pathway is strictly dependent on IKKα (Senftleben, Cao et al. 2001), and independent of IKKβ and IKKγ (Dejardin, Droin et al. 2002). Upon stimulation, TRAF proteins like TRAF2, TRAF3 and TRAF6 are recruited and activate the protein kinase NIK. Subsequently NIK selectively phosphorylates and activates the IKKα catalytic subunit. In this pathway acivated IKKα homodimers phosphorylate the precursor NF-κB2 (p100) at two C-terminal sites (Senftleben, Cao et al. 2001). p100 is subsequently polyubiquitinated and then processed to the mature subunit p52 by the proteasome (Xiao, Harhaj et al. 2001). p52, containing the Rel homology domain (RHD), and its binding partner RelB translocate into the nucleus to turn on the transcription of target genes (Sun and Chen 2004). Many data strongly suggest, that the noncanonical NF-κB pathway plays a central role in the expression of genes involved in development, maintenance and function of primary and secondary lymphoid organs (Weih and Caamano 2003), in the development, selection and survival of B and T cells and in the differentiation of antigen presenting cells such as DCs and mTECs (Zarnegar, Wang et al. 2008). Hence, the noncanonical NF-κB pathway plays an essential role in the regulation of immune central and peripheral tolerance, and therefore in autoimmune reactivity of the immune system. The canonical and noncanonical NF-κB pathways do not exist in isolation and the close cross-talk between both contributes to fine-tune signaling processes.

1.3 CYLD

1.3.1 Familial Cylindromatosis

Familial cylindromatosis (also called turban tumour syndrome or Brooke-Spiegler syndrome) is a rare autosomal dominantly inherited disease characterized by the development of multiple

benign tumours of the skin appendages (Oiso et al. 2004). The tumours are known as cylindromas due to their characteristic microscopic architecture and are believed to arise from or recapitulate the appearance of the eccrine or apocrine cells of the skin that secrete sweat and scent, respectively. In familial cylindromatosis, the cylindromas usually begin to appear in the second or third decade, accumulating in number and increasing slowly in size throughout adult life (Bignell, Warren et al. 2000). It was shown, that this disease is caused by a variety of mutations in the gene encoding the CYLD protein. To date, 23 different mutations of *cyld* have been identified in cases of familial cylindromatosis. Most of these mutations result in truncated CYLD proteins due to translational frameshift mutations, nonsense mutations, splice site mutations, or missense mutations (Guangyong Zheng et al. 2004). The susceptibility gene *cyld* has the genetic attributes of a tumour suppressor gene. As with all classical tumour suppressors, both copies of the gene must be inactivated to produce cylindromas. This usually arise from a mutation in one copy and a deletion of the region of the chromosome carrying the other copy (Wilkinson 2003).

1.3.2 The function of the CYLD protein

Cyld was originally identified as a tumour suppressor, that is mutated in patients with familial cylindromatosis (Biggs, Wooster et al. 1995). The responsible cylindromatosis gene comprises 20 exons, extending over 56 kb of genomic DNA (Bignell et al. 2000). The CYLD gene encodes several protein-interaction domains, including three cytoskeletal-associated protein-glycine-conserved (CAP-Gly) domains, two prolin-rich motifs and a zinc-finger-like domain (Bignell et al. 2000). The CAP-Gly domains are typically found in proteins that coordinate the attachment of organelles to microtubules indicating a role for CYLD in cytoskeleton formation (Bignell et al. 2000). Indeed, CYLD was shown to have microtubule-association function, which is dependent on the first CAP-Gly domain (Gao 2008). The prolin-rich motifs mediate the interaction with proteins containing a Src homology 3 (SH3) domain (Li 2005). Whether or not CYLD interacts with such proteins is still unclear. The human *cyld* gene is located on chromosome 16q12.1 and encodes a protein that encompasses 956 amino acids, containing a C-terminal catalytic domain with sequence homology to ubiquitin-specific proteases (USP) family members (Bignell et al. 2000; Kovalenko 2003). The CYLD protein harbors a NEMO (IKKγ) binding site located between amino acids 470 and 684 and a TRAF2 binding site located between CYLD amino acids 394 and 470 (Kovalenko et al. 2003). CYLD is known to be a member of the family of deubiquinating enzymes (DUB) with restricted substrate specificity and its deubiquitinating activity was shown to down-

regulate NF-κB activity by removing activating ubiquitin molecules from TRAF2 and NEMO (Brummelkamp, Nijman et al. 2003; Kovalenko 2003; Trompouki, Hatzivassiliou et al. 2003). Hence, mutations of CYLD at the C-terminal region disrupt its DUB catalytic activity and cause dysregulated activation of the NF-κB pathway, which in turn promotes cell survival and tumourigenesis.

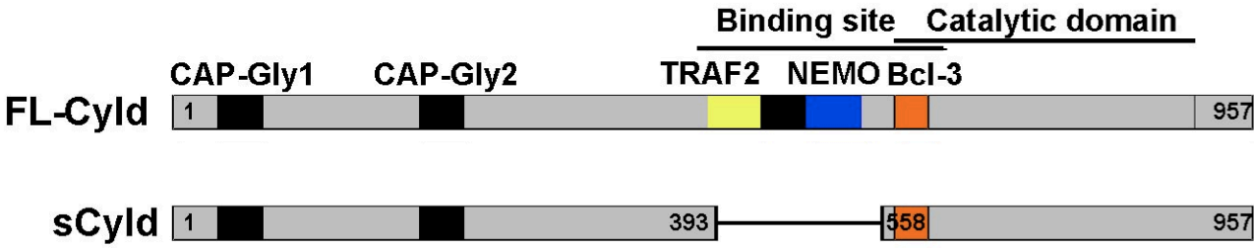

Figure 5: Structure of the FL-CYLD and sCYLD protein. FL-CYLD and sCYLD exhibit both their catalytic domain at the C-terminus. In contrast to FL-CYLD, sCYLD lacks the TRAF2 and NEMO binding sites and the third CAP-Gly domain, while it still retains the Bcl-3 binding site. Picture was taken from (Hövelmeyer, Wunderlich et al. 2007).

The naturally occuring short splice variant of CYLD is normally found in murine cells in addition to full lenght CYLD (FL-CYLD) and misses exon 7 and 8 of the *cyld* gene (Hövelmeyer, Wunderlich et al. 2007). Therefore, sCYLD still retains DUB activity but is devoid of the domain that mediates binding to TRAF2 and NEMO.

1.3.3 The role of CYLD in NF-κB signaling

CYLD has been identified by three distinct laboratories as DUB enzyme that has an essential role in the NF-κB signaling pathway (Brummelkamp et al. 2003; Kovalenko et al. 2003; Trompouki et al. 2003). Brummelkamp *et al.* could show by RNAi-based functional screening study, that inhibition of CYLD resulted in enhanced NF-κB activity (Brummelkamp et al. 2003). Furthermore, a yeast two-hybrid screening assay identified that CYLD physically interacts with NEMO, a regulatory subunit of the IκB kinase IKK (Kovalenko 2003; Trompouki, Hatzivassiliou et al. 2003). This interaction occurs through a prolin-rich sequence located near the N-terminus of NEMO and the third CAP-Gly domain of CYLD (Saito, Kigawa et al. 2004). Moreover, CoIP assays revealed the association of CYLD with TRAF2 and TRAF6, suggesting that the effect of CYLD on NF-κB activation is mediated by CYLD-dependent deubiquitination of TRAF2 and TRAF6 (Brummelkamp, Nijman et al. 2003; Kovalenko 2003; Trompouki, Hatzivassiliou et al. 2003). In another report, Regamey *et al.* identified a direct interaction between TRAF-interacting protein (TRIP) and CYLD, which resulted in a downregulation of the NF-κB activity following TNF-α stimulation (Regamey,

Hohl et al. 2003). In previous studies, Reiley *et al.* suggest that inducible phosphorylation of CYLD between the amino acids 420-446 is an important mechanism of its regulation (Reiley, Zhang et al. 2005). They indicated that signal-induced TRAF2 ubiquitination is associated with phosphorylation of CYLD, since when endogenous CYLD is replaced with a phosphorylation-defective CYLD mutant, the inducible ubiquitination of TRAF2 is severely attenuated. The latter implicates, that phosphorylation serves as a mechanism that temporarily inactivates the DUB activity of CYLD, allowing the accumulation of ubiquitin-conjugated TRAF2. Further, Reiley *et al.* indicated that IKK regulates the function of DUB CYLD because CYLD undergoes rapid and transient phosphorylation in cells stimulated with various known IKK inducers. Additionally, they demonstrated that CYLD phosphorylation is dependent on IKKγ, since it is blocked in IKKγ-deficient Jurkat cells. In addition to its function as DUB, CYLD can also be ubiquitinated at K^{48} upon hypoxia-induced NF-κB activation in cancer cell lines infected with high-risk human papillomavirus (HPV) serotypes. Ubiquitinated CYLD is then targeted for proteosomal degradation resulting in prolonged NF-κB activation (An, Mo et al. 2008). Hence, post-translational modifications of CYLD such as phosphorylation and ubiquitination appear to be critical for its function and activity in the NF-κB signaling pathway.

1.3.4 The role of CYLD in thymocyte development

CYLD was the first DUB which was found to regulate thymocyte development (Reiley et al. 2006). In contrast to the negative regulatory function of CYLD in the NF-κB pathway, it was shown to positively regulate TCR signaling in thymocytes. Reiley *et al.* demonstrated, that CYLD-deficient mice have decreased numbers of SP thymocytes and peripheral T cells, indicating a regulatory role for CYLD in the DP-SP transition of thymocytes (Reiley et al. 2006). Mechanistically, CYLD positively regulates the Src-family protein tyrosine kinase Lck, which is required for TCR-proximal signaling and thymocyte development (Molina 1992). CYLD was shown not to be required for Lck activation, but instead for recruiting activated Lck to its substrate Zap70. The kinase Zap70 is known to specifically regulate the development of SP thymocytes (Starr, Jameson et al. 2003). Hence, thymocytes of CYLD-deficient mice display defects in TCR-stimulated phosphorylation of Zap70 and downstream signaling events, which results in attenuated positive selection of SP thymocytes. The ubiquitination of Lck is mediated by c-CBL and known to be a negative mechanism that regulates the signaling function of Lck (Rao 2002), because ubiquitination of Lck results in its proteosomal degradation. Importantly, CYLD can remove both K^{63}- and K^{48}-linked polyubiquitin chains from Lck, in contrast to its selectivity in removing only K^{63}-linked polyubiquitin chains from TRAF2 and Bcl-3.

These findings implicate, that polyubiquitin chains might regulate Lck function by both degradation-dependent and -independent mechanism.

1.4 Inflammatory bowel disease

Inflammatory bowel disease (IBD) is a chronic, disabling and often relapsing disorder associated with high morbidity. The onset of IBD typically occurs in the second and third decades of life and patients suffer from rectal bleeding, severe diarrhea, abdominal pain, fever, and weight loss. In the healthy gut, the mucosal immune system ensures the balance between pro- and anti-inflammatory mediators by allowing an effective defense against luminal pathogens but preventing an overwhelming immune reaction directed against harmless luminal antigens like components of food or nonpathological bacteria (Atreya, Atreya et al. 2008). In IBD this immunological balance is strongly impaired shifting towards the pro-inflammatory side. Crohn's disease (CD) and ulcerative colitis (UC) are two distinct forms of IBD that share related characteristics. The pathological process of both diseases involves inflammation, ulceration and subsequent regeneration of intestinal mucosa (Warren and Sommers 1954; Finkelstein, Sasatomi et al. 2002). Although the specific causes of IBD are poorly understood, the pathological natures of UC and CD are well defined. UC involves the colon but largely spares the small intestine except the terminal ileum. Inflammation is located in the mucosa, while the deeper layers of the gut are usually not affected. In contrast, CD primarily involves the small and large bowel. The inflammatory infiltrate in CD involves the entire thickness of the intestinal wall and classically contains numerous epithelioid cell granulomas. In IBD, the innate immune response plays an essential role. Upon activation, DCs and macrophages secrete several pro-inflammatory cytokines such as IL-6, IL-12, IL-23 and TNF-α, which actively regulate the inflammatory response in CD in UC. After secretion, these cytokines trigger and differentiate a large number of T cells activating the adaptive immune response. In addition to innate immune cells, mucosal $CD4^+$ T cells were shown to play a central role in both the induction and persistence of chronic inflammation by producing pro-inflammatory cytokines. CD is considered as a T_H1 disease, since the mucosa of patients is dominated by $CD4^+$ T cells producing IFNγ, IL-2, IL-12 and TNF (Monteleone, Biancone et al. 1997). In contrast, the mucosa in patients with UC is dominated by $CD4^+$ T cells with a T_H2 phenotype, characterized by the production of TGF-β and IL-5 but no IL-4 (Fuss, Neurath et al. 1996), indicating UC as a T_H2-mediated disease. However, the concept of CD being a T_H1- and UC

being a T_H2-mediated disease has been challanged by studies reporting an up-regulation of IL-4 or IL-5 in CD (Desreumaux, Brandt et al. 1997; Carvalho, Elia et al. 2003), and T_H1 cytokines in UC (Tsukada, Nakamura et al. 2002; Y. Sawa 2003).

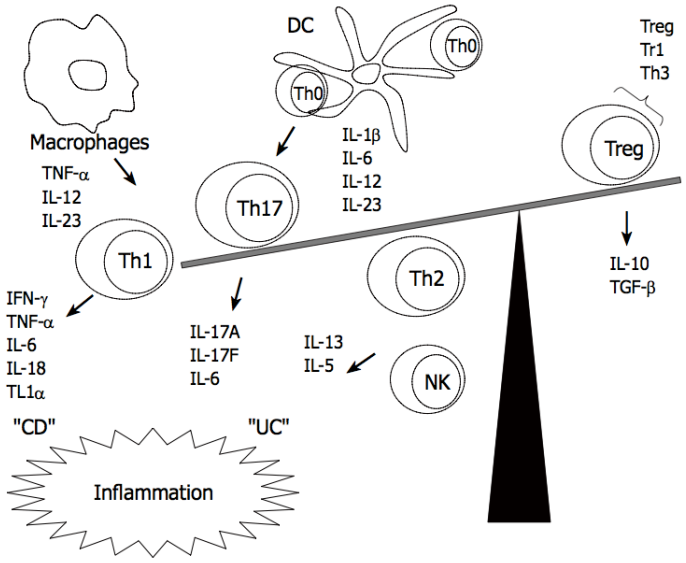

Figure 6: Cytokine imbalance between effector and T regulatory cells in IBD. In patients with IBD, pro-inflammatory cytokines produced by T_H17 and T_H1 cells abolish the effect of anti-inflammatory cytokines secreted by Tregs. Cytokines derived from APCs following contact with microbial products trigger the differentiation of T_H17 and T_H1 cells or have a direct pro-inflammatory effect by TNF-α production. CD = Crohn's disease; UC = Ulcerative colitis

Recently, T_H17 cells were identified to play an essential role in the development of autoimmunity and inflammatory responses such as IBD (Mangan 2006). It has been shown, that the T_H17-secreted cytokine IL-17 is overexpressed in the inflamed mucosa from active CD and UC patients and may therefore contribute to the pathophysiology of IBD (Fujino, Andoh et al. 2003). Also Tregs play a major role in the maintenance of the gut homeostasis, since they suppress the differentiation and function of T_H1 and T_H2 cells by the production of the anti-inflammatory cytokine IL-10. This was demonstrated by experiments using IL-10-deficient Tregs which fail to protect from IBD (Asseman, Mauze et al. 1999). The important inhibitory function of IL-10 could be further manifested by the fact, that IL-10-deficient mice spontaneously develop IBD, associated with a T_H1-polarized immune response (Kuhn, Lohler et al. 1993). Therefore, a cytokine imbalance between effector T cells and Tregs is implicated in the development of IBD. Altogether, APCs, T_H1, T_H2, Tregs and T_H17 cells and their cytokines play a complex role in IBD. It is well known, that mutational genes can affect the development of IBD via certain signaling pathways. The abnormal signaling can lead to dysregulation of the inflammatory response, which is crucial in the pathogenesis of IBD. Disorders of signaling pathways can act on the intestinal barrier and cause an uncontrolled release of effector T cells, which mediate inflammation in CD. In genome-wide association studies more than 50 distinct loci that confer IBD susceptibility could be identified. Recently, mutations in the gene encoding NOD2 (also designated CARD15 and IBD1) were strongly associated with an in-

creased risk of developing CD but not UC (Hugot, Chamaillard et al. 2001; Ogura, Bonen et al. 2001; Cuthbert, Fisher et al. 2002). NOD2 activation is implicated in the induction of NF-κB and the mitogen-activated protein kinase (MAPK) pathway resulting in the production of pro-inflammatory mediators. Importantly, the *cyld* gene is located next to *nod2*, suggesting an intriguing possibility that CYLD may also be involved in the regulation of human IBD.

1.5 Experimental autoimmune encephalomyelitis

Multiple sclerosis (MS) is one of the most common chronic inflammatory disorders of the central nervous system (CNS), which is characterized by inflammation, destruction of myelin sheaths, axonal injury and atrophy of the CNS (Steinman 1996). The disease usually begins in the young adulthood and affects women more frequently than men. Moreover, the risk to develop MS is significantly higher in family members of patients with the disease (Ebers, Sadovnick et al. 1995), indicating a genetic predisposition to MS (Ebers and Dyment 1998).

Experimental autoimmune encephalomyelitis (EAE) was established nearly 70 years ago as an animal model for MS (Rivers, Sprunt et al. 1933), because it shares some clinical and pathological features with MS. EAE is a $CD4^+$ T cell-mediated demyelinating disease of the CNS induced by active immunization with myelin antigens and Freund's adjuvant (Wekerle, Kojima et al. 1994). Upon immunization, myelin-specific effector T cells are primed and expand in peripheral lymph nodes. Then, the activated $CD4^+$ T cells migrate into the CNS, where they cross the blood brain barrier (BBB). In the CNS, the infiltrated $CD4^+$ T cells are reactivated by local APCs presenting myelin peptides and start to initiate tissue inflammation. The entry of primed T cells into the CNS is dependent on the expression of the integrin $\alpha_4\beta_1$ (VLA-4), which interacts with the adhesion molecule VCAM expressed by inflamed endothelial cells (Yednock 1992).

Until recently, T_H1 cells were thought to be the main effector T cells responsible for the autoimmune inflammation, because EAE can be induced by adoptive transfer of myelin-reactive T_H1 cells (Baron 1993; Kuchroo, Martin et al. 1993). However, more recent studies have highlighted an essential role of T_H17 cells in the onset and maintenance of EAE (Steinman 2007). It was shown, that mice lacking RORγt, IL-17 or IL-23 as well as mice treated with IL-17 blocking antibodies are less susceptible to EAE than control mice (Hofstetter 2005; Langrish 2005; Ivanov 2006; Komiyama 2006). Moreover, T_H17 cells could be detected in

inflamed brain lesions from patients suffering from MS (Tzartos 2008). Therefore, it currently appears that both T_H1 and T_H17 cells have pathogenic potential in MS (Stromnes, Cerretti et al. 2008).

1.6 Objectives

In our laboratory, we focus on the analysis of CYLD function in the immune system making use of the $CYLD^{ko}$ as well as the $CYLD^{ex7/8}$ mice, which exclusively overexpress sCYLD while FL-CYLD is completely absent. sCYLD is lacking exon 7 and 8 of the *cyld* gene and is therefore devoid of the TRAF2 and NEMO binding site while it still retains an intact Bcl-3 binding site. $CYLD^{ex7/8}$ mice have enlarged spleens and secondary lymphoid organs due to a massive accumulation of B cells as a result of enhanced survival and expression of NF-κB. Moreover, bone marrow derived DCs (BMDC) from these mice show a hyperactive phenotype *in vitro* and *in vivo*, accompanied by increased nuclear translocation of Bcl-3. Because sCYLD is important in B cell and DC regulation, we decided to investigate the impact of sCYLD in T cell development and function. To examine a possible effect of sCYLD in positive and negative selection of thymocytes, $CYLD^{ex7/8}$ mice were crossed to HY TCR transgenic mice and thymocytes of the different genotypes were analyzed by flow cytometry. Since CYLD was demonstrated to be essential in TCR signaling of thymocytes, we examined the effect of sCYLD in TCR signaling by Western Blot analysis. Additionally, the activation of T cells of $CYLD^{ko}$, $CYLD^{ex7/8}$ and control mice was analyzed *in vitro* and *in vivo* by examining NF-κB signaling, proliferative response and cytokine production. Moreover, the functional capacity of Treg cells overexpressing sCYLD was evaluated. Because the *cyld* gene was shown to be downregulated in patients with IBD, we examined the contribution of sCYLD in the development of intestinal pathology by using an adoptive transfer model of colitis and analyzing mice by mini-endoscopy. As additional model of autoimmunity MOG-induced EAE was used.

2 Materials and Methods

2.1 Chemicals and Biological Material

Chemicals were purchased from Sigma (Steinheim), Fluka Chemie (Switzerland), Merck (Darmstadt) or AppliChem (Darmstadt) unless stated otherwise. Solutions were prepared with double distilled water (ddH_2O).

Sterility of solutions and chemicals used in cell culture was maintained by working under a sterile hood (Heraeus, Germany).

Name of chemical	Supplier
β-Mercaptoethanol (β-ME)	Fluka Chemie GmbH, Switzerland
Acetone	Merck, Darmstadt
Agar	Gibco Life Technologies GmbH, Karlsruhe
Agarose, electrophoresis grade	AppliChem, Darmstadt
L-Arabinose	Sigma-Aldrich, Steinheim
Bovine serum albumine (BSA)	Sigma-Aldrich, Steinheim
Calcium chloride	Sigma-Aldrich, Steinheim
Chloroform	Merck, Darmstadt
Citric acid	Fluka Chemie GmbH, Switzerland
2'-Deoxyguanosine Monohydrate	AppliChem, Darmstadt
Diethylpyrocarbonate (DEPC)	AppliChem, Darmstadt
Dextran sulfate	AppliChem, Darmstadt
Dextrose	Merck, Darmstadt
Diethylpyrocarbonate (DEPC)	AppliChem, Darmstadt
Dithiothreitol (DTT)	Boehringer Mannheim GmbH, Mannheim

dNTPs	Pharmacia Biotech, USA
Ethanol, abs.	AppliChem, Darmstadt
Ethidium bromide	Sigma-Aldrich, Steinheim
Ethylendiamine tetraacetate (EDTA)	Fluka Chemie GmbH, Switzerland
Fetal calf serum (FCS)	Boehringer Mannheim GmbH, Mannheim
Ficoll 400	Amersham Pharmacia, Freiburg
Glacial acetic acid	Fluka Chemie GmbH, Switzerland
Hydrochloric acid (37 %)	Merck, Darmstadt
Isopropanol	AppliChem, Darmstadt
Magnesium chloride	Sigma-Aldrich, Steinheim
Magnesium chloride (for PCR)	Gibco Life Technologies GmbH, Karlsruhe
Mineral oil	Sigma-Aldrich, Steinheim
Orange G	Chroma Gesellschaft Schmidt & Co, Stuttgart
Phenol	Sigma-Aldrich, Steinheim
Potassium acetate	Fluka Chemie GmbH, Switzerland
Potassium chloride	Merck, Darmstadt
Proteinase K	Roche, Switzerland
Sodium azide	Fluka Chemie GmbH, Switzerland
Sodium carbonate	Fluka Chemie GmbH, Switzerland
Sodium chloride	AppliChem, Darmstadt
Sodium citrate	Fluka Chemie GmbH, Switzerland
Sodium dodecyl sulfate	AppliChem, Darmstadt

Sodium hydrogencarbonate	Fluka Chemie GmbH, Switzerland
Sodium hydroxide	Fluka Chemie GmbH, Switzerland
Tris base	Fluka Chemie GmbH, Switzerland
Tris/ HCl	AppliChem, Darmstadt
Tween 20	Sigma-Aldrich, Steinheim

Table 1: Chemicals

2.2 Molecular biology

Standard methods of molecular biology were performed – if not otherwise stated – according to protocols described in Sambrook *et al.* (Sambrook 1989).

2.2.1 Preparation of genomic DNA

Cells or tail biopsy (0,5cm) were lysed over night (o/n) at 56°C in lysis buffer (10mM Tris-HCl, ph 8; 10mM EDTA; 150mM NaCl; 0.2% (w/v) SDS; 400mg/ml proteinase K). Undissolved debris was pelleted (13000 rpm, 10 min) and the supernatant was mixed with an equal volume of isopropanol to precipitate the DNA. Subsequently, DNA was pelleted by centrifugation, washed in 70% (v/v) EtOH, dried at RT, and resuspendet in TE buffer (10mM Tris-HCl, pH 8; 1mM EDTA).

2.2.2 Polymerase chain reaction (PCR)

PCR (Saiki, Scharf et al. 1985; Mullis and Faloona 1987) was used to screen mice for the presence of targeted alleles or transgenes from tail tip DNA (primers shown in Table 2). Reactions were performed in either Hybaid machines (MWG-Biotech, Ebersberg, Germany) or Triothermocyclers (Biometra, Göttingen, Germany). Genotyping of mice was generally performed in a total volume of 30 µl in the following reaction mix: 10 pmol of each primer, 0.5 U of *Thermus aquaticus* (Taq) DNA polymerase (1U/µl, Segenetics, Bonn, Germany), 25 mM dNTPs, 10 mM Tris-HCl pH 8.3, 50 mM KCl, 2.5 mM $MgCl_2$, 100 ng template DNA. Amplification started with denaturation for 4 min at 94 °C followed by 30-35 cycles of 94 °C for 30 sec, 54-63 °C for 30-60 sec, 72 °C for 30-60 sec and a final extension step at 72 °C for 10 min.

Name of primer	Sequence (5´-3´)	$T_{Ann.}$ °C	Direction
CYLD wt	CAT GGA AGG AGG CTG CGG TGG AGG AGA T	58	sense
CYLD 1	CCT ATG TGG TAC TGA CCA GA	58	anti-sense
CYLD 2	GTG AAT GAA GCT AGG CCA TAC	58	anti-sense
F4	ACA ACA TGG ATC CCA GGT TG	60	sense
R4	CCG CTA ATA AAG GTC CTC TC	60	anti-sense
LacZ fwd	GCA TCG AGC TGG GTA ATA AGC GTT	63	sense
LacZ rev	GAC ACC AGA CCA ACT GGT AAT GG	63	anti-sense
Cre 3	TCC AAT TTA CTG ACC GTA CAC	56	sense
Cre 7	TCA GCT ACA CCA GAG ACG G	56	anti-sense
CD11c fwd	ACC CTG GTC ATC ATC CTG	65	sense
CD11c rev	CGG CAA ACG GAC AGA AGC	65	anti-sense
Vα3.2/2D2	CCC GGG CAA GGC TCA GCC ATG CTC CTG	58	sense
Jα18/2D2	GCG GCC GCA ATT CCC AGA GAC ATC CCT CC	58	anti-sense
HYtg fwd	ACA CAT GGA GGC TGC AGT CAC	58	sense
HYtg rev	CGT TTC TGC ACT GTT ATC ACC	58	anti-sense

Table 2: List of primers routinely used for genotyping. Sequences of oligonucleotides are shown from 5' to 3'. Direction is designated sense, if the primer orientation coincides with transcriptional orientation, and anti-sense if otherwise.

2.2.3 RNA isolation and Quantitative Real Time PCR

RNA from mouse T cells was prepared using the RNeasy Mini kit (QIAGEN, Hilden, Germany) according to the manufacturer's instructions. DNA was removed by DNAseI digestion (QIAGEN, Hilden, Germany). RNA was subsequently used for Quantitative Real Time PCR in an iCycler (Light Cycler 1.2, Roche) using the QuantiRect SYBR Green RT-PCR Kit (QIAGEN, Hilden, Germany) according to the manufacturer's protocol. Primers for Quantitative Real Time PCR were obtained from Qiagen as described on their homepage

https://www1.qiagen.com/GeneGlobe/Default.aspx. Expression was normalized to that of the house-keeping gene GAPDH.

2.2.4 Agarose Gel Electrophoresis and DNA Gel Extraction

Separation of DNA fragments by size was achieved by electrophoresis in agarose gels (0.8% - 2% (w/v); 1x TAE (Sambrook et al. 1989); 0.5 mg/ml ethidium bromide). DNA fragments were recovered from agarose gel slices with either the QIAEX II or the QIAquick Gel Extraction Kit (QIAGEN, Hilden, Germany) following the manufacturer's instructions.

2.2.5 Quantification of DNA and RNA

The concentration of nucleic acids was determined by measuring the absorption of the sample at 260 nm and 280 nm, respectively, in a spectrophotometer. An OD260 of 1 corresponds to approximately 50 µg/ml for double stranded DNA or 40 µg/ml for RNA and single stranded DNA. Purity of nucleic acids was estimated by the ratio OD260/OD280, with 1.8 and 2.0 optimal for DNA and RNA, respectively. Alternatively, the DNA was electrophoresed in an agarose gel, and the concentration was evaluated from the band intensity in comparison with a standard.

2.3 Cell biology

2.3.1 Preparation of single cell suspensions from lymphoid organs

Organs of interest were taken and placed into ice-cold PBA (PBS-BSA-azide (NaN_3); PBS, 0.1% (w/v) BSA, 0.01% NaN_3). Thymus, spleen and lymph nodes were passed through a nylon cell strainer (40µm, BD Falcon; Heidelberg, Germany) to obtain single cell suspensions. Bones were flushed with medium (DMEM, 10% (v/v) FCS, 2 mM L-glutamine) to extract bone marrow cells. Erythrocytes were lysed from spleen and thymus preparations in 140 mM NH_4Cl, 17 mM Tris-HCl pH 7.65 for 2 min at RT. To stop lysis, cells were washed with PBA, centrifugated (6 min, 1200 rpm, 4°C), resuspendet in the appropriate amount of PBA and kept on ice. For isolation of DCs, spleens were subjected to mild collagenase type II digestion (2mg/ml; Gibco) in the presence of DNase (2-4 Kuniz units/spleen of one mouse; Sigma, Steinheim, Germany) for 30 min at 37°C. Then, normal preparation of single cell suspensions by passing digested tissues through nylon cell strainers followed. Blood from the tail vein was collected in a tube with heparin (Liquemin, Roche, Mannheim, Germany) and then

layered on top of 7% (w/v) Ficoll 400 (Pharmacia, Freiburg, Germany). After 1400 g centrifugation at 23°C for 15 min, lymphocytes were recovered from the interphase of the gradients and resuspended in DMEM, 10% (v/v) FCS, 2 mM L-glutamine and kept on ice.

2.3.2 Cell counting

Viable cells were assessed using the trypan blue dye exclusion test and counted using a Neubauer chamber (Assistent, Sondheim, Germany). To this end, an aliquot of the cell suspension was diluted with physiological trypan blue solution (Gibco, Long Island, NY, USA). Dead cells are stained blue whereas live cells cannot take up the dye due to their intact membrane. After counting 16 single quadrants, the counted cell number (N) was multiplied by the dilution factor (V) and the chamberfactor (10^4) resulting in the number of live cells per ml (N x V x 10^4 = cell number/ml).

2.3.3 Flow cytometry

Single cell suspensions were prepared from all tested organs and the cell number was determined. Red blood cell lysis was performed as described above. Cells (10^6 per sample) were surface stained in 30 µl PBA with combinations of fluoresceine isothiocyanate (FITC), phycoerythrine (PE) and Cy-Chrome™ (Cyc), allophycocyanin (APC) and bio-conjugated monoclonal antibodies (mAbs) for 20 min on ice. Stainings with biotinylated mAbs were followed by a secondary staining step with Streptavidin (SA)-Cychrome™ (Pharmingen) or SA-PE-Cy7. After staining, the samples were washed and resuspended in PBA. Stained cells were analyzed on a FACScan or a FACSCalibur and data were evaluated using CellQuest software (Becton Dickinson, Heidelberg, Germany). Dead cells were labeled with Topro-3 and excluded from the analysis. Monoclonal antibodies, listed in Table 3, were either homemade (C. Uthoff-Hachenberg, B. Hampel, Institute for Genetics, Cologne, Germany) or purchased from Pharmingen (San Diego , USA) or Natutec (Frankfurt, Germany).

Specificity	Clone	Reference and Supplier
B220/CD45R	RA3-6B2	(Leo et al., 1987), Pharmingen
CD4	GK.1.5/4	(Dialynas et al., 1983), Pharmingen
CD8	53-6.7	(Ledbetter and Herzberg, 1979), Pharmingen
CD19	1D3	(Springer et al., 1979), Pharmingen
CD24/HSA	M1/69	(Springer et al., 1978), Pharmingen

CD25 (IL2Ra)	7D4	(Malek et al., 1983), Pharmingen
CD44	KM114	(Miyake et al., 1990), Pharmingen
CD45Rb	16A	(Bottomly et al., 1989), Pharmingen
CD62L (L-Selectin)	MEL-14	(Gallatin et al., 1983), Pharmingen
CD69	H1.2F3	(Yokoyama et al., 1988), Pharmingen
CD86/B7.2	GL1	(Inaba et al., 1994), Pharmingen
CD90.2/Thy1.2	CFO-1	(Opitz et al., 1982), Pharmingen
FoxP3	FJK-16s	Natutec
IL-17A	TC11-18H10	Pharmingen
IFN-γ	R4-6A2	Pharmingen
TCRβ	H57-597	(Kubo et al., 1989), Pharmingen
Vα3.2	RR3-16	(Utsunomiya et al., 1991), Pharmingen
Vβ11	RR3-15	(Behlke et al., 1986), Pharmingen

Table 3: List auf antibodies used for flow cytometry

Intracellular staining for Foxp3 were done using the Foxp3 Staining Set from Natutec (Frankfurt, Germany) according to the manufacturer's instructions. Intracellular stainings for IL-17 and IFNγ were performed using the Cytofix/Cytoperm kit from BD biosciences according to the manufacturer's instructions.

2.3.4 Magnetic cell sorting and FACS sorting

Specific cell populations were either sorted or depleted from a heterogenous cell suspension by magnetic cell sorting (MACS; Miltenyi Biotec, Bergisch Gladbach, Germany). Cell populations were labeled with antibody-coupled microbeads (10 µl beads, 90 µl PBA per 10^7 cells) and separated on LS, MS or LD MACS columns in a magnetic field (Milteneyi et al. 1990). For cell sorting, T cells were purified by MACS and then stained with antibodies against various cell surface markers. T cells of individual T cell subsets were then sorted using a dual laser FACStar (Becton Dickinson). The purity of isolated populations was subsequently tested by FACS analysis: MACS-isolated T cells were normally >90% pure and sorted T cell subpopulations were 95% pure. FACS sorting was performed with the help of Abdo Konur (Department of Medicine III, Mainz, Germany).

2.3.5 CFSE labeling

CFSE (carboxyfluorescein diacetate succinimidyl ester) is a membrane-permeable fluorescent dye, which is non-fluorescent in its native form, but is rendered highly fluorescent after diffusion into the cell. The dye is then unable to diffuse out of the cell and upon one cycle of cell division the stain is halved in each of the daughter cells, which can be detected by flow cytometry. For proliferation analysis freshly isolated $CD4^+$ and $CD8^+$ T cells were labeled with CFSE (0.5mM; Molecular probes, Eugene, Oregon, USA). After washing the cells twice in 10 ml PBS, pH7.4, they were incubated with 0.5 mM CFSE in 1 ml PBS per 10^7 cells at RT for 8 min (Lyons and Parish, 1994). To stop the staining reaction 8 ml of RPMI 1640 (Gibco, Long Island, NY, USA) plus 10% FCS were added. Then the cells were washed twice in 10 ml RPMI, and resuspended in the appropriate volume of PBS or medium.

2.3.6 Culture of *ex vivo* Splenocytes and Lymphocytes

Spleens and LNs were aseptically removed from mice and then pressed through a sterile sieve. Erythrocytes were lysed for 2 min by NH_4Cl (140 mM NH_4Cl, 17 mM Tris-Hcl pH 7. 65). Splenocytes and lymphocytes were kept in RPMI 1640 supplemented with 10 % (v/v) FCS (decomplemented), 1 mM sodium pyruvate, 2 mM L-glutamine, 1 x non-essential amino acids, 0.1 mM 2-β-mercaptoethanol and 10 mM HEPES (Gibco), supplemented with various activation compounds (e.g. anti-CD3, anti-CD3/CD28, ConA, MOGp35-55) in the indicated concentration for no longer than four days at 37°C.

2.3.7 T cell activation

T cells and APCs were - if necessary – purified using MACS (see section 2.3.4). For proliferation studies T cells were labeled with CFSE (see section 2.3.5) and plated at 0.2-0.5 x 10^6 cells per well in round or flat bottom 96-well plates, respectively. APCs were added in the appropriate concentration (B cells: 0.1 x 10^6, DCs: 0.1 x 10^5). Cells were incubated in RPMI 1640 medium plus supplements (see above), untreated or treated with anti-CD3 (1 µg/ml), anti-CD3 (1 µg/ml) / anti-CD28 (6 ng/ml), ConA (10 µg/ml) or with different concentrations of MOGp35-55. Supernatants were collected for cytokine analysis and labeled cells were analyzed by flow cytometry after various time points.

2.3.8 Flow Cytomix

Multiple cytokine and chemokine levels were detected using FlowCytomixTM technology (BenderMedsystems, Vienna) according to the manufacturer's instructions.

2.3.9 Treg Suppression Assay *in vitro*

Culture medium was IMDM (Gibco, Long Island, NY, USA) supplemented with 5 % (v/v) FCS (decomplemented), 1 mM sodium pyruvate, 2 mM L-glutamine, 1 x non-essential amino acids, 0.1 mM 2-b-mercaptoethanol and 10 mM HEPES (Gibco). 2 x 10^4 conventional $CD4^+CD25^-$ T cells were stimulated using 96-well round bottom microplates in a total volume of 0.2 ml in the presence or absence of different numbers of freshly isolated $CD4^+CD25^+$ T cells. Mitomycin C-treated (60µg/ml/10^7 cells for 30 min) A20 B tumour cells (2 x 10^3/well) as accessory cells and anti-CD3 mAbs were used as stimulus. After 96 h, [^{3}H]thymidine was added to the cultures (0.5 µCi/well) and [^{3}H]thymidine uptake was assessed by β scintillation counting after additional 18 h.

2.4 Histological Analysis and Immunohistochemestry

Shock frozen tissues were sectioned in 5-8 µm slices, fixed in ice cold acetone for 10 min and air dried for 10 min. Using a Pap pen, the tissue was outlined on the glass slide, placed in a wet chamber and TBS was added for 5 min at RT. Slides were then incubated with quenching buffer containing 0.3% (v/v) H_2O_2 for 30 min and washed once with TBS. The sections were incubated with avidin solution and biotin solution for 15 min each and subsequently washed three times with TBS. The sections were then incubated with the primary antibodies for 60 min. After incubation, the sections were washed 3 times with TBS and incubated with secondary reagents for 60 min. Sections were washed three times with TBS. The slides were incubated with freshly prepared POX solution for 10 min and subsequently washed with TBS. The AP was developed using the Alkaline Phosphatase Substrate Kit III, washed three times with TBS and air dried before mounting with glycerol or crystal mount.

2.5 Biochemistry

2.5.1 Protein extract preparations

Protein lysates from mouse organs were prepared either freshly or from frozen tissue. Tissue was diced into small pieces using a clean razor blade. Then, RIPA buffer (1xPBS, 1% (v/v) NP-40) was added at 3 ml/g tissue supplemented with various protease inhibitors. Samples were centrifuged at 13000 rpm for 5 min to separate supernatants from debris. Supernatants were transferred to fresh tubes and protein concentrations were determined in a photometer using Bradford assay. Protein extracts were diluted with RIPA buffer to 15 mg/ml before adding running buffer (3 x SDS sample buffer, NEB, Schwalbach, Germany) and DTT (30 x DTT, NEB, Schwalbach, Germany) to 200 µg of protein extracts. To separate the cytoplasmic protein fractions from the nuclear extracts, cells were resuspended at 10^6/15 µl in hypotonic solution (10 mM Hepes [pH 7.9], 10 mM KCl, 2 mM $MgCl_2$, 0.5 mM DTT, 0.1 mM EDTA, supplemented with various protein inhibitors) and incubated at 4 °C for 10 min. Then NP-40 was added to 1% (v/v) and the cells were centrifuged at 13000 rpm for 1 min. The supernatant containing the cytoplasmic fraction was recovered from the nuclear pellet and the nuclear pellet was resuspended in 10^6/10 µl cells of high salt buffer (20 mM Hepes [pH 7.9], 420 mM NaCl, 1.5 mM $MgCl_2$, 0.5 mM DTT, 0.2 mM EDTA and 10% (v/v) glycerol) and incubated on ice for 30 min. Nuclear extracts were recovered after centrifugation at 10000 rpm for 10 min at 4 °C and stored at – 80 °C.

2.5.2 Western Blot

Protein extracts were electrophoresed by SDS-PAGE (8-15% (v/v)) (Laemmli, 1970) and transferred to Immobilon-PVDF membranes (Millipore, Bedford, USA). The membranes were blocked with 5% (w/v) NF-milk/PBS or 5% (w/v) BSA/PBS for 1 h and probed using primary antibodies. Membranes were then incubated with goat anti-rabbit IgG-horseradish peroxidase (HRP) conjugates (Vector, Burlingame, USA) as secondary antibody and developed using the ECL or ECL+ kit.

Specificity	Clone/Supplier
Tubulin	2148, Cell Signaling
IκBα	C21, Santa Cruz
CYLD	Homemade
TRAF3	M-20, Santa Cruz
RelB	C-19, Santa Cruz
p100	4882, Cell Signaling
c-Rel (p65)	C22B4, Cell Signaling
Zap70	2701, Cell Signaling
p-Zap70	99F2, Cell Signaling
Lck	2752, Cell Signaling
p-Lck	2751, Cell Signaling
PLC-γ 1	H-3, Santa Cruz
p-PLC-γ 1	D9H10, Cell Signaling

Table 4: List of antibodies used for Western Blotting

2.6 Mouse experiments

Tail bleeding as well as the general handling of mice was performed according to Hogan (Hogan, 1987) and Silver (Silver 1995).

2.6.1 Mice

C57BL/6 mice were obtained from Charles River or Jackson Laboratories, C57BL/6 Thy1.1 mice were taken from breeding in our animal facility. $CYLD^{FL}$ mice (Hövelmeyer et al. 2007) were crossed to CD4-Cre (Wolfer et al. 2001) and CD11c-Cre mice (Caton et al. 2007) to specifically delete FL-CYLD in T cells of CYLD CD4-Cre mice and in DCs of CYLD CD11c-Cre mice. $CYLD^{FL}$ mice were used as control mice. $CYLD^{ex7/8}$ mice (Hövelmeyer et

al. 2007) were crossed to 2D2 (Bettelli et al. 2003) and HY TCR (Uematsu et al. 1988) transgenic mouse strains. $CYLD^{ex7/8}$ mice were further crossed to $RAG1^{-/-}$ deficient and DEREG mice (Lahl et al. 2007). All mice were generated on the C57BL/6 genetic background or bred for at least 10 generations to this background and housed in specific pathogen-free conditions. All animal experiments were in accordance with the guidelines of the Central Animal Facility Institution of the University of Mainz (ZVTE, University of Mainz).

2.6.2 Adoptive Cell Transfer

After enrichment, cell suspensions were washed with PBS, counted, and diluted to the desired concentration. Cells were injected in PBS intravenously (i.v.) into the tail vein of recipient mice (200 µl/mouse). For proliferation studies of T cells, cells were CFSE-labeled before transfer (see section 2.3.5), recipient mice were sacrificed 5 days after cell transfer, and cells were analyzed by FACS. To better track transferred T cells by FACS, 2D2tg $Thy1.2^{+}$ cells were transferred to $Thy1.1^{+}$ recipients.

2.6.3 Induction and assessment of EAE

MOGp35-55 peptide (amino acid sequence: MEVGWYRSPFSRVVHLYRNGK) was obtained from Research Genetics (Huntsville, Alabama, USA). Active EAE was induced by immunization with 50 µg of MOGp35-55 emulsified in CFA (Difco Laboratories, Detroit, Michigan, USA) supplemented with 8 mg/ml of heat-inactivated *Myobacterium tuberculosis* H37RA (Difco Laboratories, Detroit, Michigan, USA). The emulsion was administered as a 100 µl subcutaneous (s.c.) injection into the tail base. Mice also received 200 ng of Pertussis toxin (Sigma Aldrich, Steinheim, Germany) i.p. on the day of immunization and two days later. Clinical assessment of EAE was performed daily according to the following criteria: 0, no disease; 1, decreased tail tone; 2, abnormal gait (ataxia) and/or impaired righting reflex (hind limb weakness or partial paralysis); 3, partial hind limb paralysis; 4, complete hind limb paralysis; 5, hind limb paralysis with partial fore limb paralysis; 6, moribund or dead.

2.6.4 Adoptive Transfer Colitis

5×10^5 naive $CD4^{+}$ T cells were purified using MACS (see section 2.3.4) and injected intraperitoneally (i.p.) in 6- to 8-week old $RAG1^{-/-}$ mice. After the cell transfer mice were weekly weight and scored by mini-endoscopy.

2.6.5 Treg suppression assay *in vivo*

5 x 10^5 MACS purified naive $CD4^+$ $CD25^-$ T cells from WT mice were injected i.p. in 6- to 8-week old $RAG1^{-/-}$ deficient mice alone or with the same number of WT or $CYLD^{ex7/8}$ MACS purified $CD4^+$ $CD25^+$ Treg cells. After the cell transfer $RAG1^{-/-}$ recipients were weekly weight and monitored by mini-endoscopy.

2.6.6 *In vivo* high resolution mini-endoscopy analysis of the colon

For monitoring of colitis activity, a high resolution video endoscopic system (Karl Storz) for mice was used. To determine colitis activity in $RAG1^{-/-}$ $CYLD^{ex7/8}$ and control mice before and after cell transfer, mice were anesthetized by injecting a mixture of ketamine (Ketavest 100mg/ml $^{-1}$, Pfizer) and xylazine (Rompun 2%, Bayer Healthcare) i.p. and monitored by mini-endoscopy at indicated timepoints. Endoscopic scoring of five parameters (translucency, granularity, fibrin, vascularity and stool) was performed.

2.6.7 Statistics

Values are typically as mean ± SEM (standard error of mean). Statistical significance was assessed using 2-tailed Student's *t*-test. P-values < 0.05 were regarded significant, displayed by '*' in the figures (** = p-values < 0.005; *** = p-values < 0.0005).

3 Results

3.1 Overexpression of short CYLD leads to a strong reduction of the T cell compartment in CYLD$^{ex7/8}$ mice

The tumour suppressor gene *cyld* was shown to be required for T cell development by regulating TCR-proximal signaling in thymocytes. Further, it exhibits an essential role in regulating T cell activation and homeostasis. Previously it was shown that CYLD mRNA can be expressed as two splice variants in mice. The full-length transcript codes for a protein of 106 kDa, the shorter transcript for a protein of 86 kDa. The shorter CYLD lacks exons 7 and 8 and is the result of alternative splicing from exon 6 to 9. In this thesis, the role of the naturally occurring short splice variant of CYLD (sCYLD) in the context of T cells was investigated using CYLD$^{ex7/8}$ mice, a mouse strain that expresses solely and excessively sCYLD while lacking the full length CYLD (FL-CYLD).

To examine whether deletion of FL-CYLD, while retaining the sCYLD splice form influences T cell development, we analyzed thymi of CYLD$^{ex7/8}$, CYLD^{ko} and wild type (WT) mice. CYLD mutant mice showed significant reductions in cell numbers in the thymus compared to controls (Fig. 7).

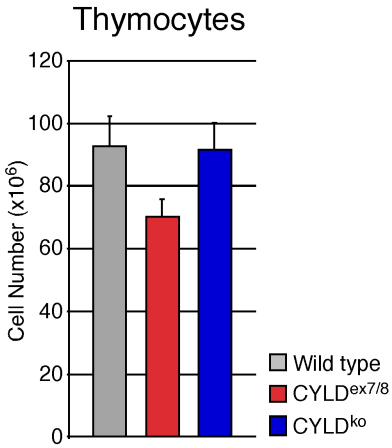

Figure 7: Decreased thymocytes in CYLD$^{ex7/8}$ mice compared to controls. Bar charts showing absolute number of thymocytes from CYLD$^{ex7/8}$, CYLD^{ko} and WT mice. Values represent mean ± SEM.

To determine in which step of thymocyte development *cyld* plays a crucial role, we next analyzed early T cell development using CD25 and CD44 cell surface markers. However, we did not observe any changes in this early developmental step (Fig. 8A, upper panel). Next, we stained thymocytes with CD4 and CD8 surface markers and detected a significant reduction of single positive (SP) CD4 and CD8 thymocytes in CYLD$^{ex7/8}$ thymi as compared to WT and

CYLD^{ko} thymocytes (Fig. 8B). But neither deletion of FL-CYLD nor of both CYLD isoforms changed the ratio between early thymocyte populations significantly (Fig. 8A, lower panel).

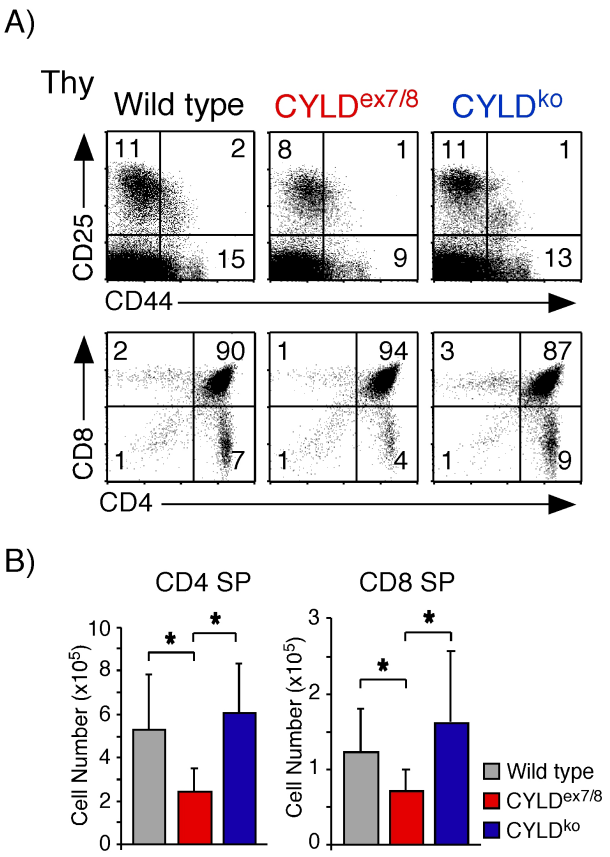

Figure 8: Strong reduction of CD4 and CD8 SP thymocytes in CYLD$^{ex7/8}$ mice. FACS analysis of thymocytes from 8-10-week-old CYLD$^{ex7/8}$, CYLD^{ko} and WT control mice. (A, upper panel) DN thymocytes were analyzed for CD25 and CD44 surface expression. (A, lower panel) Thymocytes pregated on lymphocytes were analyzed for CD4 and CD8 expression. (B, left) Bar charts indicate total cell number of CD4 SP and (B, right) CD8 SP thymocytes from the indicated genotypes. Values represent mean ± SEM.

To understand whether deletion of FL-CYLD influences peripheral T cell homoeostasis, we analyzed CD4$^+$ and CD8$^+$ T cell subpopulations in the peripheral immune organs. Strikingly, CD8$^+$ and CD4$^+$ T cells were drastically reduced in percentage (Fig. 9A, left) and total lymphocyte number (Fig. 9A, right) in CYLD$^{ex7/8}$ spleens compared to splenic cells of CYLD^{ko} and WT control mice, correlating to the reduction of their progenitor cells in the thymus. Further, the ratio of splenic CD4$^+$ to CD8$^+$ among T cells (gated on CD90.2$^+$) is changed in CYLD$^{ex7/8}$ mice compared to WT mice, tilting much more towards the CD4$^+$ compartment (Fig. 9B). Importantly, we did not detect any changes in total numbers or ratio of the T cell population in the CYLD^{ko} mice. Next, we analyzed the numbers and ratio of T cells also in the lymph nodes (LNs). As can be seen in Fig. 9C and D, also in the LNs the ratio of CD4:CD8 T cells changed compared to the WT mice, although the total number of CD4$^+$ or CD8$^+$ T cells was constant compared to WT LNs. We conclude that the loss of FL-CYLD, accompanied with the overexpression of sCYLD, results in skewing the CD4:CD8 ratio towards the CD4$^+$ T cells in the thymus and in peripheral organs.

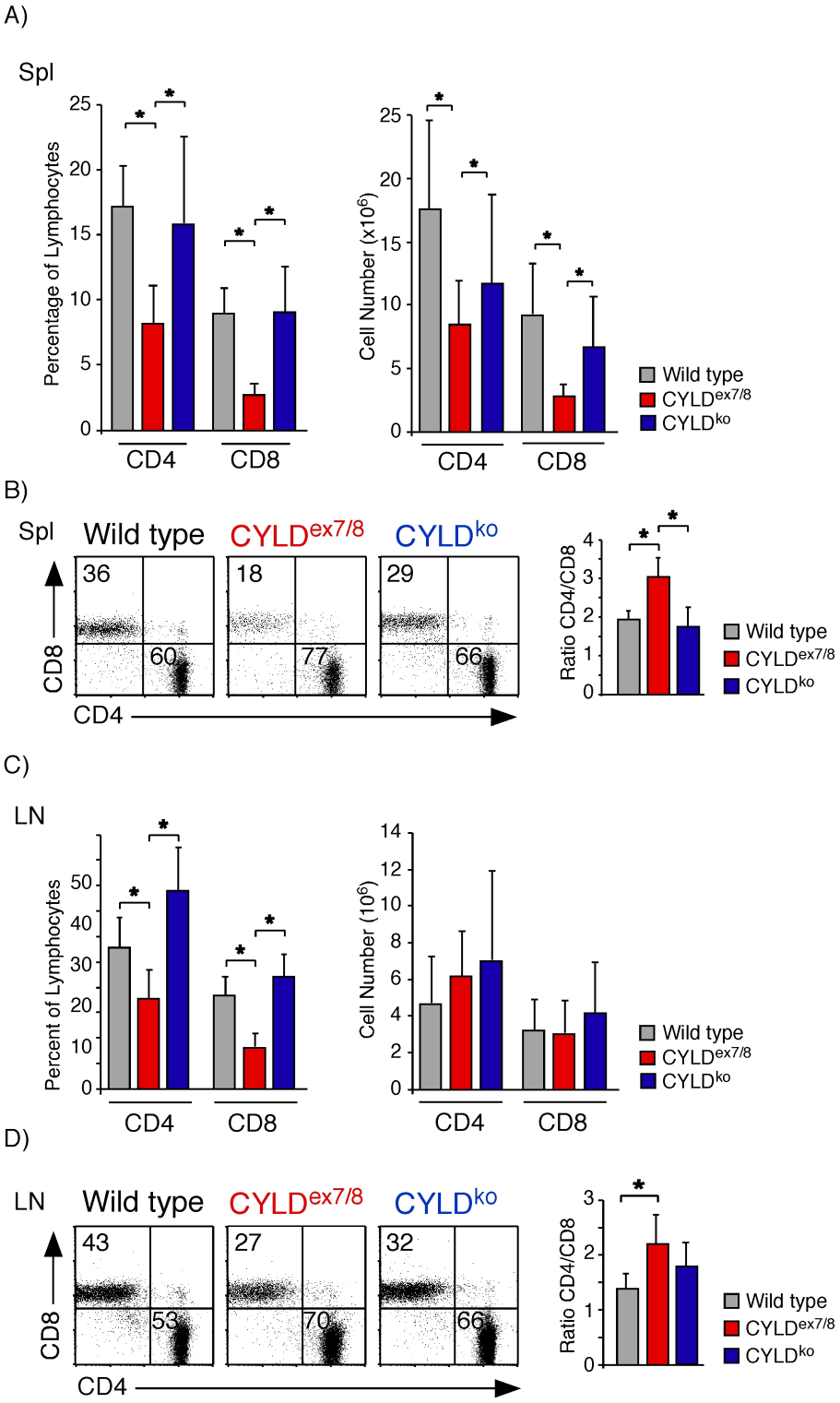

Figure 9: Decreased CD4$^+$ and CD8$^+$ peripheral T cells in CYLD$^{ex7/8}$ mice. (A, left) Bar charts display the percentage and (A, right) the total cell number of splenic CD4$^+$ and CD8$^+$ T cells. (B, left) FACS analysis of splenic cells gated on lymphocytes and TCRβ. Cell surface markers are shown as coordinates. (B, right) Bar charts show the ratio of splenic CD4/CD8 T cells from the indicated genotypes. Values represent mean ± SEM. (C, left) Bar charts show the percentage and (C, right) the total cell number of lymphoid CD4$^+$ and CD8$^+$ T cells of the indicated genotypes. Values represent mean ± SEM. (D, left) FACS analysis of splenic cells. Cells were gated on lymphocytes and TCRβ and analyzed for CD4 and CD8 surface expression. (D, right) Bar charts show the ratio of lymphoid CD4/CD8 T cells from the indicated genotypes. Values represent mean ± SEM.

Since overexpression of sCYLD in the absence of FL-CYLD affected the T cell development in CYLD$^{ex7/8}$ mice, we further investigated the expression levels of full length and short CYLD RNA in WT thymocytes as well as sCYLD in CYLD$^{ex7/8}$ thymocytes. Interestingly, full length CYLD was highly upregulated in DP as well as CD4 SP WT thymocytes (Fig. 10A). A similar picture could be seen for the RNA expression of the sCYLD splice variant in WT mice. Investigating the expression of short CYLD in CYLD mutant thymocytes, we detected increased levels in DN as well as CD4 SP thymocytes (Fig. 10B).

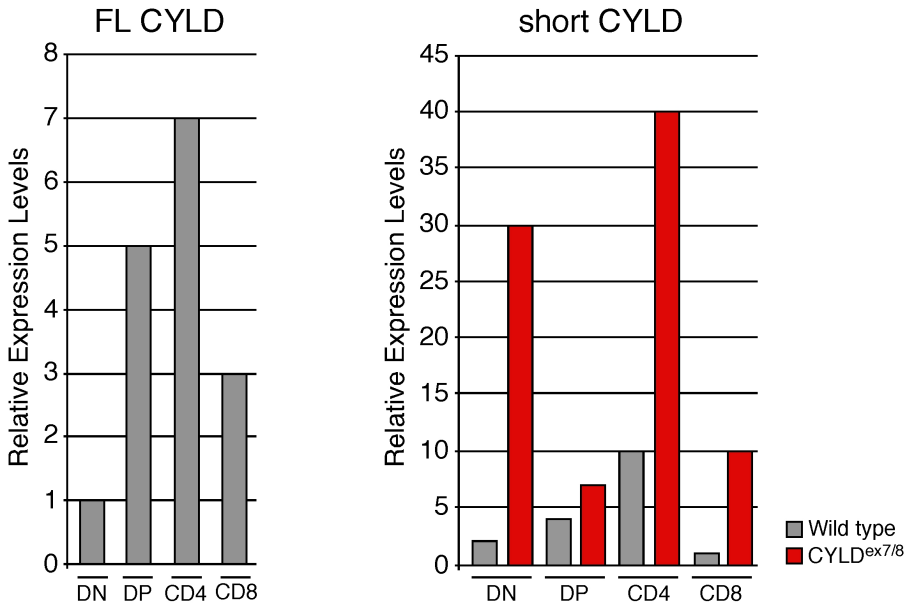

Figure 10: Relative expression of FL-CYLD and short CYLD in thymocytes. Quantitative Real Time PCR of sorted DN, DP, CD4 SP and CD8 SP thymocytes of the indicated genotypes. Left, relative expression of FL-CYLD. Right, relative expression of sCYLD. Gene expression levels were normalized to HPRT from each mRNA preparation.

3.2 Impaired TCR signaling in CYLD$^{ex7/8}$ thymocytes

To understand the molecular mechanisms mediating the abnormal T cell responses in CYLD$^{ex7/8}$ mice, we examined TCR signaling in thymocytes. It was previously shown, that CYLD positively regulates Lck function and TCR-proximal signaling in thymocytes (Reiley et al. 2006). First, we analyzed if overexpression of sCYLD has an effect on Lck activation. The activation of Lck can be detected based on its phosphorylation at a conserved tyrosine residue located in the kinase domain (Tyr 394). Activation of thymocytes by crosslinking of CD3 and CD4 displayed similar phosphorylation of Lck in WT and CYLD$^{ex7/8}$ thymocytes (Fig. 11). However, we found less phosphorylated Lck in CYLD^{ko} thymocytes, contrary to the CYLD deficient mice previously published (Reiley et al. 2006) where no difference in Lck phosphorylation between WT and CYLD deficient thymocytes could be detected.

Moreover, immunoblot analysis with antibody specific for Zap70 showed a reduced phosphorylation of this protein in CYLD$^{ex7/8}$ thymocytes compared to WT. As expected, for CYLD^{ko} thymocytes phosphorylation of Zap70 could not be detected. Furthermore, the activation of phospholipase Cγ-1 (PLCγ-1), which is downstream of Zap70 signaling, can be detected by its phosphorylation on Tyr 783. Paradoxly, we observed more p-PLCγ-1 in stimulated CYLD$^{ex7/8}$ as in WT thymocytes. For CYLD^{ko} thymocytes, we detected less activated p-PLCγ-1 corresponding to the missing Zap70 phoshorylation. These data show, that overexpression of sCYLD has an effect on TCR signaling by partially inhibiting the activation of Zap70.

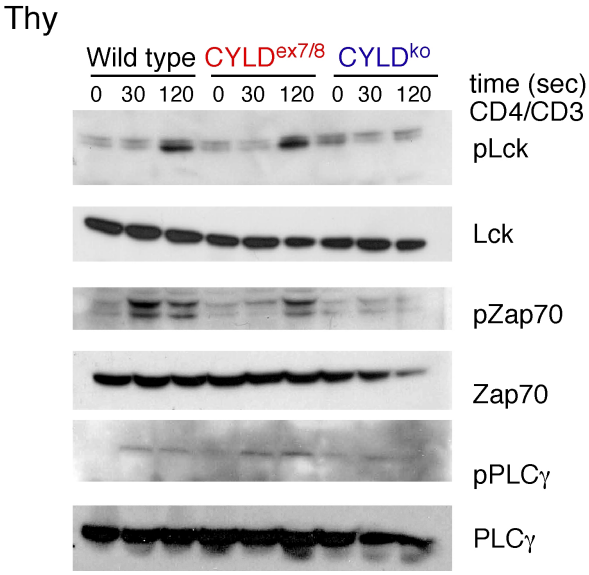

Figure 11: TCR signaling in CYLD$^{ex7/8}$ thymocytes. Total thymocytes from WT, CYLD$^{ex7/8}$ and CYLD^{ko} mice were left untreated or were stimulated with anti-CD3 plus anti-CD4 (timepoints indicated over lanes). Cell lysates were analyzed by immunoblot for Lck, Zap70 and PLCγ−1 phosphorylation.

3.3 Impaired thymic selection in CYLD$^{ex7/8}$ thymocytes on HY TCR transgenic background

The reduced numbers of CD4$^+$ and CD8$^+$ T cells in the thymus and periphery of CYLD$^{ex7/8}$ mice could be a consequence of alterations in the thymic selection process. Thus, we analyzed positive and negative selection of thymocytes by crossing the CYLD$^{ex7/8}$ mice onto the HY TCR transgenic background. The transgenic HY TCR recognizes the Y-chromosomal peptide smcy (Markiewitz et al. 1998) in the context of H-2D^b (Uematsu et al. 1998). In male mice, T cells expressing the male antigen-reactive HY TCR are deleted in the DP stage of T cell development whereas in female mice most of the transgenic thymocytes are positively selected into the CD8 compartment. Interestingly, in male HYtg CYLD$^{ex7/8}$ mice we found an increased population of DP as well as CD8 SP thymocytes (Fig. 12A, upper panel) showing that

the negative selection of HY TCR^+ DP thymocytes was impaired. Additionally, also HYtg $CYLD^{ko}$ mice exhibited a profound population of DP thymocytes (Fig. 12A, upper panel). Next, we examined positive selection of T cell development by analyzing female HYtg $CYLD^{ex7/8}$ mice. Here, we observed a profound effect on positive selection indicated by a 3-fold increased population of DP thymocytes in $CYLD^{ex7/8}$ and $CYLD^{ko}$ mice compared to controls (Fig. 12A, lower panel). Moreover, we analyzed the expression level of the HY-specific TCR, using the clonotypic antibody T3.70. When levels of HY TCR were measured in the different developmental stages of T cell development, we found that overexpression of sCYLD led to a much higher proportion of $T3.70^+$ T cells compared to HYtg control mice (Fig. 12B). This difference is especially apparent in the male mice (Fig. 12B, upper panel). These findings indicate that overexpression of sCYLD has an effect on TCR expression that leads to partial rescue of negative selection and possibly to the generation of self-reactive T cells.

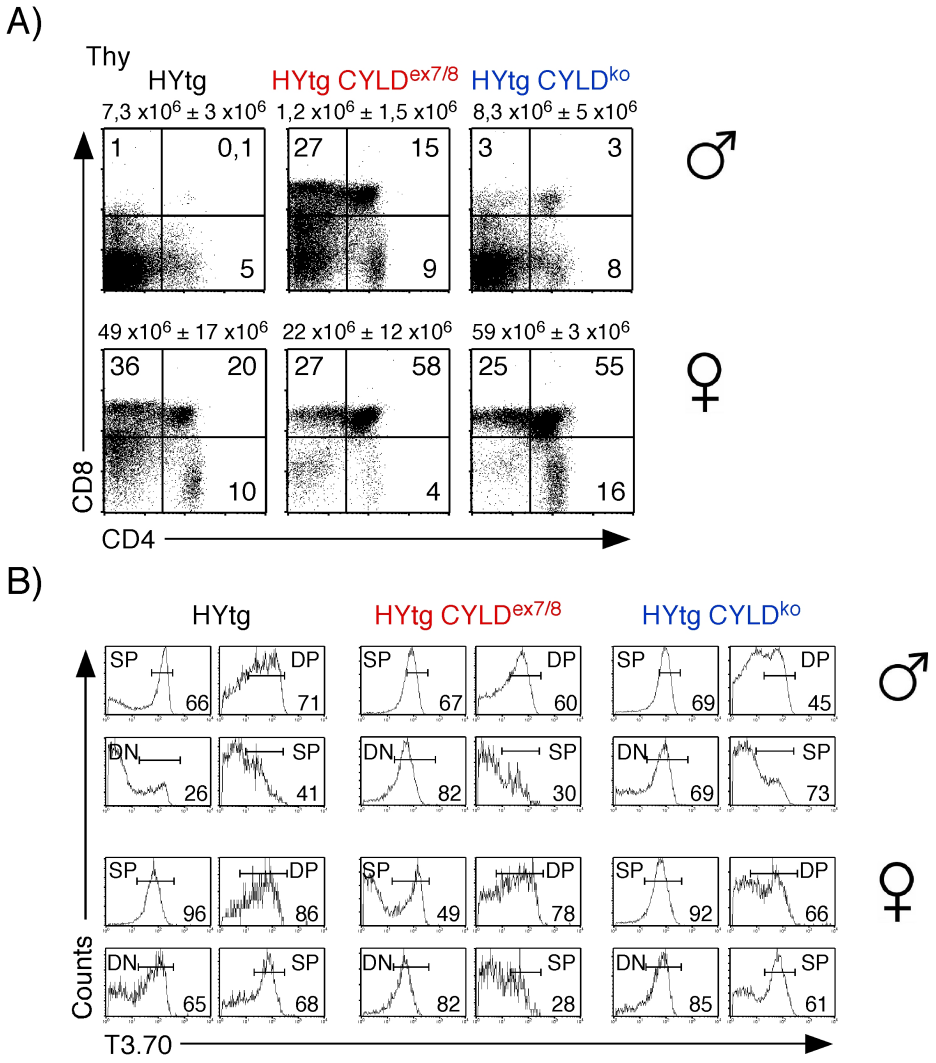

Figure 12: Positive and negative selection of thymocytes in HYtg CYLD$^{ex7/8}$ mice. (A) FACS analysis of total thymocytes from male (upper panel) and female (lower panel) mice of the indicated genotypes. Cells were analyzed for the expression of CD4 and CD8 surface markers. (B) Histogram plots show the percentage of T3.70 expression in the different developmental stages of T cell development (DN=double negative, DP=double positive, SP=single positive).

Further, we analyzed CD4$^+$ and CD8$^+$ T cells in the periphery of HYtg CYLD$^{ex7/8}$ mice compared to controls. In female mice overexpressing sCYLD, we observed a strong reduction of both CD4$^+$ and CD8$^+$ T cells in LN as well as spleens, whereas the complete CYLD knockout behaved like control HYtg mice (Fig. 13, upper panel). Investigating male mice on HYtg background, we found less CD8$^+$ T cells in LNs and spleens of CYLD$^{ex7/8}$ mice (Fig. 13, lower panel). Taken together, these results indicate a pivotal role for CYLD in both the positive and negative selection process in the thymus.

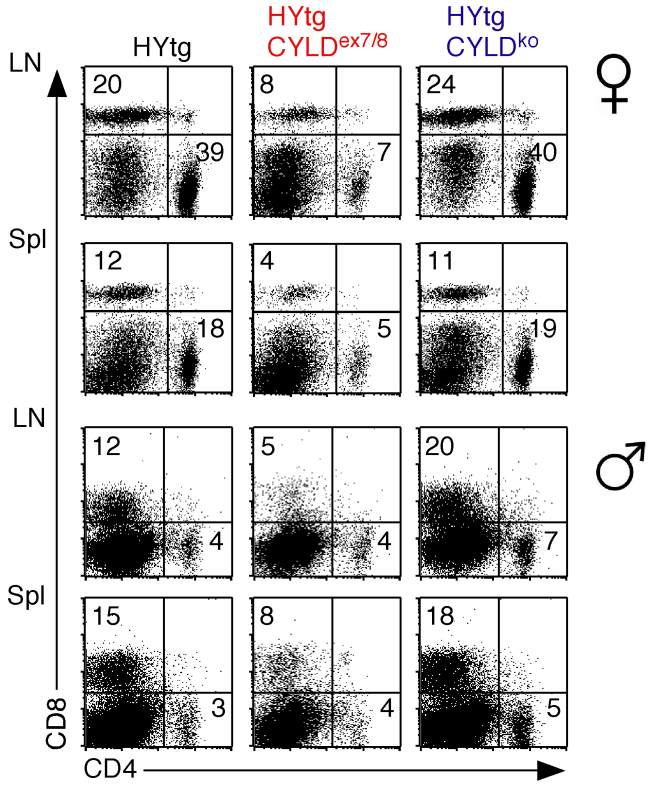

Figure 13: CD4 and CD8 peripheral T cells in HYtg CYLD$^{ex7/8}$ mice. FACS analysis of total cells from LN and Spl of the HYtg, HYtg CYLD$^{ex7/8}$ and HYtg CYLD^{ko} mice. Dot plots show the percentage of CD4 and CD8 surface expression.

3.4 Deminished development of mTECs in CYLD$^{ex7/8}$ thymi

The thymus is the primary lymphoid organ responsible for the development, selection and output of a diverse and self-tolerant T lymphocyte pool into the periphery. Since we detected a strong defect in positive and negative selection of thymocytes in CYLD$^{ex7/8}$ mice, we examined the structure of the thymus by histology. Of note, by keratin-5 and H&E staining we observed a distortion of the cortico-medullary boundary of CYLD$^{ex7/8}$ thymi whereas the thymic structure of CYLD^{ko} thymi was unchanged (Fig. 14, first and second lane). Furthermore, the medullary compartment was decreased in size in CYLD$^{ex7/8}$ thymi. Importantly, by staining for PECAM-1, we detected an enlargement of blood vessels in the thymi of CYLD$^{ex7/8}$ mice when compared to WT and CYLD^{ko} mice (Fig. 14, third lane).

During T cell development, thymocytes undergo negative and positive selection processes by interacting with the microenvironment of the thymus generated by thymic epithelial cells (TECs). Cortical TECs (cTECs) build up the cortical compartment of the thymus and are essential for selecting thymocytes that are capable of recognizing self-major histocompatibility complex. The medullary compartment is built up by medullary TECs (mTECs) playing an important role in self-tolerance by eliminating self-reactive T cells. Because the structure and size of the medullary compartment from CYLD$^{ex7/8}$ thymi was altered compared to controls,

we examined the expression of UEA-1, a marker for mature mTECs. Interestingly, the number of mature mTECs was decreased in CYLD$^{ex7/8}$ thymi compared to controls (Fig. 14, fourth lane). Additionally, we stained for Cld 3/4, which is a marker for Aire expressing mTECs. Aire is an important transcription factor expressed by mTECs, which promotes the ectopic expression of peripheral tissue-specific antigens (TSAs). As shown in Figure 14 (last lane), we detected a reduction of Cld 3/4 positive mTECs in the medullary compartment of CYLD$^{ex7/8}$ mice, whereas there was no difference between CYLD^{ko} and WT thymi.

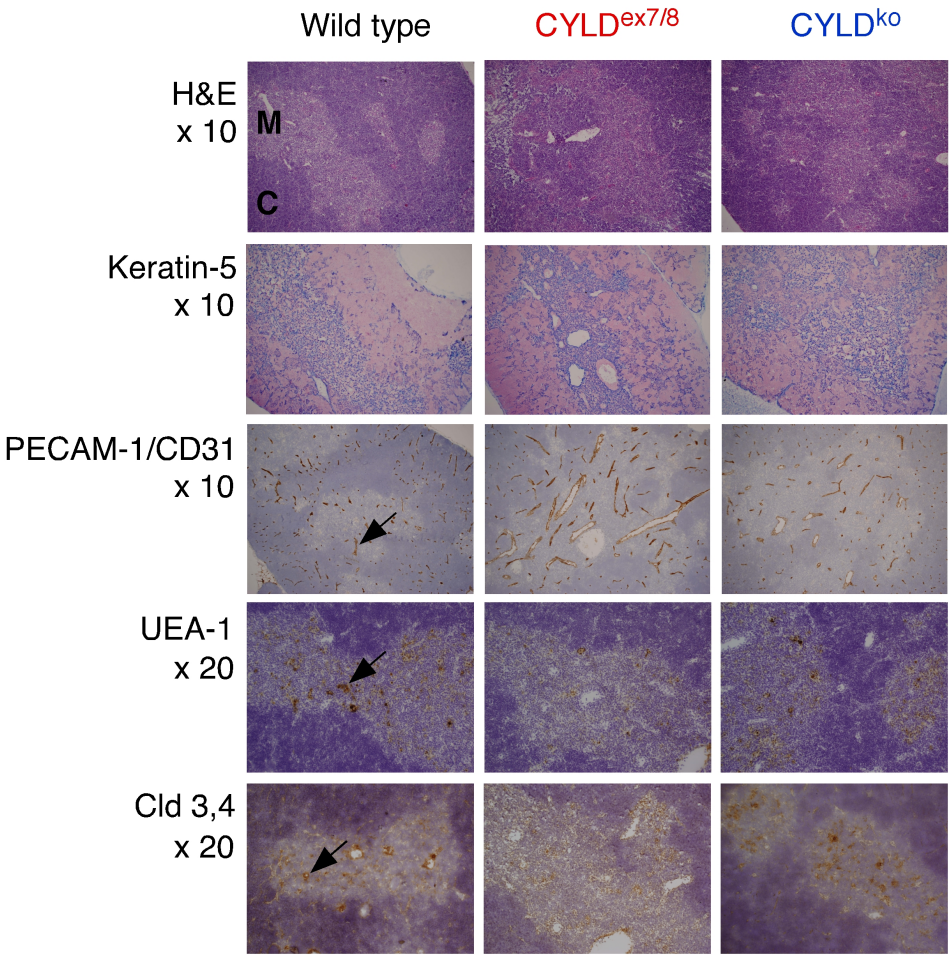

Figure 14: Histological analysis of CYLD$^{ex7/8}$ thymi. Cryosections of thymi from 4- to 6-week-old WT, CYLD$^{ex7/8}$ and CYLD^{ko} mice were stained with hematoxylin and eosin (H&E), Keratin-5, PECAM-1/CD31, UEA-1 and Cld 3/4. Magnifications as indicated were used. Arrows indicate positive cells.

In addition to the histological analysis of CYLD$^{ex7/8}$ thymi, quantification of total cell numbers revealed a strong decrease of CYLD$^{ex7/8}$ mTECs as well, whereas the numbers of total cTECs was similar to WT (Fig. 15A). Recent studies reported, that the activation of the non-canonical NF-κB pathway is known to be crucial for the development of fully functional mTECs (Weih et al. 1995). Further, it was shown that RelB, a member of the noncanonical

NF-κB pathway, plays a critical role in the regulation of Aire expression and the survival of Aire expressing cells in the thymus. Therefore, we investigated the expression of RelB in mTECs by RT PCR. Importantly, we detected a reduction in the expression of RelB in CYLD$^{ex7/8}$ mTECs compared to WT mTECs (Fig. 15B). Hence, these data implicate that short CYLD plays a major role in the development of mTECs by regulating RelB expression.

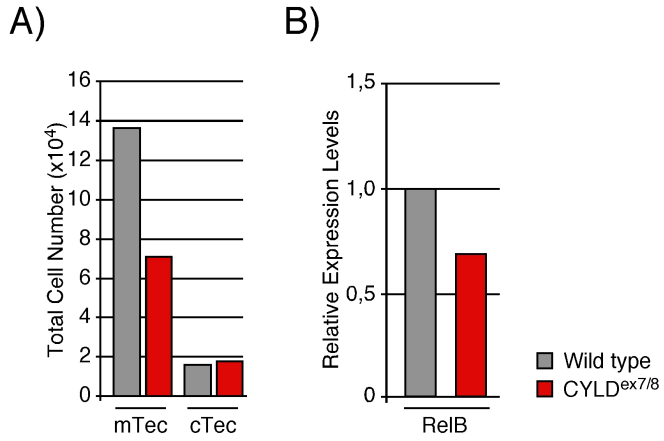

Figure 15: Decreased numbers of mTECs in CYLD$^{ex7/8}$ thymi. (A) Quantification of total numbers of mTECs and cTECs from WT and CYLD$^{ex7/8}$ thymi (n=3). (B) Quantitative Real Time PCR of sorted mTECs of the indicated genotypes. Bar charts display the relative expression of RelB. Gene expression levels were normalized to HPRT from each mRNA preparation and normalized to WT (n=4).

3.5 Hyperresponsiveness of CYLD$^{ex7/8}$ T cells

Next, we were interested if short CYLD is important in regulating peripheral T cell activation. Therefore, we analyzed the role of sCYLD in T cell activation *in vitro* as well as *in vivo*. First, for the *in vitro* proliferation assay, we cultured CFSE labeled T cells with agonistic anti-CD3 antibodies or Concanavalin A (ConA) and examined the responsiveness of CYLD$^{ex7/8}$ T cells on day 4 by FACS cytometry (Fig. 16A). Surprisingly, CYLD$^{ex7/8}$ T cells did not proliferate properly in response to an anti-CD3 or ConA stimulus in contrast to the controls. In addition, most of the CYLD$^{ex7/8}$ CD4^{+} as well as CD8^{+} T cells could not be detected anymore. This could be due to hyporesponsiveness of the T cells or activation induced cell death (AICD).

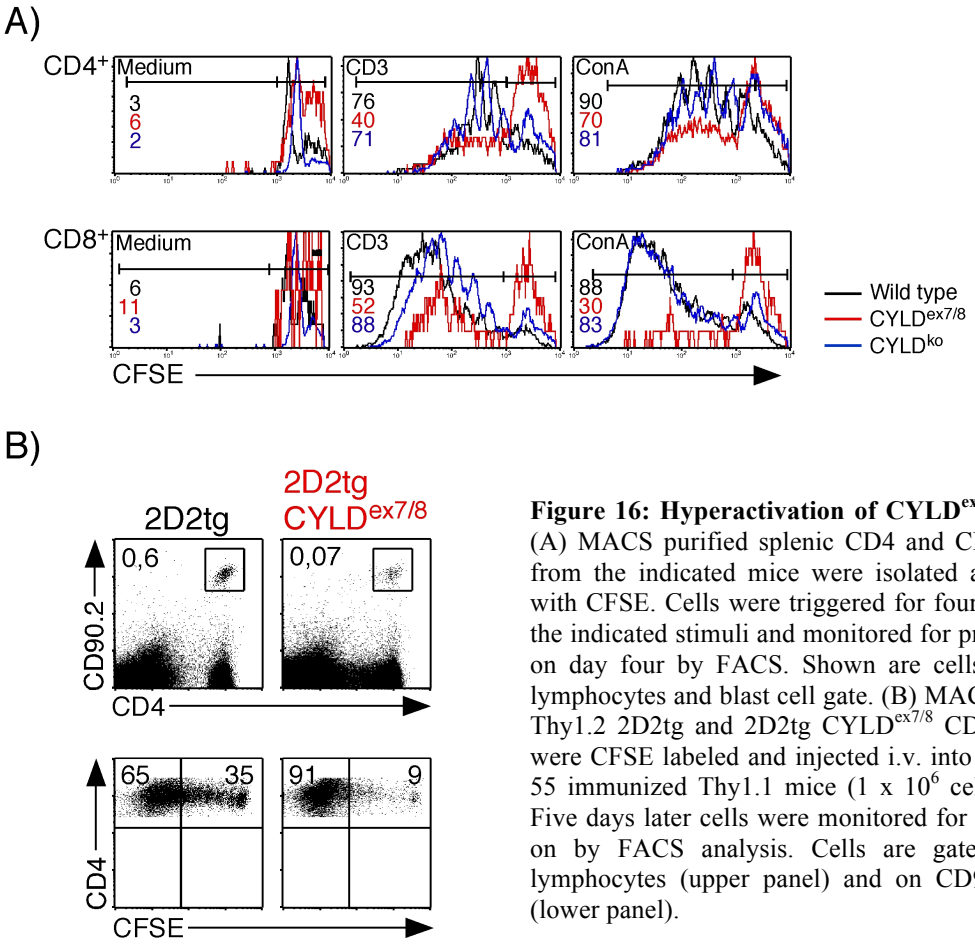

Figure 16: Hyperactivation of CYLD$^{ex7/8}$ T cells. (A) MACS purified splenic CD4 and CD8 T cells from the indicated mice were isolated and loaded with CFSE. Cells were triggered for four days with the indicated stimuli and monitored for proliferation on day four by FACS. Shown are cells gated on lymphocytes and blast cell gate. (B) MACS purified Thy1.2 2D2tg and 2D2tg CYLD$^{ex7/8}$ CD4$^+$ T cells were CFSE labeled and injected i.v. into MOGp35-55 immunized Thy1.1 mice (1 x 10^6 cells/mouse). Five days later cells were monitored for proliferation by FACS analysis. Cells are gated on live lymphocytes (upper panel) and on CD90.2$^+$ cells (lower panel).

To answer this question in a more physiological context, we investigated the activation of CYLD$^{ex7/8}$ CD4$^+$ T cells *in vivo*. Therefore, CYLD$^{ex7/8}$ mice were crossed onto the 2D2tg background, a TCR transgenic mouse strain specific for the MOG 35-55 peptide. We injected CFSE-labeled CD4$^+$ T cells isolated from 2D2tg CYLD$^{ex7/8}$ and 2D2tg mice into MOG-immunized mice and analyzed the cells by FACS cytometry on day 5. It is important to note, that we detected 10 fold less of the transferred 2D2tg CYLD$^{ex7/8}$ CD4$^+$ T cells in the spleen compared to control cells (Fig. 16B, upper panel). Strikingly, the remaining cells proliferated to a greater extend compared to control WT cells (Fig. 16B, lower panel).

Further, to analyze the survival capacities of those T cells, CYLD$^{ex7/8}$, CYLD^{ko} and WT CD90.2 T cells were cultured in T cell media without stimulation and monitored daily for their survival capacity by counting and FACS analysis (Fig. 17). CYLD$^{ex7/8}$ CD4$^+$ as well as CD8$^+$ T cells showed a reduced survival capacity compared to control WT T cells. Already on day 1 the numbers of CYLD mutant CD4$^+$ T cells were significantly reduced whereas a strong reduction of CYLD mutant CD8$^+$ T cells could be detected on day 3. In contrast, CD8$^+$ T cells

of the CYLD^{ko} displayed a greater survival capacity as CD8^{+} T cells from WT mice. This data suggest that short CYLD plays a pivotal role in the regulation of peripheral T cell activation as well as survival.

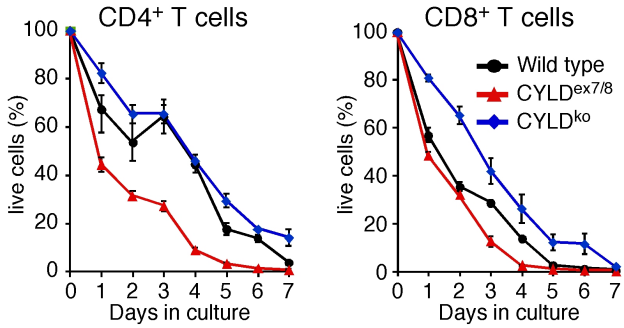

Figure 17: Decreased survival capacity of CYLD$^{ex7/8}$ T cells. MACS purified CD90.2 T cells (1 x 10^{6}) of WT, CYLD$^{ex7/8}$ and CYLD^{ko} mice were cultured in T cell medium without stimulation for the indicated timepoints. Numbers of surviving cells were determined by counting viable cells and by FACS analysis of CD4^{+} and CD8^{+} T cells. Each time point represents the average of three individual experiments with n=3 mice ± SEM.

Moreover, we wanted to investigate how the CYLD mutation influences T cell differentiation *in vivo* compared to CYLD^{ko} and WT T cells. Naive and memory/effector T cells can be separated by the expression of the co-receptors CD44 and CD62L in peripheral T cells. As can be seen in Figure 18A, T cells isolated from CYLD mutant mice are drastically different in their expression of these surface markers compared to WT T cells. Interestingly, we observed a large increase in the proportion of CD44^{high} CD62L^{low} effector/memory CD4^{+} T cells in lymph nodes as well as spleens of CYLD$^{ex7/8}$ mice compared to control mice. This is a strong indication that most of the T cells in CYLD$^{ex7/8}$ mice undergo activation, even without further external stimuli. Once activated, CD4^{+} T cells can further differentiate to different subtypes, based on the pattern of cytokine secretion. Of these, T_H1 and T_H17 cells are characterized by the production of Interferon- γ (IFNγ) and IL-17A, respectively. We have therefore isolated T cells from mesenteric LNs (mLN), where T cells are likely to encounter foreign antigen coming from the gut and performed intracellular staining for IL-17A as well as IFNγ. As seen in Figure 18B, a large proportion of CYLD$^{ex7/8}$ T cells produce IL-17A, when compared to WT or CYLD^{ko} mice. Interestingly, the T cells of the CYLD^{ko} contain 4% T_H1 cells like CYLD mutant T cells, a significant elevation of these cells compared to WT mice (Fig. 18B).

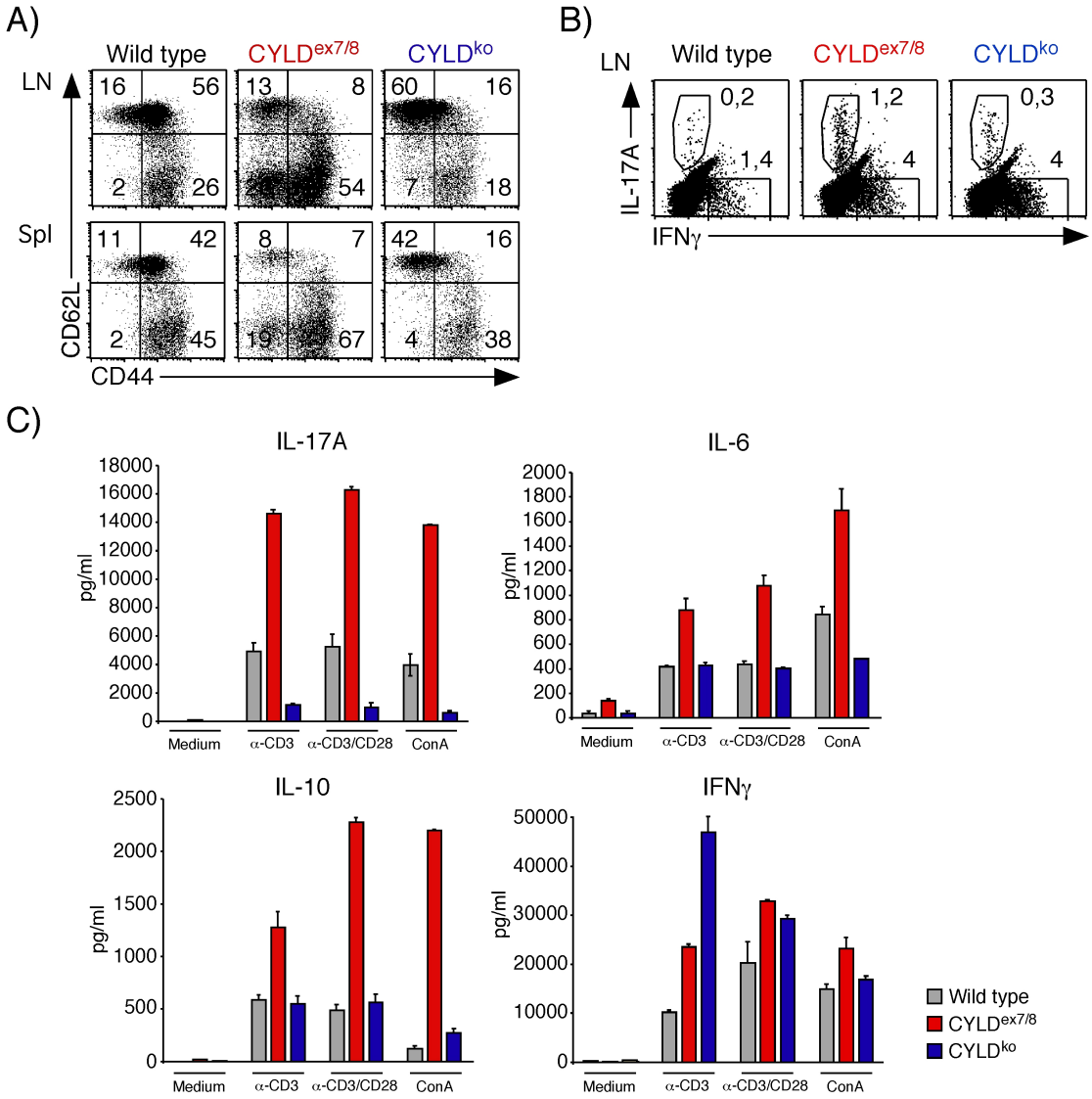

Figure 18: CYLD$^{ex7/8}$ T cells are highly activated and secret high amounts of inflammatory cytokines. (A) Flow cytometry of lymphnodes and splenocytes from WT, CYLD$^{ex7/8}$ and CYLD^{ko} mice, stained with antibodies along margins. Cells are gated on live lymphocytes and CD4^{+} T cells. (B) Flow cytometry of intracellular IL-17A and IFNγ in CD4^{+} T cells isolated from LN of the indicated genotypes. (C) CD4^{+} T cells of WT, CYLD$^{ex7/8}$ and CYLD^{ko} mice were stimulated 48h with the indicated stimuli. Supernatant were analyzed for IL-17A, IL-6, IL-10 and IFNγ by Cytometric Bead Array (CBA).

Next, we measured if this increase in inflammatory T cell population is accompanied by an augmentation of cytokine secretion. LN cells were isolated, activated, and cytokine secretion was measured by Cytometric Bead Array (CBA). As seen in Figure 18C, T cells isolated from CYLD$^{ex7/8}$ mice secreted much higher levels of IL-17A, IL-6 and IL-10, following stimulation with anti-CD3, anti-CD3/CD28 or in the presence of ConA. In contrast, there was only a marginal upregulation of IFNγ secretion compared to WT T cells, and even that was only seen in the presence of anti-CD3 alone (Fig. 18C). Moreover, T cells isolated from CYLD^{ko} mice did not secrete more IL-6 and IL-10 compared to WT T cells, and on the contrary, secreted less

IL-17A. Surprisingly, these cells secreted very high levels of IFNγ when compared to WT or CYLD$^{ex7/8}$ T cells, but also here only when anti-CD3 alone was used (Fig. 18C). These results indicate that CYLD mutant T cells, especially CYLD$^{ex7/8}$ T cells, contain a large population of cells already activated and differentiated to functional effector T cells.

3.6 Constitutive activation of the noncanonical NF-κB pathway

Previously, it was shown that full length CYLD acts on different proteins involved in the NF-κB pathway (Brummelkamp et al. 2003; Troumpauki et al. 2003; Kovalenko et al. 2003; Reiley et al. 2006). To further examine the mechanism of abnormal T cell responses in the absence of FL-CYLD, we investigated the activation of transcription factors of the NF-κB family. Whole cell lysates of thymocytes and MACS purified peripheral CD4$^+$ T cells from three different WT, CYLD$^{ex7/8}$ and CYLD^{ko} mice were isolated and subjected to Western Blot analysis. We could detect remarkable high amounts of the noncanonical NF-κB members RelB and p100 in non-stimulated CYLD$^{ex7/8}$ thymocytes (Fig. 19A) as well as peripheral CD4$^+$ T cells (Fig. 19B) indicating constitutive activation of the noncanonical NF-κB pathway. However, the canonical NF-κB pathway did not seem to be affected as shown by normal expression levels of p65. In addition, also on RNA level we found high levels of RelB and NF-κB2 (p100) in CYLD$^{ex7/8}$ thymocytes (Fig. 19C) as well as CD4$^+$ and CD8$^+$ peripheral T cells (Fig. 19D,E). Altogether, these data suggest that the overexpression of sCYLD while FL-CYLD is absent leads to a constitutive activation of the noncanonical NF-κB pathway, even without external stimulation.

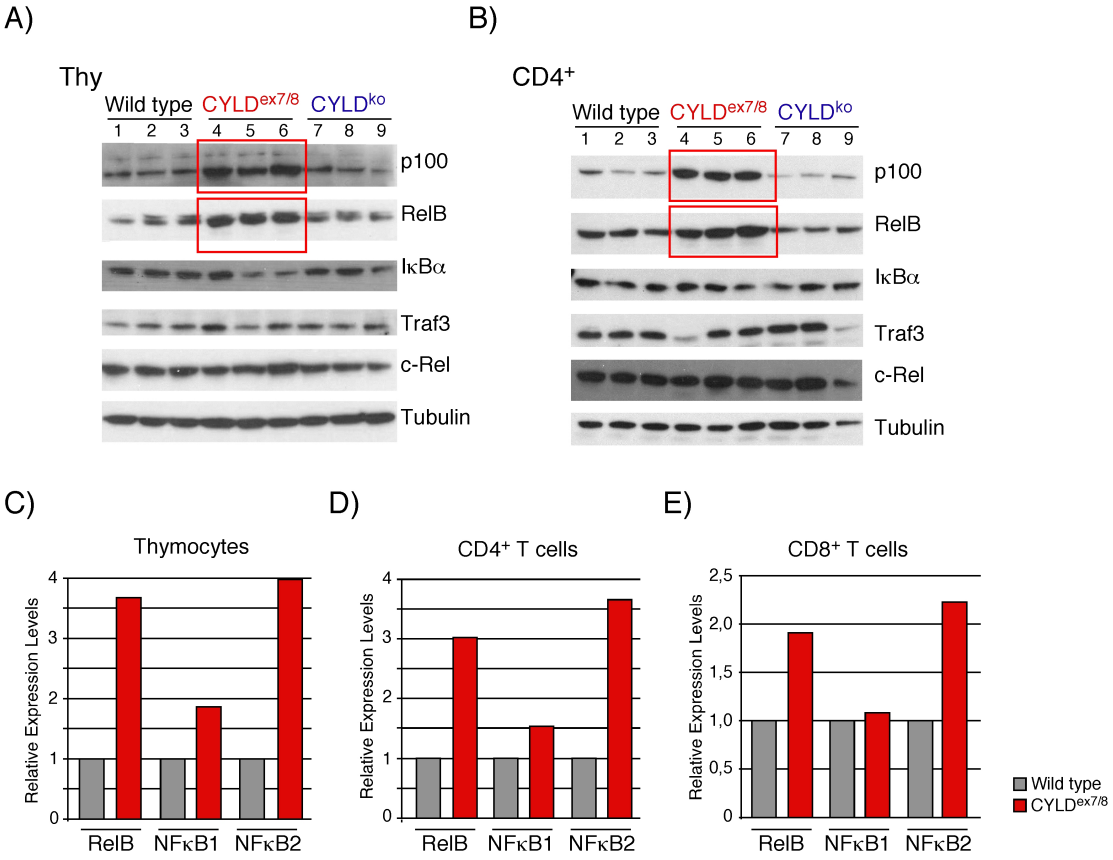

Figure 19: CYLD$^{ex7/8}$ T cells display constitutive activation of the noncanonical NF-κB pathway. (A-B) Cell extracts of whole thymocytes (A) and peripheral CD4$^+$ T cells (B) from three different WT (lane 1-3), three different CYLD$^{ex7/8}$ (lane 4-6) and three different CYLD^{ko} mice (lane 7-9) isolated in the same experiment were examined by Western Blot using antibodies against the indicated proteins. Tubulin-specific antibody was used as loading control. (C-E) Quantitative RT-PCR analysis of the indicated genes in thymocytes (C), peripheral CD4$^+$ T cells (D) and peripheral CD8$^+$ T cells (E). mRNA expression was normalized to HPRT mRNA. Each bar represents the average of three individual mice.

3.7 Regulatory T cells of CYLD$^{ex7/8}$ mice display reduced suppressive capacities

Naturally arising regulatory T cells (Treg cells) are essential for the maintenance of immunological self-tolerance and immune homeostasis by suppressing the activation and expansion of potentially self-reactive T cells. Treg cells are characterized by constitutive expression of the IL-2 receptor α chain (CD25) and the forkhead family transcription factor Foxp3 and they constitute 5–10% of peripheral CD4$^+$ T cells in naive mice. FACS analysis of Treg cells by staining for the surface marker CD4 and for intracellular Foxp3 (gated on CD4$^+$) revealed a five fold increase of Treg cells in thymi of CYLD$^{ex7/8}$ mice when compared to controls (Fig. 20A, upper panel). Investigating the level of Treg cells in the periphery, we also observed a profound population of these cells in LNs as well as spleens of CYLD mutant mice, whereas the CYLD^{ko} behaved like WT control mice (Fig. 20A, middle and lower panel). Of note, most

of the Foxp3$^+$ T cells in LNs and spleens of CYLD$^{ex7/8}$ mice were negative for the expression of the surface marker CD25 (Fig. 20B). It was shown before that CYLD$^{-/-}$ mice (Lee et al. 2010) display an increased Treg frequency in both the thymus and the spleen due to enhanced NF-κB activity. However, these cells were positive for CD25 surface expression in contrast to the enhanced Foxp3$^+$CD25$^-$ population found in CYLD$^{ex7/8}$ mice.

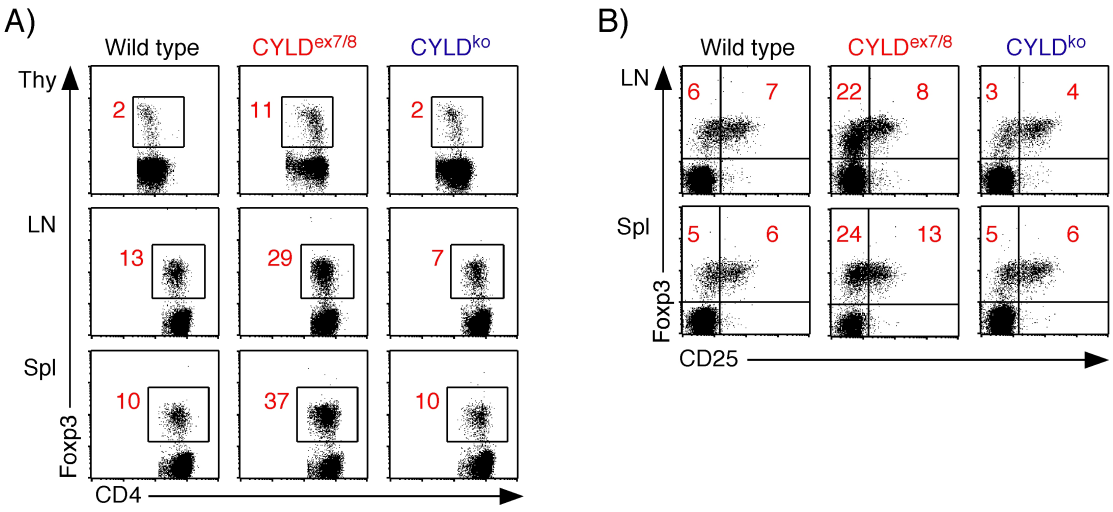

Figure 20: Increased amounts of regulatory T cells in CYLD$^{ex7/8}$ mice. (A) Flow cytometric analysis of intracellular Foxp3 expression on thymocytes, lymph node cells and splenocytes from the indicated genotypes. Cells are gated on CD4$^+$ T cells. (B) Flow cytometry of intracellular Foxp3 and surface CD25 expression on lymph node cells and splenocytes. Cells are gated on CD4$^+$ T cells.

Because Treg cells have the ability to suppress the proliferation of conventional CD4$^+$ T cells in a contact dependent manner, we examined the functional capacity of CYLD$^{ex7/8}$ Tregs compared to controls in an *in vitro* suppression assay. Therefore, we stimulated MACS purified CD4$^+$CD25$^-$ T cells in the presence of CD4$^+$CD25$^+$ T cells isolated from CYLD$^{ex7/8}$, CYLD^{ko} and WT mice in variable ratios and measured [^{3}H]thymidine incorporation. As shown in Figure 21A, using cells derived from WT control mice, proliferation of conventional CD4$^+$CD25$^-$ T cells was strongly reduced in the presence of CD4$^+$CD25$^+$ Treg cells. In contrast, costimulation of CD4$^+$CD25$^-$ WT T cells and CD4$^+$CD25$^+$ Treg cells derived from CYLD$^{ex7/8}$ mice did not reduce proliferation of the former population (Fig. 21B). Hence, Treg cells derived from CYLD$^{ex7/8}$ mice display a diminished suppressive capacity when co-cultured with conventional CD4$^+$ T cells. However, Treg cells isolated from CYLD^{ko} mice strongly suppressed the proliferation of co-cultured WT CD4$^+$CD25$^-$ T cells.

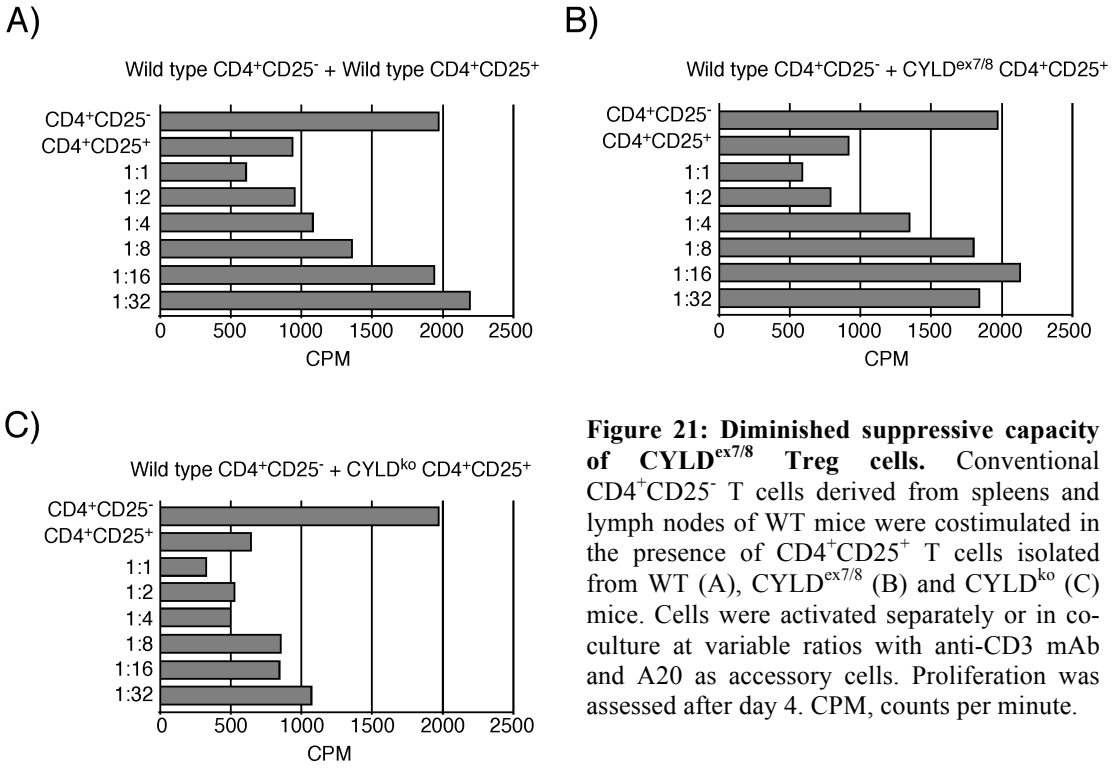

Figure 21: Diminished suppressive capacity of CYLD$^{ex7/8}$ Treg cells. Conventional CD4$^+$CD25$^-$ T cells derived from spleens and lymph nodes of WT mice were costimulated in the presence of CD4$^+$CD25$^+$ T cells isolated from WT (A), CYLD$^{ex7/8}$ (B) and CYLD^{ko} (C) mice. Cells were activated separately or in co-culture at variable ratios with anti-CD3 mAb and A20 as accessory cells. Proliferation was assessed after day 4. CPM, counts per minute.

In further experiments we wanted to investigate the suppressive function of CYLD$^{ex7/8}$, CYLD^{ko} and WT Tregs in a more physiological context *in vivo*. For this purpose we used an adoptive transfer model of colitis. In this model, Tregs have been shown to prevent and cure intestinal inflammation caused by the adoptive transfer of naive CD4$^+$CD25$^-$ T cells into immunodeficient RAG1$^{-/-}$ mice. Therefore, we MACS purified Treg cells from the indicated mice and injected them in equal numbers with CD4$^+$CD25$^-$ T cells of WT mice into RAG1$^{-/-}$ recipients. This allowed us to investigate whether the Tregs of CYLD$^{ex7/8}$ mice could inhibit T cell transfer colitis. As shown in Figure 22, RAG1$^{-/-}$ deficient mice receiving WT CD4$^+$CD25$^-$ and Treg cells displayed no features of colitis determined by mini-endoscopy (Fig. 22A), body weight (Fig. 22B) and histological analysis of the colon (Fig. 22C). As expected, the control group of RAG1$^{-/-}$ mice receiving only CD4$^+$CD25$^-$ T cells developed a strong colitis phenotype. Mini-endoscopy of the colon revealed strong signs of colonic inflammation, which included the production of fibrin, high granularity and vascularity, diarrhea and decreased translucency leading to a high clinical score of disease (Fig. 22A). Further, these mice showed a strong wasting disease (Fig. 22B) as compared to the group of RAG1$^{-/-}$ hosts receiving WT Treg cells. In addition, histological analysis of the colon revealed massive distortion of the colonic structure accompanied with cell infiltration into the lamina propria. Altogether, these signs of intestinal inflammation indicate the functional capacity of the transferred naive

$CD4^+$ T cells to induce inflammation of the colon. Importantly, correlating to the result of the *in vitro* suppression assay, also *in vivo* Treg cells of $CYLD^{ex7/8}$ mice were not able to suppress the inflammatory activity of the transferred WT $CD4^+CD25^-$ T cells, since the $RAG1^{-/-}$ recipients displayed the same inflammatory colitis phenotype as the control group (Fig. 22A-C).

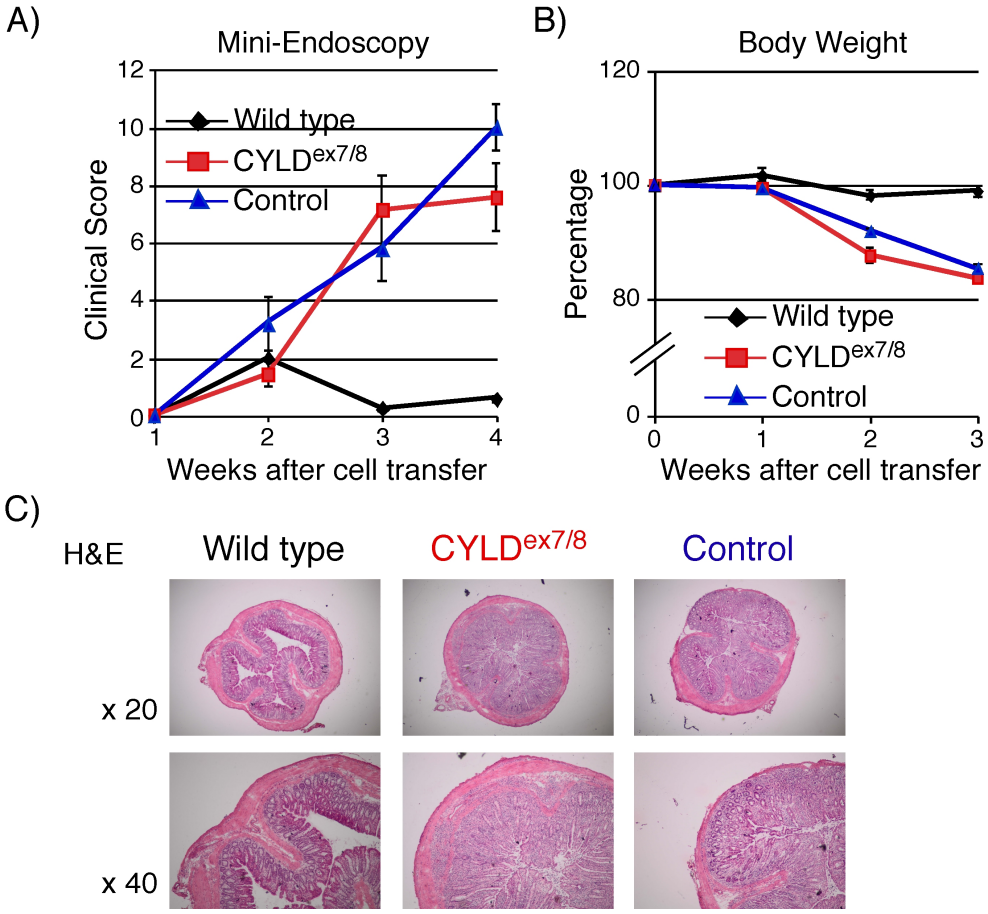

Figure 22: $CYLD^{ex7/8}$ Treg cells fail to inhibit colitis in an adaptive transfer model. Conventional $CD4^+CD25^-$ T cells isolated from WT mice were adoptively transferred into $RAG1^{-/-}$ mice alone or together with $CD4^+CD25^+$ T cells of WT or $CYLD^{ex7/8}$ mice. (A) $RAG1^{-/-}$ recipients were examined for signs of colitis (translucency, fibrin, granularity, stool, vascularity) by mini-endoscopy at the indicated timepoints. Murine endoscopic index of colitis severity (MEICS) scores are shown ± SEM. (B) Graph displays the body weight of $RAG1^{-/-}$ recipients at indicated timepoints ± SEM. (C) Histological analysis of colonic inflammation by H&E staining of colonic cryosections 4 weeks after adoptive cell transfer. Data are representative for n=5 mice of each group. Magnification was used as indicated.

Since the Treg cells of $CYLD^{ex7/8}$ mice were not able to suppress the inflammatory capacity of the transferred naive $CD4^+$ T cells, we were wondering, if the Treg cells survived after transfer into $RAG1^{-/-}$ recipients. As shown in Figure 23A, mesenteric LN cells were stained for CD4 and Foxp3 expression and analyzed by FACS cytometry. Interestingly, only 10% of transferred $CYLD^{ex7/8}$ Treg cells were observed compared to 20% of WT Treg cells. As expected, in the control recipients nearly no Tregs could be detected. Further, we examined the

incidence of transferred Treg cells in the colon from RAG1$^{-/-}$ recipients by immunohistochemistry. In contrast to WT Treg cells, Tregs of CYLD mutant mice were absent in the colon, probably indicating a defect in homing to the side of colonic inflammation (Fig. 23B). Taken together, overexpression of sCYLD leads to a defect of Treg cells to suppress an inflammatory response and to an impairment of efficient migration to the site of colonic inflammation.

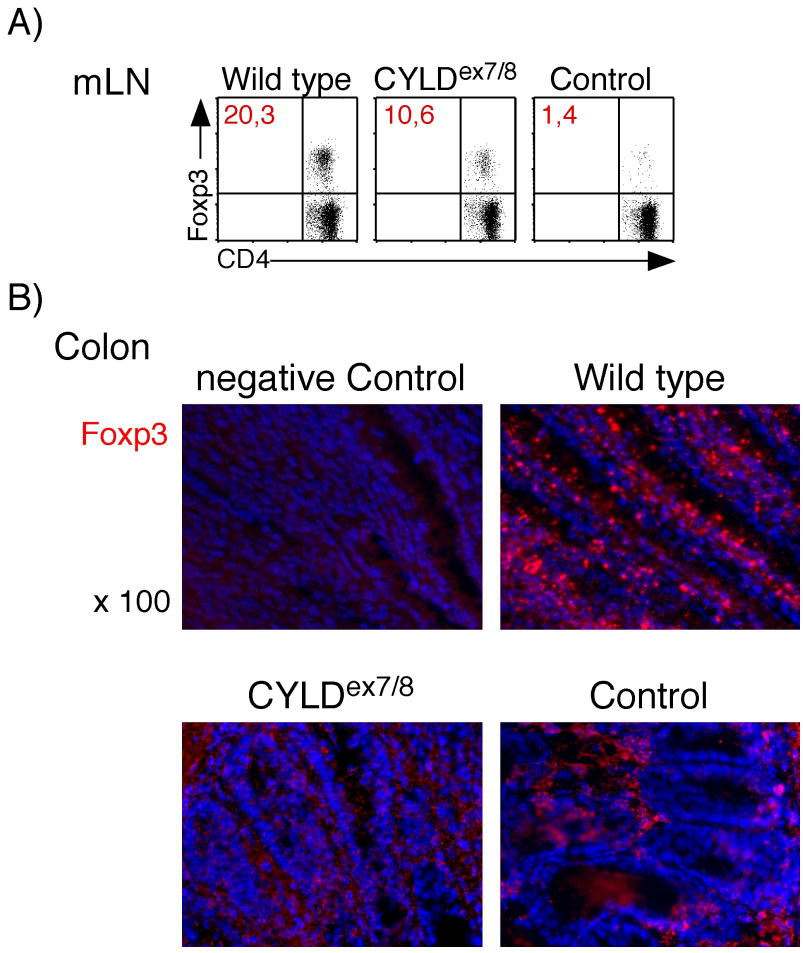

Figure 23: CYLD$^{ex7/8}$ T cells fail to home to the side of colonic inflammation. (A) Flow cytometric analysis of intracellular Foxp3 expression in CD4$^+$ T cells of mesenteric lymph nodes. (B) Colon cross-sections were immunostained with antibody for Foxp3 (red). Nuclei were counterstained with Hoechst 3342 (blue). Magnification was used as indicated.

3.8 Spontaneous colitis in CYLD$^{ex7/8}$ mice

Abnormal T cell responses are often associated with chronic inflammation and autoimmune diseases. Since CYLD$^{ex7/8}$ T cells display a hyperactive phenotype and produce high amounts of inflammatory cytokines such as IL-17A and IFNγ, we further investigated if CYLD mutant mice are more susceptible to spontaneous autoimmunity. Young CYLD$^{ex7/8}$ mice showed no

signs of autoimmunity whereas at the age of 10 months they started to develop a mild colitis phenotype indicated by histology (Fig. 24). Colons of CYLD mutant mice contained markedly more and larger lymphoid follicles or colonic patches, which are a hallmark for hapten-induced colitis and known to be implicated in the development of inflammation of human inflammatory bowel disease.

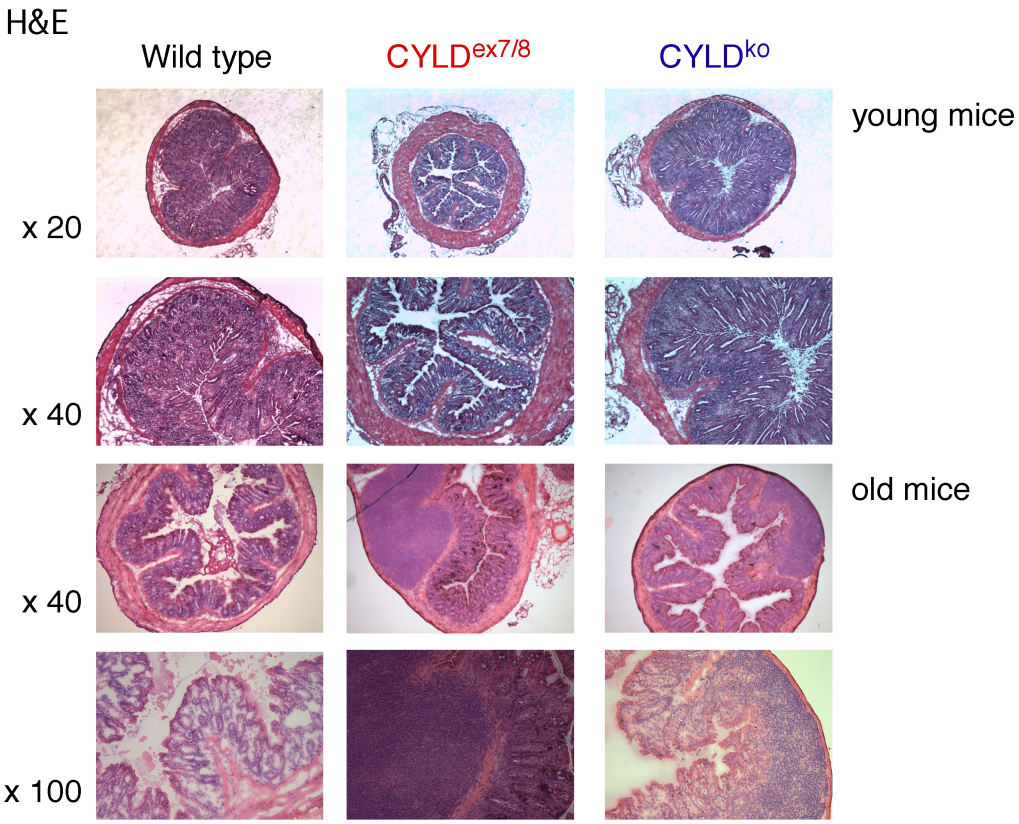

Figure 24: Aged CYLD$^{ex7/8}$ mice develop spontaneous colitis. H&E staining of colonic cryosections from WT, CYLD$^{ex7/8}$ and CYLD^{ko} mice. Mice were analyzed for colonic inflammation at the age of 8 weeks (first and second lane) and at the age of 10 months (third and fourth lane). Magnifications was used as indicated.

Interestingly, CYLD mutant mice crossed onto a TCR transgenic background, either on HY TCR or 2D2 TCR transgenic, developed a severe inflammation of the colon even at early age. First, HYtg CYLD$^{ex7/8}$ mice were suffering from a strong colitis phenotype starting with 4-weeks of age (Fig. 25A). As shown in Figure 25B, their body weight was significantly decreased compared to control mice. By mini-endoscopy we investigated the transluceny, granularity and vascularity of the colon as well as the incidence of fibrin and diarrhea. This analysis revealed a high clinical score of colonic inflammation in HYtg CYLD$^{ex7/8}$ mice compared to control mice (Fig. 25C). Correlating to this data, macroscopic examination of the intestine showed severe pancolitis affecting all parts of the colon distal from the caecum (Fig. 25D). Moreover, histological analysis by H&E staining of colonic cryosections revealed a

dramatic infiltration of lymphocytes into the lamina propria of HYtg CYLD$^{ex7/8}$ colons leading to the distortion of the whole colonic structure (Fig. 25E). These data display strong spontaneous colitis in CYLD mutant mice when crossed onto the HY TCR transgenic background.

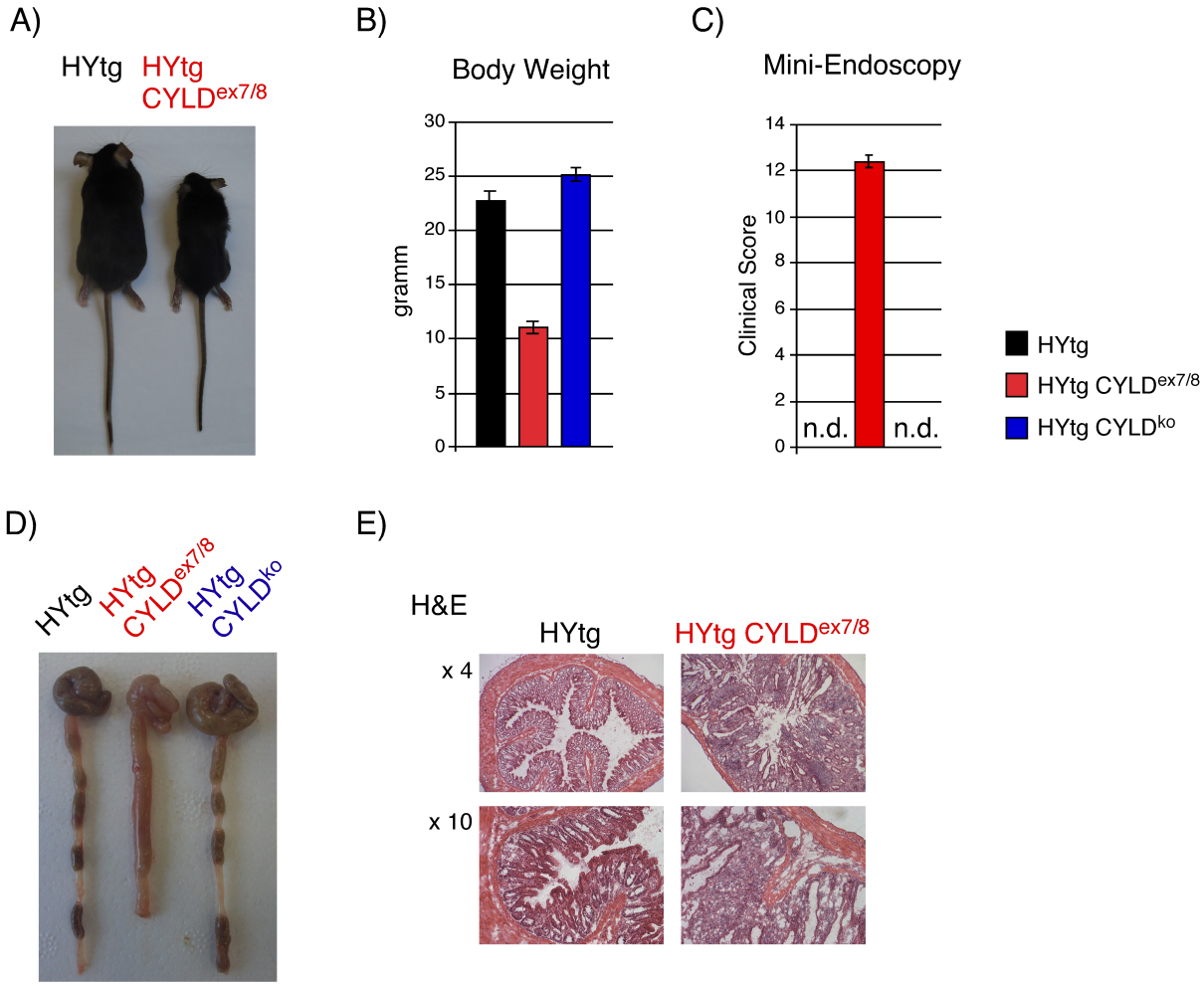

Figure 25: Spontaneous colitis in HYtg CYLD$^{ex7/8}$ mice. (A) Photographs of 8-weeks-old HYtg and HYtg CYLD$^{ex7/8}$ littermates. (B) Bar charts show the body weight of 8-week-old HYtg, HYtg CYLD$^{ex7/8}$ and HYtg CYLD^{ko} mice. Values are represented as mean ± SEM of n=3 mice of each group. (C) The indicated mice were examined by mini-endoscopy. Murine endoscopic index of colitis severity (MEICS) scores are shown ± SEM. n.d., not detectable. (D) Macroscopic examination of colons from 8-week-old HYtg, HYtg CYLD$^{ex7/8}$ and HYtg CYLD^{ko} mice. (E) H&E staining of colonic cryosections of the indicated mice. Magnification was used as indicated.

Since HYtg CYLD$^{ex7/8}$ mice develop a strong inflammatory colitis similar to the histopathology seen in patients with inflammatory bowel disease, we wanted to further characterize the colitis phenotype in these mice. Therefore, we analyzed the gene expression of pro-inflammatory cytokines in the colon, which play a major role in the intestinal immune system. The expression of pro-inflammatory genes was investigated by quantitative RT-PCR and revealed a high upregulation of IL-4, IL-6, IL-10, IL-12, IL17A, IL-22, IFNγ and TNF-α in the

colon of HYtg CYLD$^{ex7/8}$ mice already 8 weeks after birth (Fig. 26). In previous studies it was shown, that IL-6 is a central cytokine upregulated in Crohn's disease as well as Ulcerative colitis. IL-6 contributes to enhanced T cell survival and apoptosis resistance in the lamina propria at the inflamed site (Mudter and Neurath 2007). Strikingly, in HYtg CYLD$^{ex7/8}$ colons the expression of IL-6 showed a 250-fold upregulation compared to controls.

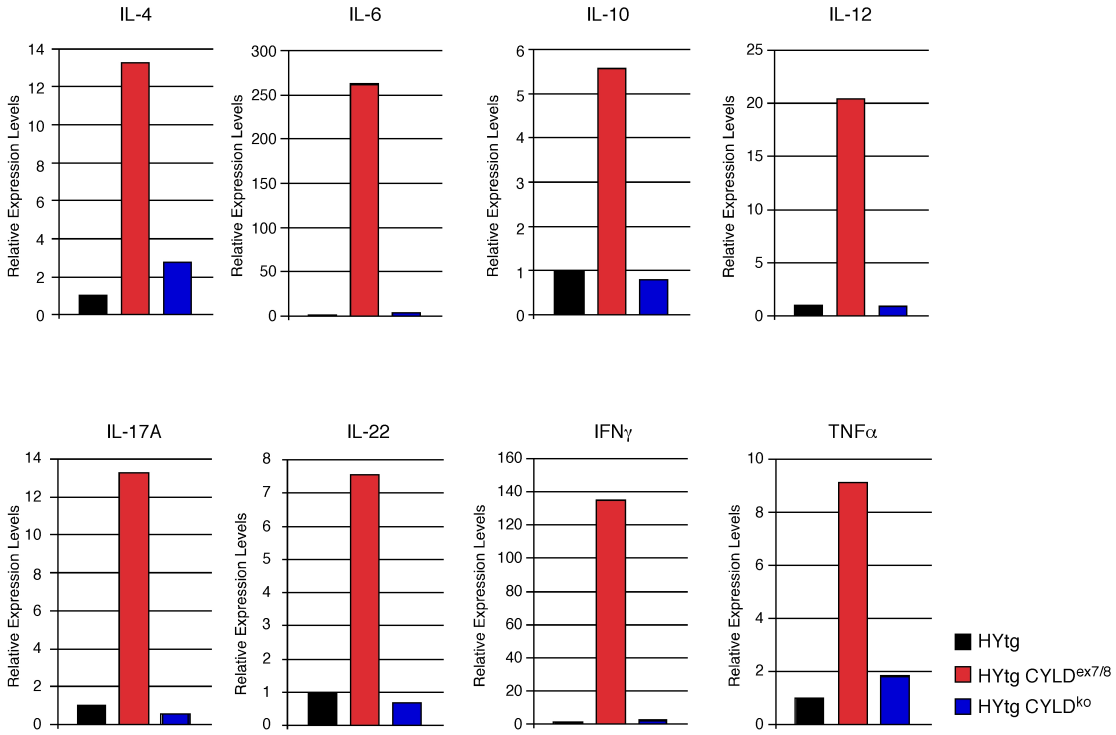

Figure 26: High upregulation of pro-inflammatory gene expression. Expression of pro-inflammatory cytokines in the colon of HYtg, HYtg CYLD$^{ex7/8}$ and HYtg CYLD^{ko} mice examined by quantitative Real Time PCR. Bar charts display the relative expression of the indicated genes. Gene expression levels were normalized to HPRT from each mRNA preparation and normalized to controls (n=2).

Because of the significant upregulation of pro-inflammatory gene expression, we wanted to investigate which cells are responsible for the inflammatory response in the colon of HYtg CYLD$^{ex7/8}$ mice. Therefore, we examined the cellular infiltrate within the mucosa by immunohistochemistry. As shown in Figure 27, inflammatory infiltrates in the colon were dominated by large numbers of CD8$^+$ T cells, CD4$^+$ T cells, F4/80$^+$ macrophages, CD11c$^+$ dendritic cells and to a lesser extent MPO$^+$ neutrophils. Thus, overexpression of sCYLD on the HY TCR transgenic background causes the spontaneous development of severe chronic colitis associated with an accumulation of innate immune cells and the presence of CD4$^+$ and CD8$^+$ T cell infiltrates.

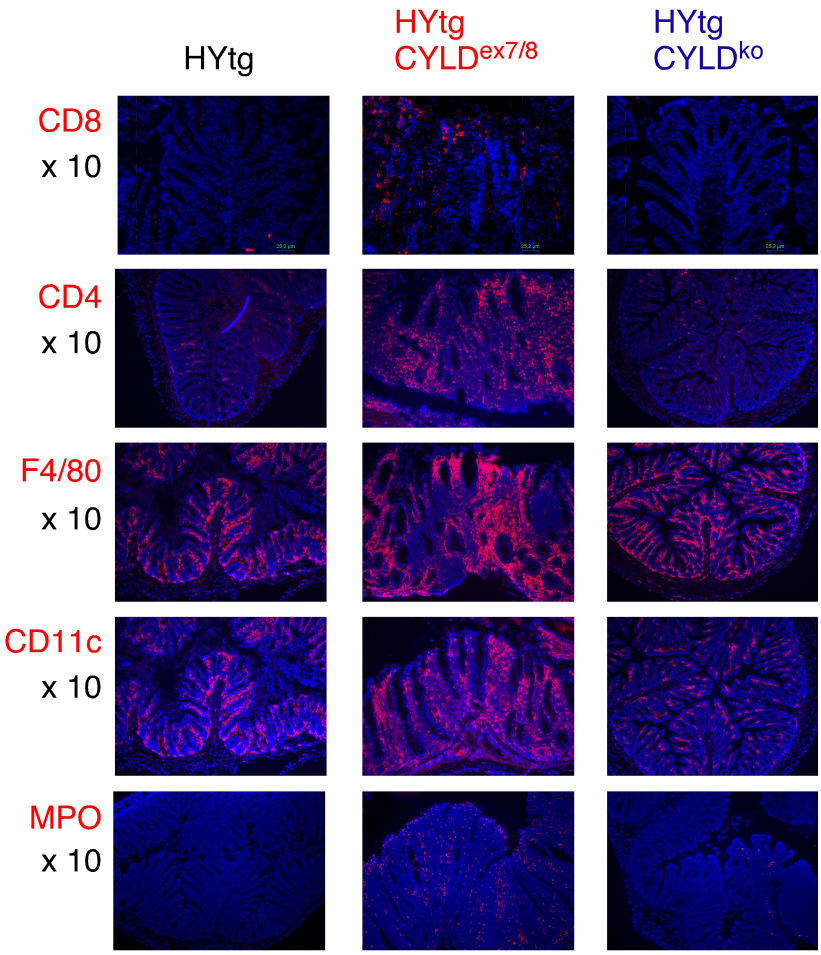

Figure 27: Inflammation in the colon of HYtg CYLD$^{ex7/8}$ mice. Colon cross-sections from HYtg, HYtg CYLD$^{ex7/8}$ and HYtg CYLD^{ko} mice were immunostained with antibodies for CD8, CD4, F4/80, CD11c and myeloperoxidase (MPO) (red). Nuclei were counterstained with DAPI (blue). Magnification was used as indicated.

The transcription factor STAT-3 has been shown before to mediate apoptosis resistance in chronic intestinal inflammation. Further, the expression and activation of STAT-3 is significantly upregulated in IBD. Patients suffering from both Crohn's disease and Ulcerative colitis exhibit increased numbers of phosphorylated STAT-3 positive cells in the lamina propria. Since the expression and activation of STAT-3 is induced via IL-6 signaling and we detected a dramatic increase of IL-6 expression in the colon of HYtg CYLD$^{ex7/8}$ mice, we wanted to examine the status of STAT-3 in the colon of these mice by immunohistochemistry. Colonic sections from HYtg CYLD$^{ex7/8}$ mice exhibited a strong increase of phospho-STAT-3 positive cells compared to controls as shown in Figure 28. The high activation of STAT-3 strongly correlated with the degree of inflammation as shown before by the high clinical score of disease and the upregulation of pro-inflammatory cytokines.

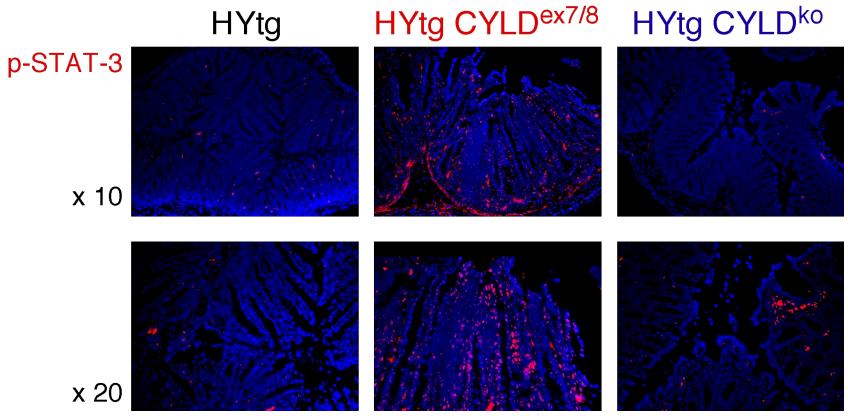

Figure 28: Increased expression of p-STAT-3 in HYtg CYLD$^{ex7/8}$ mice. Cryosections of colons from HYtg, HYtg CYLD$^{ex7/8}$ and HYtg CYLD^{ko} mice were analyzed for p-STAT-3 expression by immunohistochemistry (red). Nuclei were counterstained with DAPI (blue). Magnification was used as indicated.

Second, we examined CYLD$^{ex7/8}$ mice crossed onto the 2D2 TCR transgenic background. Interestingly, these mice were also suffering from disease at the age of 4 weeks (Fig. 29A) and displayed a strong reduction in body weight when compared to control mice (Fig. 29B). Further, high-resolution mini-endoscopy of 2D2tg CYLD$^{ex7/8}$ mice showed signs of severe colitis with thickening of the bowel wall, strong granularity of the mucosa and loss of regular vessel architecture displayed by a high clinical score of intestinal pathology (Fig. 29C). Macroscopic examination of the colon revealed a strong pancolitis as seen for the HYtg CYLD$^{ex7/8}$ mice, leading to severe shortening of the colon (Fig. 29D). Furthermore, we examined colonic cryosections from 2D2tg CYLD$^{ex7/8}$ and control mice by histology. As seen in Figure 29E, H&E staining of the colon revealed enlarged crypts, loss of goblet cells and a marked infiltration of mononuclear cells into the mucosa and submucosa.

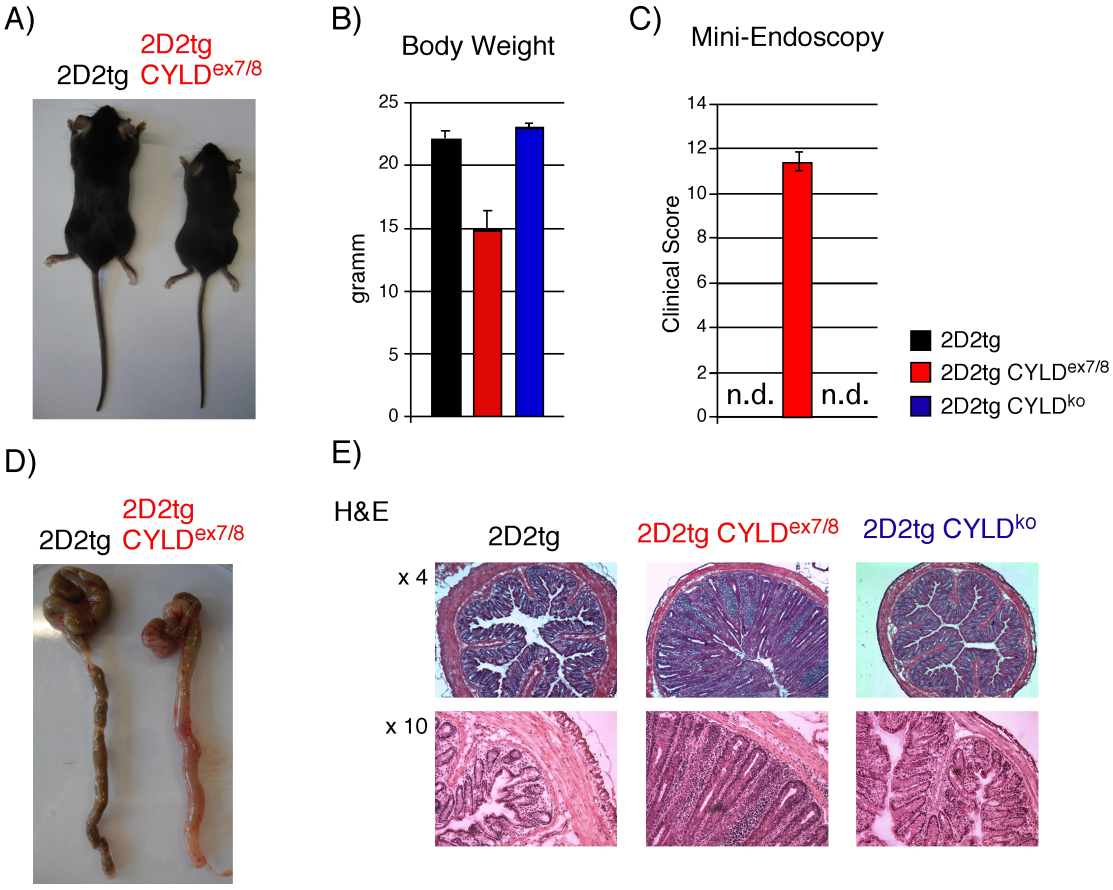

Figure 29: Spontaneous colitis in 2D2tg CYLD$^{ex7/8}$ mice. (A) Photographs of 8-weeks-old 2D2tg and 2D2tg CYLD$^{ex7/8}$ littermates. (B) Bar charts show the body weight of 8-week-old 2D2tg, 2D2tg CYLD$^{ex7/8}$ and 2D2tg CYLD^{ko} mice. Values are represented as mean ± SEM of n=3 mice of each group. (C) The indicated mice were examined by mini-endoscopy. Murine endoscopic index of colitis severity (MEICS) scores are shown ± SEM. n.d., not detectable. (D) Macroscopic examination of colons from 8-week-old 2D2tg and 2D2tg CYLD$^{ex7/8}$ mice. (E) H&E staining of colonic cryosections of the indicated mice. Magnification was used as indicated.

Moreover, we wanted to investigate which cells were responsible for the severe inflammation in the colon of 2D2tg CYLD$^{ex7/8}$ mice. Therefore, we analyzed the cellular infiltration within the mucosa by immunohistology. Thereby, we detected a massive cell infiltration of CD11c^{+} dendritic cells as well as CD4^{+} T cells and to a lesser extend neutrophils compared to controls (Fig. 30). By TdT-mediated dUTP nick end labeling (TUNEL) staining an extensive epithelial apoptosis was detected when compared to controls. Additionally, immunhistological staining of the colon for Ki-67 showed that infiltrating cells were highly proliferative. Taken together, overexpression of short CYLD on a TCR transgenic background, either HY or 2D2, causes spontaneous development of severe chronic colitis associated with massive infiltration of innate immune cells and CD4^{+} T cells into the colon leading to a strong inflammatory response.

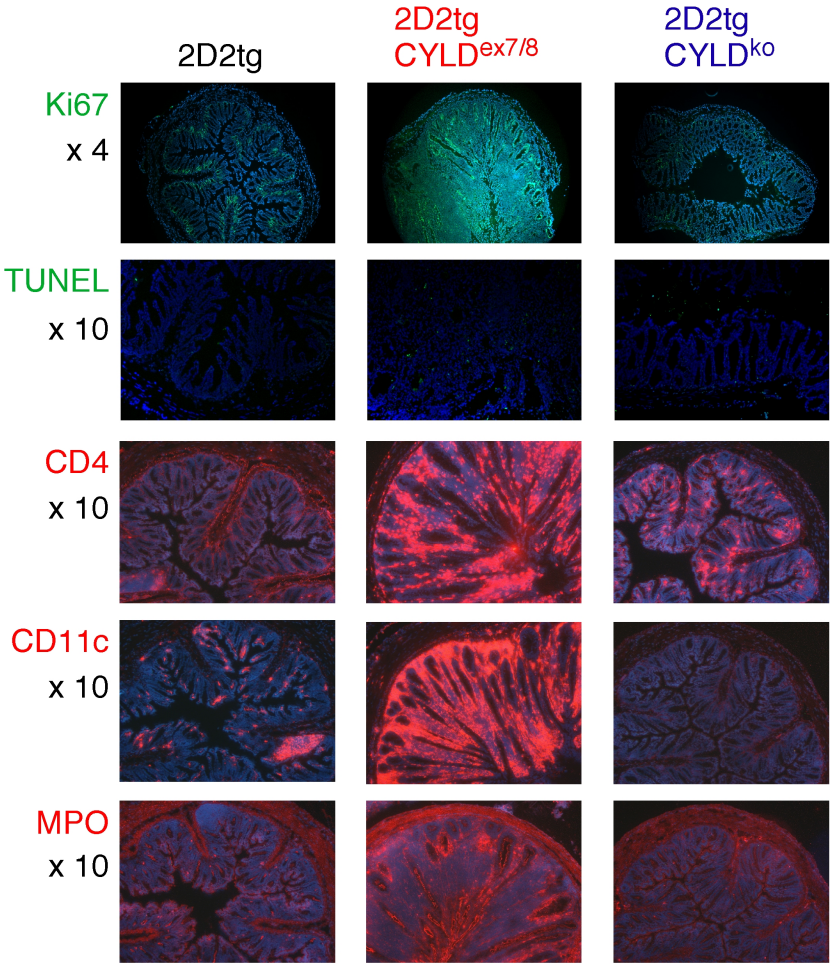

Figure 30: Inflammation in the colon of 2D2tg CYLD$^{ex7/8}$ mice. Colon cross-sections from 2D2tg, 2D2tg CYLD$^{ex7/8}$ and 2D2tg CYLD^{ko} mice were immunostained with antibodies for Ki67, TUNEL (green) and CD4, CD11c and MPO (red). Nuclei were counterstained with DAPI (blue). Magnification was used as indicated.

3.9 Naive T cells overexpressing short CYLD fail to induce colitis

Since we detected a hyperresponsive phenotype of CYLD$^{ex7/8}$ T cells, it was important to analyze whether these mutant T cells contribute to the development of IBD-like symptoms in CYLD$^{ex7/8}$ mice. Therefore, we used the murine adoptive transfer model of IBD and adoptively transferred MACS purified CD4^{+}CD25^{-} T cells from CYLD$^{ex7/8}$, CYLD^{ko} or WT mice into RAG1$^{-/-}$ mice which lack endogenous lymphocytes. The RAG1$^{-/-}$ recipients were analyzed weekly by mini-endoscopy and body weight. As shown in Figure 31A, the RAG1$^{-/-}$ recipients of WT and CYLD^{ko} T cells developed a severe colitis phenotype starting 2 weeks after adoptive cell transfer indicating the functional capacity of the transferred naive CD4^{+} T cells to induce inflammation of the colon. It is important to note, that RAG1$^{-/-}$ recipients of CYLD$^{ex7/8}$ T cells displayed no signs of intestinal pathology suggesting an impairment of these cells to induce colonic inflammation. Correlating to the high clinical score of colitis

from RAG1$^{-/-}$ recipients of WT and CYLD^{ko} T cells, these mice showed a strong reduction in their body weight 5-6 weeks after the adoptive cell transfer (Fig. 31B), which is a characteristic clinical symptom of IBD patients. As expected, RAG1$^{-/-}$ mice receiving CYLD$^{ex7/8}$ T cells displayed no substantial weight loss, which correlated to the low clinical score of colitis measured by mini-endoscopy. Figure 31C shows the macroscopic examination of the colon from RAG1$^{-/-}$ hosts 5 weeks after the adoptive cell transfer. The transfer of naive WT as well as CYLD^{ko} CD4^{+} T cells led to colonic inflammation indicated by high granularity, translucency and severe diarrhea, whereas these IBD-like pathological phenotypes were not detected in RAG1$^{-/-}$ hosts of CYLD$^{ex7/8}$ CD4^{+} T cells. Further, CD4^{+} T cells of CYLD mutant mice had no efficient T cell repopulation in the spleens 6 weeks after the adoptive cell transfer, in contrast to WT and CYLD^{ko} CD4^{+} T cells (Fig. 31D).

Moreover, we investigated the colons of RAG1$^{-/-}$ recipients by immunohistochemistry as shown in Figure 32. The analysis for cell proliferation of infiltrating cells was assessed by Ki67 staining of the colon. In contrast to RAG1$^{-/-}$ hosts of WT and CYLD^{ko} T cells, in RAG1$^{-/-}$ hosts of CYLD$^{ex7/8}$ T cells we observed proliferating cells only in the base of intestinal crypts. In addition, we stained colonic cryosections for CD4^{+} and TUNEL in order to examine, if the transferred CYLD$^{ex7/8}$ T cells had died after the adoptive transfer and therefore were not able to induce colonic inflammation. Importantly, we found less infiltrating CD4^{+} CYLD$^{ex7/8}$ T cells in the colon of RAG1$^{-/-}$ hosts when compared to control groups. Further, these cells displayed less apoptosis compared to transferred WT or CYLD^{ko} CD4^{+} T cells. In another staining, we could also show a strong colonic infiltration of dendritic cells (CD11c) as well as neutrophils (MPO) in RAG1$^{-/-}$ hosts of CYLD^{ko} and WT CD4^{+} T cells, indicating a severe inflammatory cell response. In contrast, nearly no infiltration could be detected in RAG1$^{-/-}$ hosts of CYLD mutant cells. These findings demonstrate, that CD4^{+} T cells from CYLD$^{ex7/8}$ mice are incapable of inducing IBD-like features in RAG1$^{-/-}$ hosts accompanied by a defect to home into the gut after adoptive transfer.

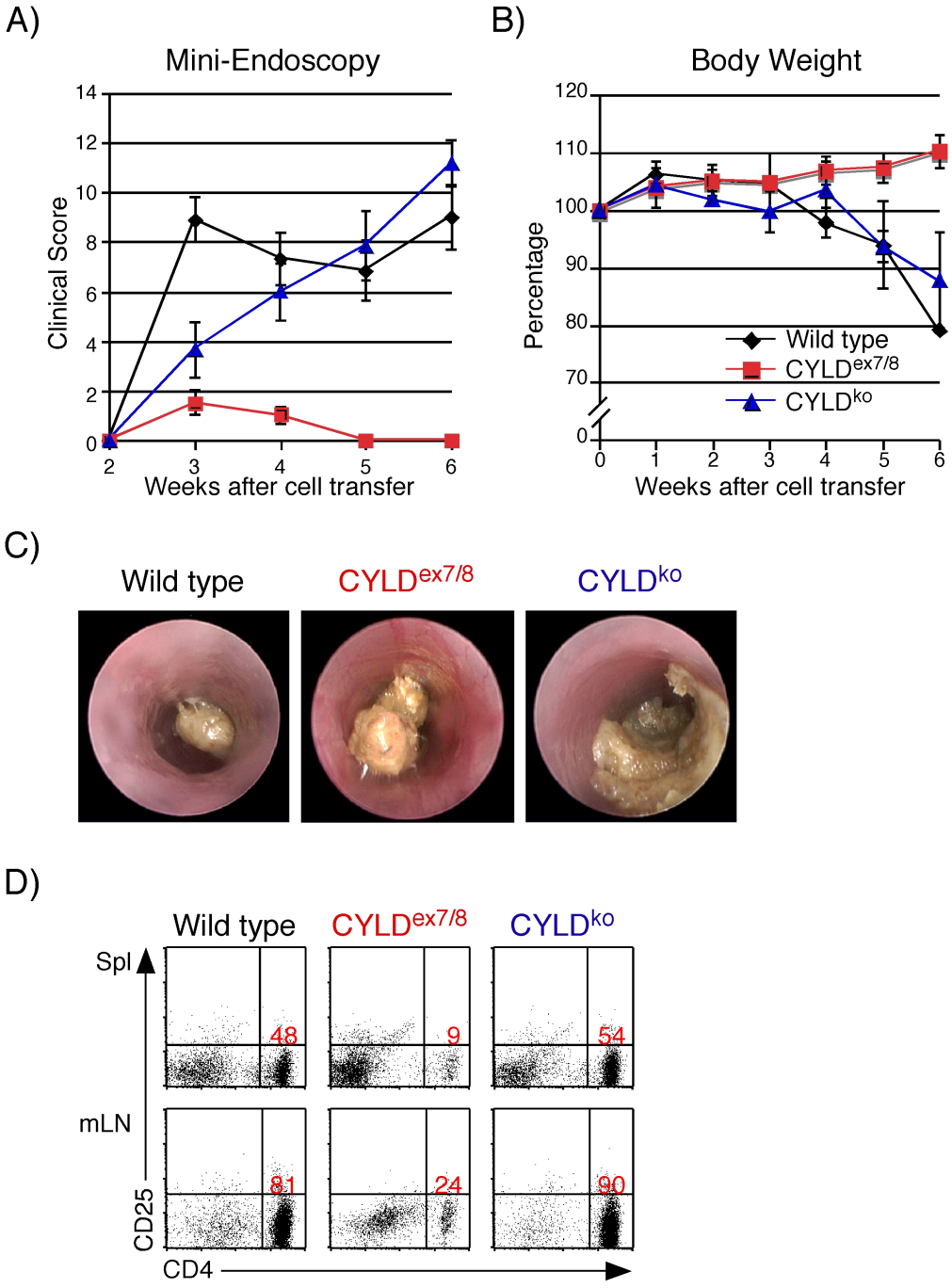

Figure 31: CYLD$^{ex7/8}$ T cells fail to induce colitis. RAG1$^{-/-}$ mice were reconstituted with WT, CYLD$^{ex7/8}$ or CYLD^{ko} naive CD4^{+}CD25^{-} T cells. (A) Graph shows the clinical score of disease from RAG1$^{-/-}$ recipients investigated by mini-endoscopy for the indicated timepoints. Murine endoscopic index of colitis severity (MEICS) scores are shown ± SEM. (B) Graph displays the body weight of RAG1$^{-/-}$ recipients. (C) Photographs of colons from RAG1$^{-/-}$ recipients 5 weeks after adoptive cell transfer. (D) FACS analysis of Spl and mLN of RAG1$^{-/-}$ hosts receiving WT, CYLD$^{ex7/8}$ or CYLD^{ko} naive CD4^{+}CD25^{-} T cells 6 weeks after adoptive cell transfer. Cells were gated on lymphocytes and stained for CD4 and CD25 surface expression.

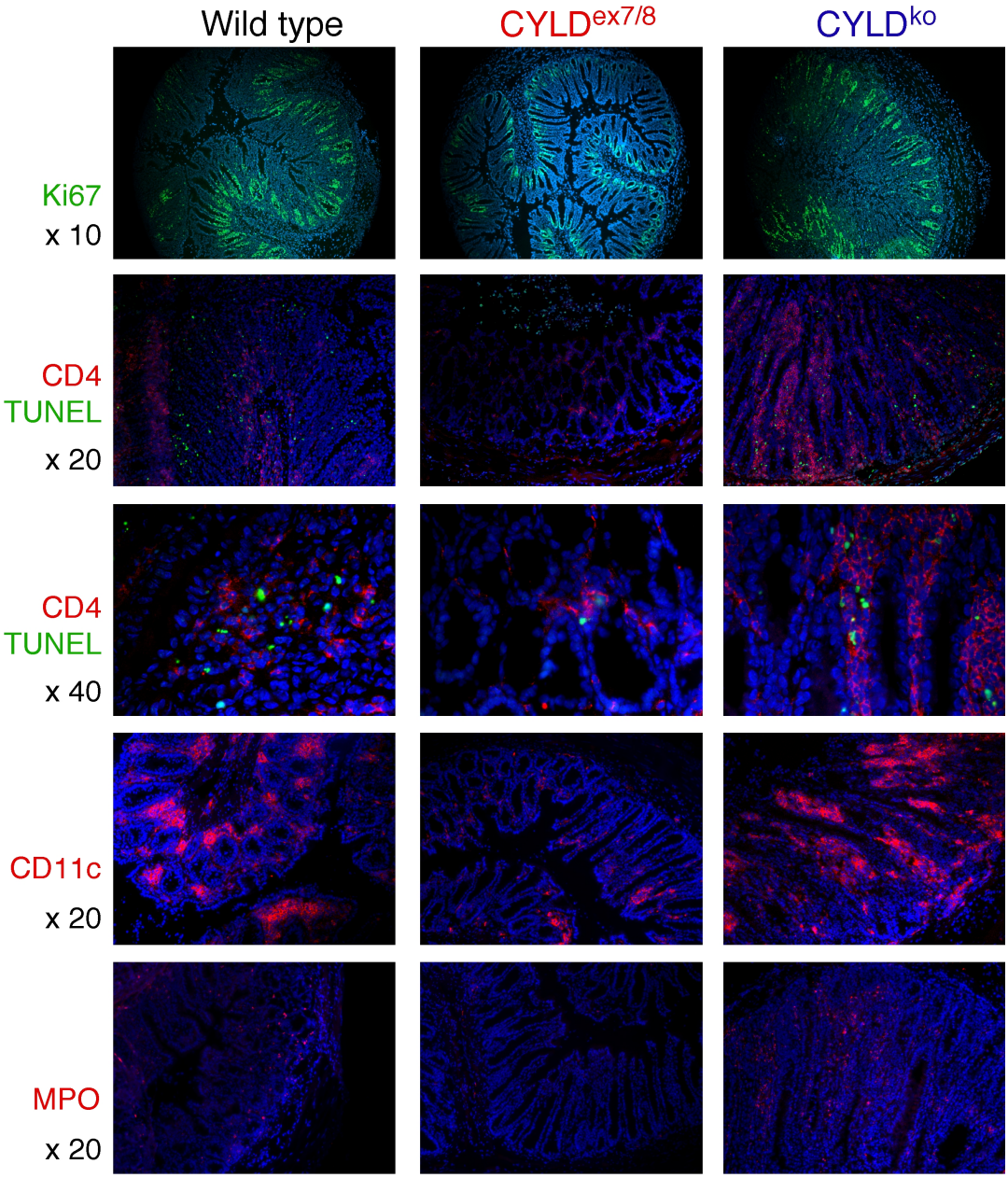

Figure 32: Naive CYLD$^{ex7/8}$ CD4^{+} T cells fail to induce colonic inflammation in an adaptive transfer model of colitis. Colonic cryosections from RAG1$^{-/-}$ hosts receiving WT, CYLD$^{ex7/8}$ or CYLD^{ko} naive CD4^{+}CD25^{-} T cells were stained with the indicated antibodies. Magnification was used as indicated. Nuclei were counter-stained with Dapi (blue).

When we examined Foxp3^{+} Treg cells in CYLD mutant mice, we detected a huge population of Treg cells negative for the surface expression of CD25 (Fig. 20). Because we performed the adoptive transfer experiment to induce colitis based on CD4^{+}CD25^{-} cells, we did not exclude Treg cells negative for the surface expression of CD25. These cells could inhibit the induction of colitis by naive CD4^{+} T cells in RAG1$^{-/-}$ host and therefore suppress the intestinal inflammation. In order to exclude this, we crossed CYLD$^{ex7/8}$ mice to DEREG mice, which express the diphteria toxin receptor (DTR) eGFP fusion protein under the control of the foxp3

promoter allowing for both detection and inducible depletion of $Foxp3^+$ Tregs. Further, we challenged DEREG $CYLD^{ex7/8}$ and DEREG control mice 3 days along with diphteria toxin (Dtx) in order to deplete all $Foxp3^+$ Treg cells. After all Treg cells were depleted, we injected MACS purified $CD4^+CD25^-$ cells from these mice into $RAG1^{-/-}$ hosts to induce colitis. This system allowed us to investigate if the $RAG1^{-/-}$ hosts of $CYLD^{ex7/8}$ $CD4^+$ T cells would show no signs of colitis (Fig. 31) because of the insufficient capacity of $CYLD^{ex7/8}$ T cells to induce colitis or because of the transfer of $Foxp3^+$ $CD4^+CD25^-$ Treg cells inhibiting colonic inflammation. After the adoptive cell transfer, we analyzed the $RAG1^{-/-}$ hosts weekly by mini-endoscopy and body weight. As shown in Figure 33A, 4 weeks after adoptive cell transfer $RAG1^{-/-}$ recipients of WT as well as $CYLD^{ex7/8;wt}$ cells developed a strong intestinal pathology indicated by a high clinical score of disease. The severe sickness of the mice was accompanied by a substantial loss of body weight (Fig. 33B). As shown in the previous experiment (Fig. 31), CYLD mutant $CD4^+$ T cells were insufficient to induce colonic inflammation indicated by mini-endoscopy and body weight (Fig. 33A, B). Moreover, macroscopic examination of the colon displayed a high granularity and vascularity, diarrhea and reduced translucency after transfer of WT and $CYLD^{ex7/8;wt}$ $CD4^+$ T cells, whereas the colons of $RAG1^{-/-}$ recipients of $CYLD^{ex7/8}$ $CD4^+$ T cells appeared completely healthy (Fig. 33C, upper panel). In addition, $RAG1^{-/-}$ recipients of WT and $CYLD^{ex7/8;wt}$ $CD4^+$ T cells but not those of $CYLD^{ex7/8}$ $CD4^+$ T cells showed a strong infiltration of lymphocytes into the periportal vein of the liver (Fig. 33C, middle panel) as well as the colon (Fig. 33C, lower panel). Thus, these findings implicate that indeed naive $CD4^+$ T cells of $CYLD^{ex7/8}$ mice are insufficient to induce intestinal inflammation.

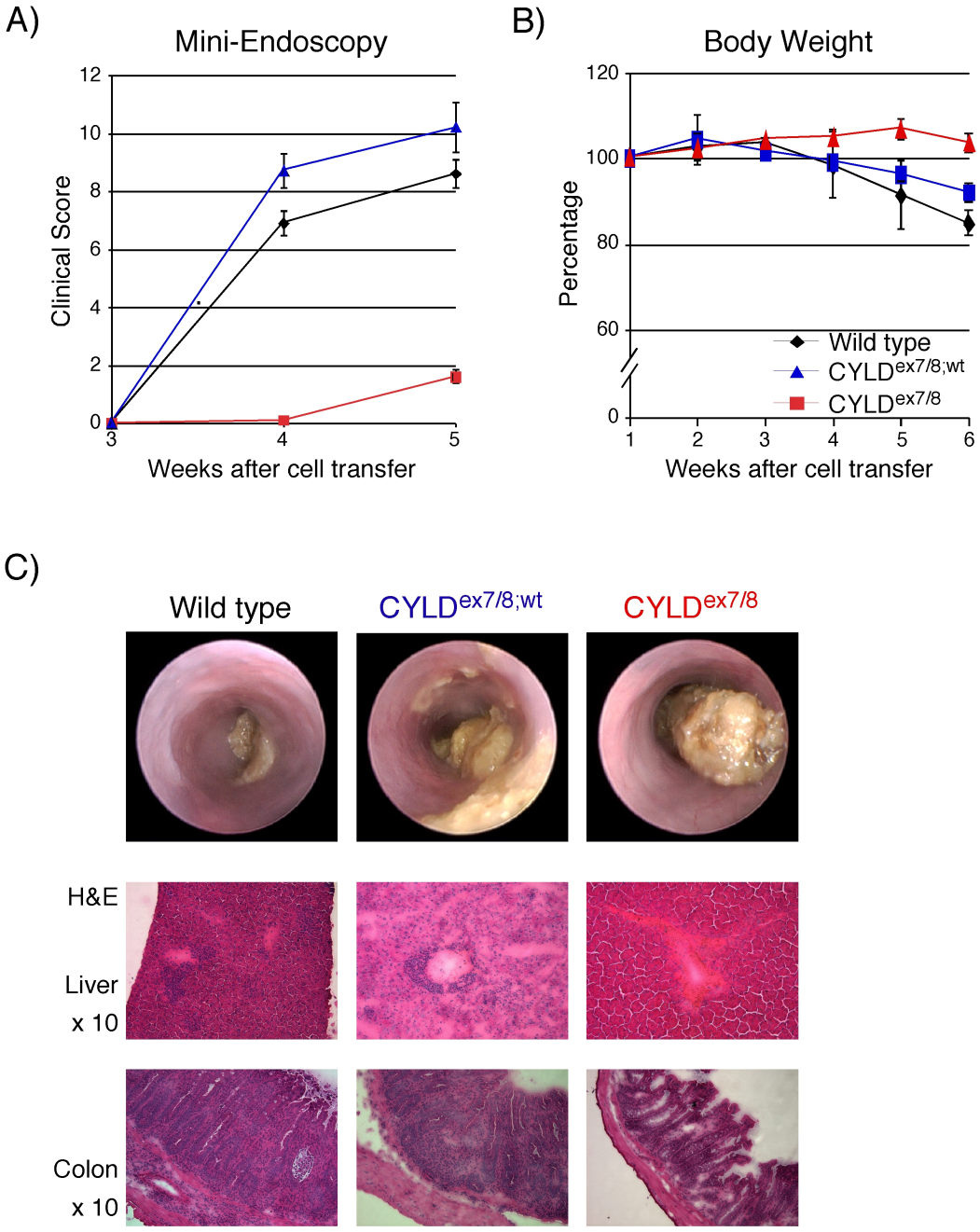

Figure 33: Naive CYLD$^{ex7/8}$ T cells fail to induce colitis. DEREG, DEREG CYLD$^{ex7/8;wt}$ and DEREG CYLD$^{ex7/8}$ mice were treated with Dtx to deplete Tregs. After Treg depletion, MACS purified naive CD4^{+}CD25^{-} T cells from these mice were transferred into RAG1$^{-/-}$ hosts. (A) Graph shows the clinical score of disease from RAG1$^{-/-}$ recipients investigated by mini-endoscopy for the indicated time points. (B) Graph displays the body weight of RAG1$^{-/-}$ recipients for the indicated time points. (C) Photographs of colons from RAG1$^{-/-}$ recipients 5 weeks after adoptive cell transfer (upper row). Cryosections from liver (middle row) and colon (lower row) from RAG1$^{-/-}$ hosts analyzed by H&E staining. Magnification was used as indicated.

3.10 Spontaneous colitis in RAG1$^{-/-}$CYLD$^{ex7/8}$ mice

In further experiments we wanted to understand the commitment of the different cell populations to the IBD-like phenotype we observed in CYLD$^{ex7/8}$ mice. To address this question, we crossed the CYLD mutant mice with RAG1$^{-/-}$ mice that lack endogenous lymphocytes. In order to investigate if RAG1$^{-/-}$CYLD$^{ex7/8}$ mice were more susceptible to colitis, we used the adoptive transfer model of colitis, in which the transfer of naive CD4^{+} T cells into RAG1$^{-/-}$ recipients induces inflammation in the complete colon. Therefore, we injected naive WT CD4^{+}CD25^{-} T cells into 8-weeks old RAG1$^{-/-}$CYLD$^{ex7/8}$, RAG1$^{-/-}$CYLD$^{ex7/8;wt}$ and RAG1$^{-/-}$ control mice. RAG1$^{-/-}$CYLD$^{ex7/8}$ as well as RAG1$^{-/-}$CYLD$^{ex7/8;wt}$ recipients showed a significant higher clinical score of colitis as the control group assessed by mini-endoscopy (Fig. 34A). In addition, they showed a massive loss of body weight already 12 days after the adoptive cell transfer (Fig. 34B). Two mice of the RAG1$^{-/-}$CYLD$^{ex7/8}$ group died already 8 days after the cell transfer, due to suffering from marked colitis accompanied by diarrhea and substantial reduction of body weight. As shown in Figure 34C, we examined colonic cryosections from the different mice by histology and stained for H&E. Consistently, histological assessment of the colon from RAG1$^{-/-}$CYLD$^{ex7/8;wt}$ and RAG1$^{-/-}$CYLD$^{ex7/8}$ mice revealed a massive mononuclear cell infiltration into the mucosa as well as submucosa leading to the distortion of the colonic structure (Fig. 34C).

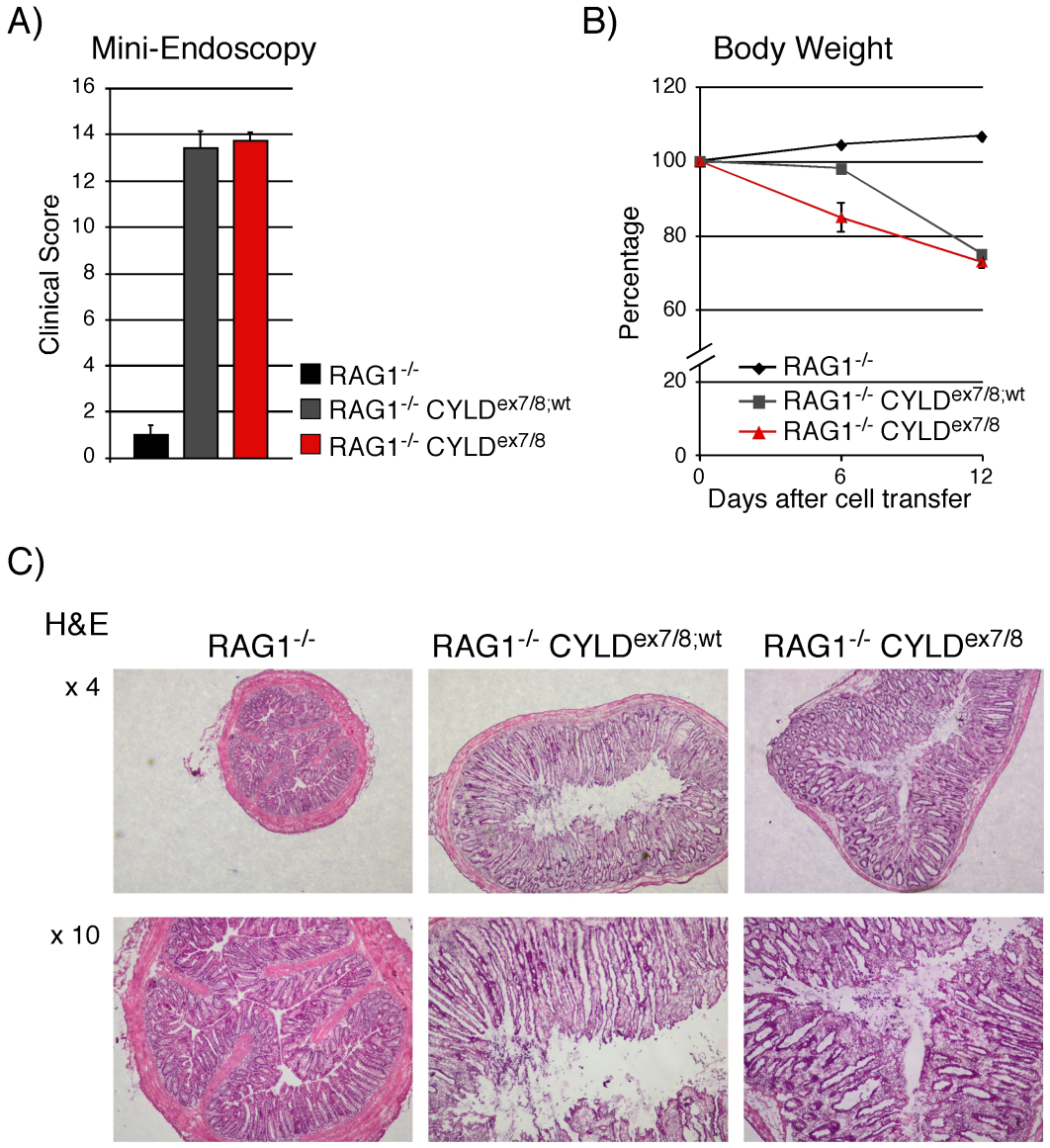

Figure 34: Development of severe colitis in RAG1$^{-/-}$CYLD$^{ex7/8;wt}$ and RAG1$^{-/-}$CYLD$^{ex7/8}$ mice upon adoptive cell transfer. RAG1$^{-/-}$, RAG1$^{-/-}$CYLD$^{ex7/8;wt}$ and RAG1$^{-/-}$CYLD$^{ex7/8}$ mice were reconstituted with naive WT CD4^{+} T cells. (A) Bars show the clinical score of disease from the indicated mice investigated by mini-endoscopy at day 12. (B) Graph displays the body weight of the indicated mice. (C) Colonic cryosections of RAG1$^{-/-}$, RAG1$^{-/-}$CYLD$^{ex7/8;wt}$ and RAG1$^{-/-}$CYLD$^{ex7/8}$ hosts were analyzed by H&E staining 12 days after adoptive cell transfer. Magnification was used as indicated.

Since 8-weeks old RAG1$^{-/-}$CYLD$^{ex7/8;wt}$ as well as RAG1$^{-/-}$CYLD$^{ex7/8}$ mice developed such a strong inflammatory response already 12 days after the adoptive cell transfer, we wanted to clarify if aging CYLD mutant mice on RAG1$^{-/-}$ background were susceptible to spontaneous intestinal pathology. Importantly, when we analyzed older RAG1$^{-/-}$CYLD$^{ex7/8}$ and RAG1$^{-/-}$CYLD$^{ex7/8;wt}$ mice at the age of 16-20 weeks by macroscopic examination (Fig. 35A), we detected a dramatic spontaneous inflammation of the intestine. Colons of these mice displayed high granularity, vascularity as well as severe diarrhea. In addition, the colon was not translu-

cent anymore compared to control RAG1$^{-/-}$ mice. Of note, the colonic inflammation was stronger in RAG1$^{-/-}$CYLD$^{ex7/8}$ mice than in RAG1$^{-/-}$CYLD$^{ex7/8;wt}$ mice. Moreover, mini-endoscopy of the colon revealed a high clinical score of intestinal pathology in CYLD mutant mice (Fig. 35B).

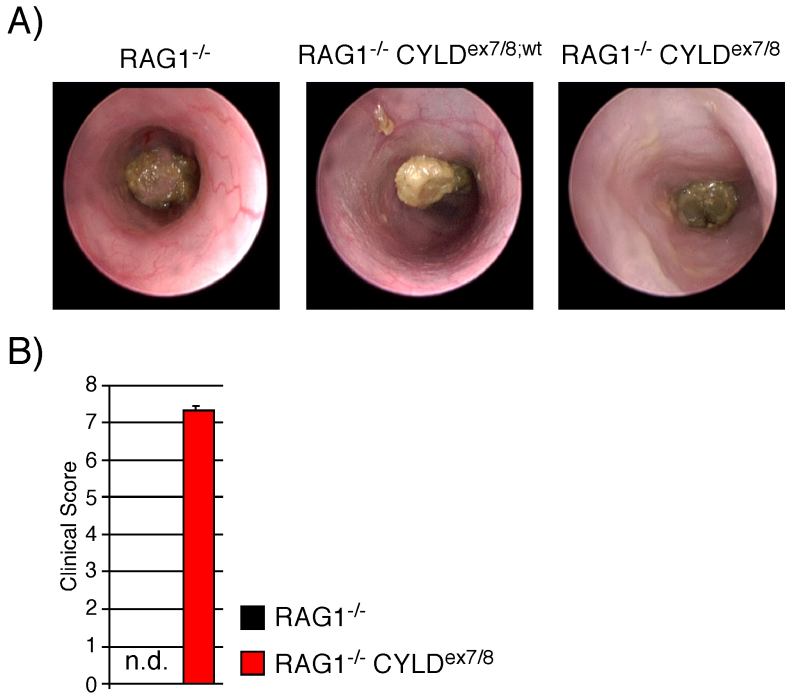

Figure 35: Spontaneous colonic inflammation in RAG1$^{-/-}$CYLD$^{ex7/8}$ and RAG1$^{-/-}$CYLD$^{ex7/8}$ mice. (A) Photographs of colons from RAG1$^{-/-}$, RAG1$^{-/-}$CYLD$^{ex7/8;wt}$ and RAG1$^{-/-}$CYLD$^{ex7/8}$ mice with the age of 5 months. (B) Bar charts indicate the clinical score of disease from the indicated mice with the age of 5 months. n.d., not detectable.

In order to characterize the colitis phenotype in these mice, we examined the gene expression of pro-inflammatory cytokines in the colon by quantitative RT-PCR. As shown in Figure 36, a high upregulation of IL-6, IL-10, IL-12, IL17A, IL-22, IL-23, IFNγ and TNF-α in the colon of RAG1$^{-/-}$CYLD$^{ex7/8}$ mice could be detected. Strikingly, we detected a 140-fold upregulation of the expression of the cytokine IL-22, which is known to be produced by dendritic cells in response to extracellular bacteria and contributes to the pathogenesis of inflammatory bowel disease. In addition, the expression of the inflammatory cytokine IL-6 was strongly upregulated in RAG1$^{-/-}$CYLD$^{ex7/8}$ mice compared to controls, highlighting the severity of colonic inflammation in these mice.

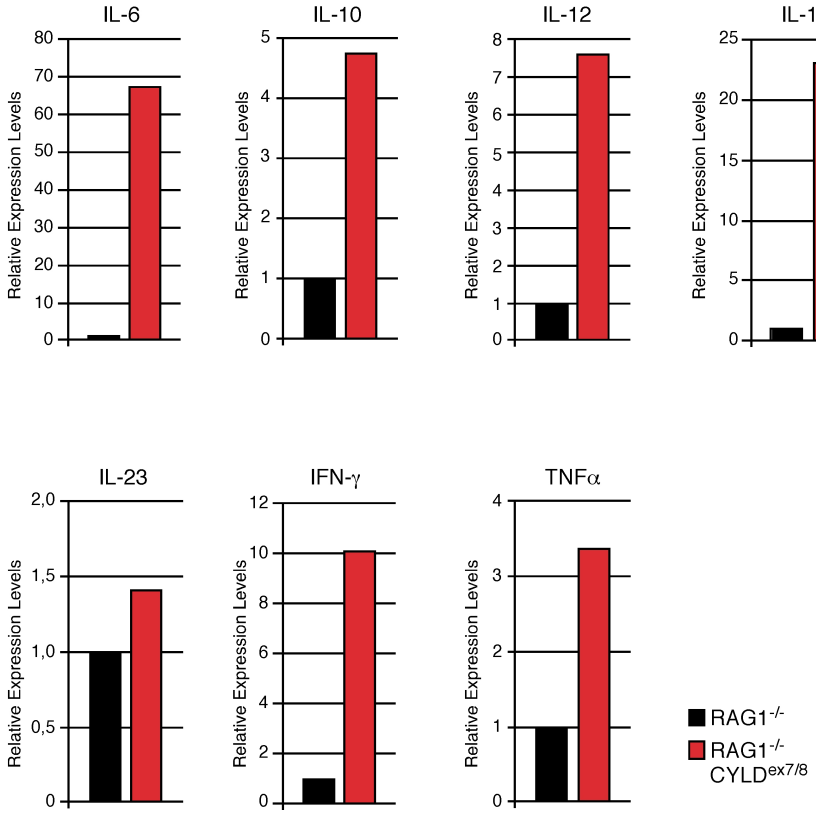

Figure 36: High upregulation of pro-inflammatory gene expression in RAG1$^{-/-}$ CYLD$^{ex7/8}$ colons. Expression of pro-inflammatory cytokines in the colon of RAG1$^{-/-}$ and RAG1$^{-/-}$ CYLD$^{ex7/8}$ mice examined by quantitative Real Time PCR. Bar charts display the relative expression of the indicated genes. Gene expression levels were normalized to HPRT from each mRNA preparation and normalized to controls (n=2).

Additionally, we analyzed the structure of the colon from the indicated mice by H&E staining. We detected enlarged crypts and a marked infiltration of mononuclear cells into the mucosa pointing massive inflammation in CYLD mutant mice on RAG1$^{-/-}$ background (Fig. 37A). Because RAG1$^{-/-}$ mice are deficient for lymphocytes we wanted to examine which cells are responsible for the inflammatory response. Immunohistochemestry of the colon from RAG1$^{-/-}$CYLD$^{ex7/8;wt}$ indicated a severe infiltration of F4/80^{+} macrophages, MPO^{+} neutrophils and to a lower extent CD11c^{+} dendritic cells (Fig. 37B). It is important to note, that this phenotype was even enhanced in RAG1$^{-/-}$CYLD$^{ex7/8}$ mice. Thus, overexpression of short CYLD on a RAG1 deficient background results in severe colonic inflammation accompanied with a massive pro-inflammatory gene expression in colonic tissue.

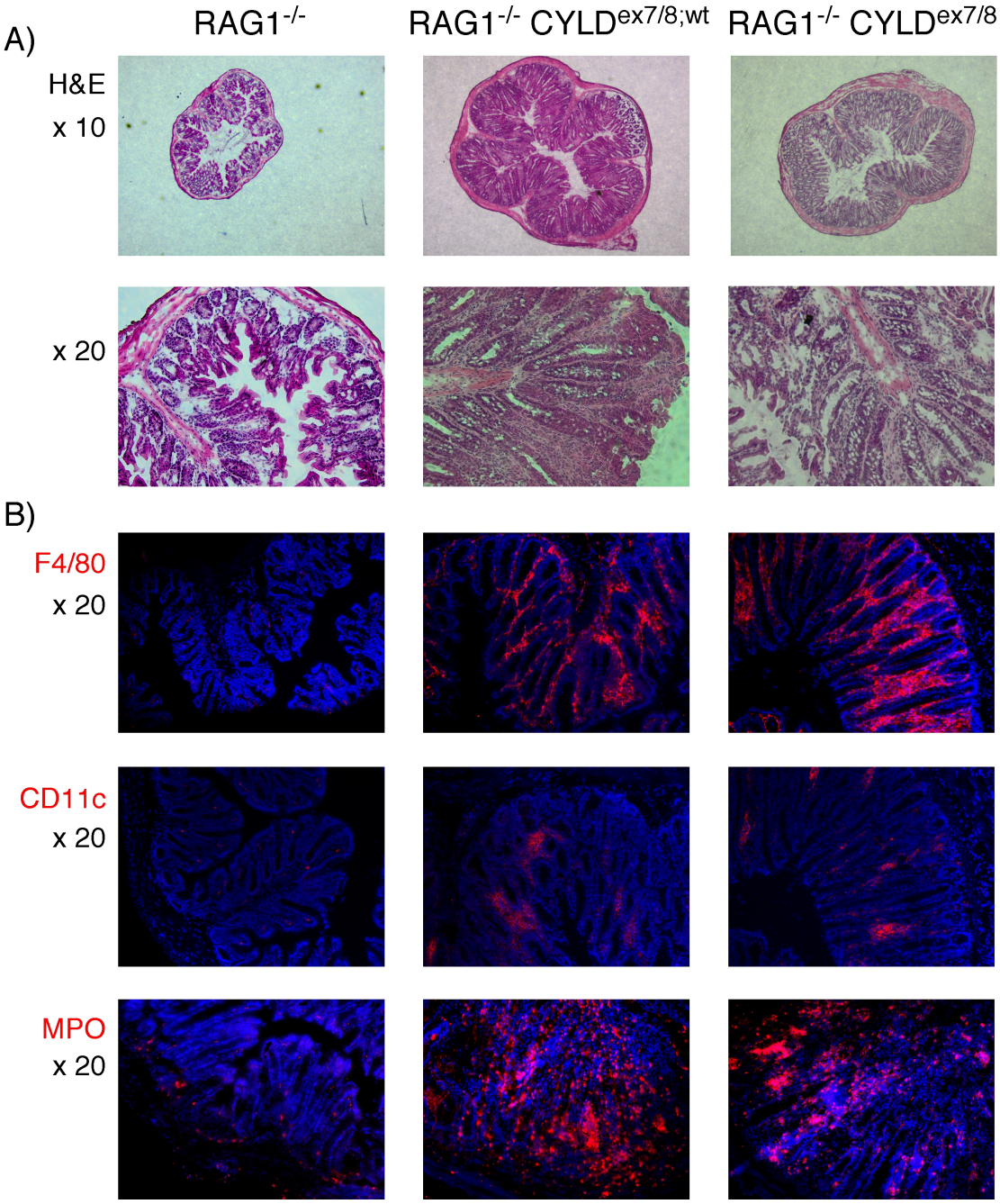

Figure 37: Massive infiltration of innate immune cells into the colon of RAG1$^{-/-}$CYLD$^{ex7/8}$ mice. (a) Histological analysis of colonic cryosections from RAG1$^{-/-}$, RAG1$^{-/-}$CYLD$^{ex7/8;wt}$ and RAG1$^{-/-}$CYLD$^{ex7/8}$ mice. Cryosections were stained for H&E. Magnification was used as indicated. (b) Immunohistochemistry of colonic cryosections from the indicated mice stained with antibodies against F4/80, CD11c and MPO (red). Nuclei were counterstained with Dapi (blue). Magnification was used as indicated.

Previously, Srokowski *et al.* showed that overexpression of sCYLD leads to a hyperactive phenotype of dendritic cells *in vitro* as well as *in vivo*. Since RAG1$^{-/-}$CYLD$^{ex7/8}$ mice develop spontaneous colitis accompanied with a remarkable infiltration of DCs into the inflamed colon, we wanted to examine the activation phenotype of DCs in these mice. Therefore, we first

investigated the expression levels of CD86 and MHCII as marker for activation on CYLD mutant DCs compared to controls. As shown in Figure 38A, MHCII and CD86 surface expression of splenic dendritic cells was highly upregulated in both, RAG1$^{-/-}$CYLD$^{ex7/8;wt}$ and RAG1$^{-/-}$CYLD$^{ex7/8}$ mice when compared to control mice. This result display a hyperactivation phenotype of DCs in RAG1$^{-/-}$CYLD$^{ex7/8;wt}$ and RAG1$^{-/-}$CYLD$^{ex7/8}$ mice as reported for CYLD$^{ex7/8}$ dendritic cells by Srokowski *et al*.

Because of the severe colitis phenotype in RAG1$^{-/-}$CYLD$^{ex7/8}$ mice and the strong infiltration of dendritic cells into the inflamed colon, we further analyzed their presentation capacity when isolated from RAG1$^{-/-}$CYLD$^{ex7/8}$, RAG1$^{-/-}$CYLD$^{ex7/8;wt}$ and control mice. Presentation efficiency of dendritic cells was measured by 2D2tg CD4^{+} T cell proliferation and division. Interestingly, dendritic cells isolated from RAG1$^{-/-}$CYLD$^{ex7/8}$ mice activated co-cultured CD4^{+} T cells to a greater extent than control cells (Fig. 38B), independently of the concentration of MOG peptide. Also RAG1$^{-/-}$CYLD$^{ex7/8;wt}$ dendritic cells showed increased activation capacity, but not as strong as RAG1$^{-/-}$CYLD$^{ex7/8}$ dendritic cells.

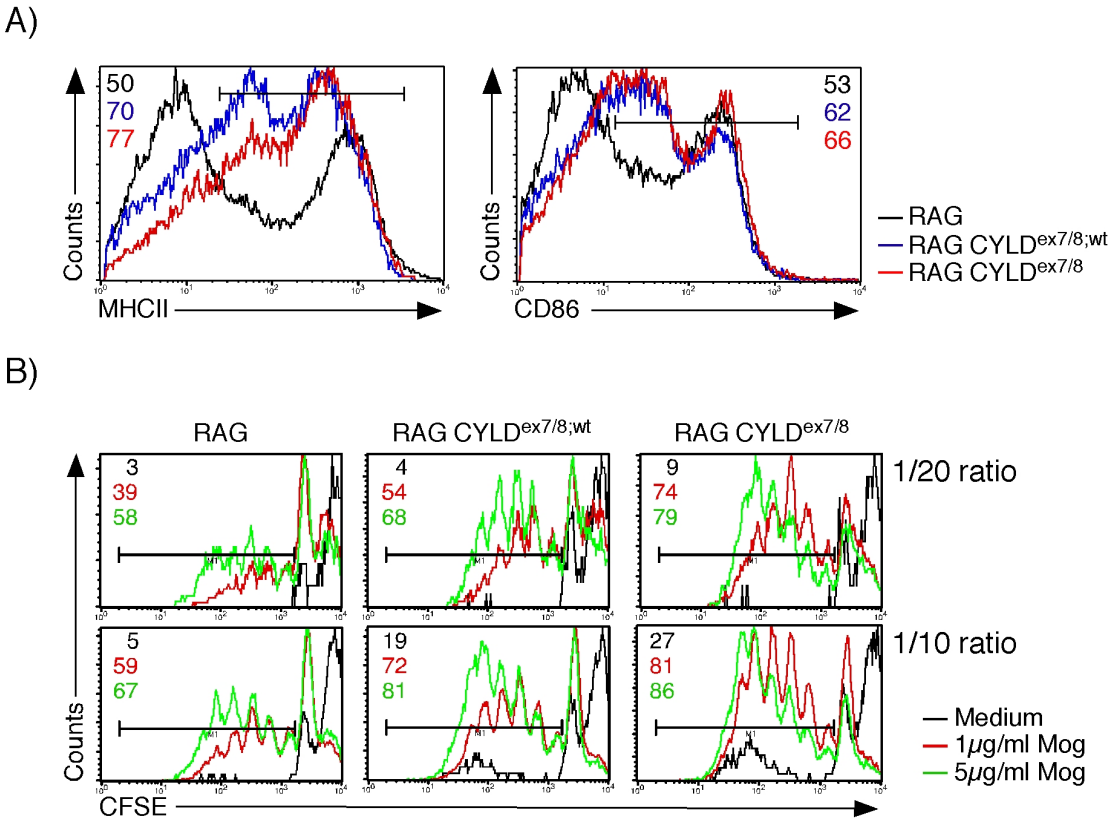

Figure 38: Hyperactivation of CYLD mutant dendritic cells. (a) Histrograms display the expression levels of MHCII (left) and CD86 (right) of the indicated genotypes. (b) Dendritic cells from RAG1$^{-/-}$, RAG1$^{-/-}$CYLD$^{ex7/8;wt}$ or RAG1$^{-/-}$CYLD$^{ex7/8;wt}$ mice were peptide loaded with 1µg/ml (red) or 5µg/ml (green) MOGp35-55 class II restricted peptide and then co-cultured with CFSE labeled purified 2D2tg CD4^{+} T cells in a ratio of 1/10 (upper panel) or 1/20 (lower panel). As a control DCs with no peptide loading were also co-cultured with CFSE labeled 2D2tg CD4^{+} T cells (black). Four days later 2D2tg CD4^{+} T cells were monitored for proliferation by FACS analysis and CFSE intensity is shown as histograms. Numbers above marker line indicate the percentage of positive cells in this region. Cells are gated on CD4^{+} T cells.

3.11 Generation of autoantibodies in TCR transgenic CYLD$^{ex7/8}$ mice

Previously, it was reported by Hövelmeyer *et al.* that CYLD$^{ex7/8}$ mice exhibit elevated levels of IgG1, IgG2a, IgG2b and IgA antibody titers compared to WT mice (Hövelmeyer et al. 2007). It is known that high levels of immunoglobulin as well as the generation of autoantibodies is often associated with autoimmunity. Since both, HY and 2D2 TCR transgenic CYLD$^{ex7/8}$ mice develop severe spontaneous colitis we were interested to investigate if this autoimmune phenotype is correlated to the generation of nuclear autoantibodies. Therefore, we tested sera of TCR transgenic 8-week-old CYLD$^{ex7/8}$ mice for the development of autoantibodies. As seen in Fig. 39, the staining of Hep-2 cells with sera from HYtg CYLD$^{ex7/8}$, 2D2tg CYLD$^{ex7/8}$ and control mice revealed the presence of antinuclear antibodies (ANA) in both, HYtg CYLD$^{ex7/8}$ and 2D2tg CYLD$^{ex7/8}$ mice, whereas no antinuclear antibodies could be detected in control mice. These findings display, that overexpression of short CYLD re-

sults in the production of autoantibodies correlating to the autoimmune phenotype detected in CYLD$^{ex7/8}$ mice.

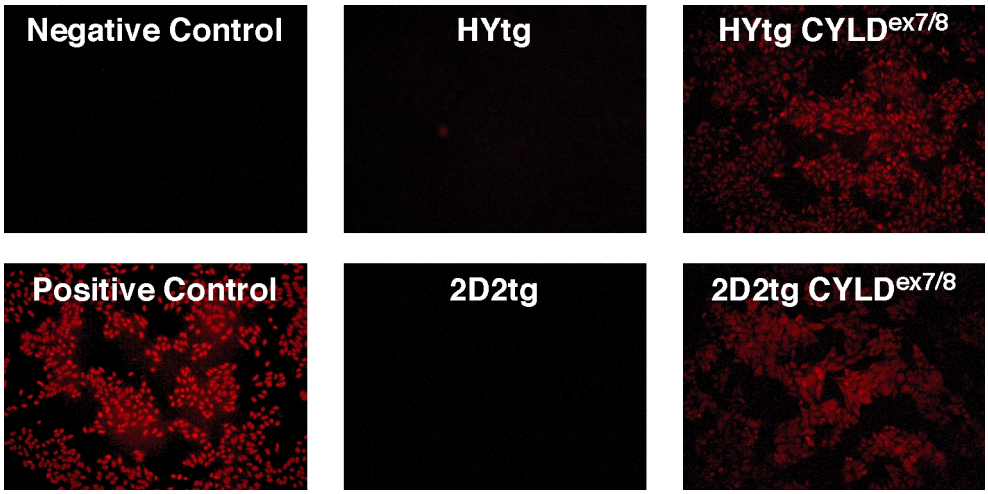

Figure 39: Hep-2 cells were stained and loaded with sera from HYtg CYLD$^{ex7/8}$, 2D2tg CYLD$^{ex7/8}$ and control mice. Positive control serum was taken from MRL/lpr mice. Magnification was x 10. Data are representative for n=3 mice.

3.12 CYLD$^{ex7/8}$ mice are hypersusceptible to EAE

Multiple sclerosis is a chronic neurological disorder of the central nervous system (CNS), which is characterized by inflammation, demyelination, axonal injury and atrophy of the CNS. The well-established mouse model for MS is known as experimental autoimmune encephalomyelitis (EAE), which is induced by active immunization with myelin components like myelin oligodendrocyte glycoprotein (MOG) accompanied by Freund's adjuvant. T_H1, T_H17 as well as Treg cells were shown to play major roles in autoimmune brain inflammation. In CYLD mutant mice we observed a hyperactive phenotype of CYLD$^{ex7/8}$ CD4$^+$ T cells accompanied by a massive production of the inflammatory cytokines IL-6, IL-17A and IFNγ. In addition, we could show that Treg cells of these mice were not able to suppress an inflammatory response. Therefore, we asked if CYLD mutant mice were more susceptible to the induction of EAE compared to CYLD^{ko} and WT mice. As additional control groups we used mice with specific overexpression of sCYLD in T cells (CYLD^{FL} CD4-Cre) or in dendritic cells (CYLD^{FL} CD11c-Cre). In order to test the susceptibility to MOG-induced EAE we immunized the five different groups of mice with the MOG 35-55 peptide in Complete Freund's adjuvant and analyzed disease progression by clinical evaluation (Fig. 40). CYLD mutant mice displayed a delayed onset of disease when compared to control mice but developed an increased severity of EAE while the WT mice were already recovering. Interestingly, signs of

paralysis in CYLD^{FL} CD11c-Cre mice started earlier compared to control animals and they developed the highest clinical score of disease. However, in CYLD^{FL} CD4-Cre mice the incidence of EAE was drastically reduced in comparison to WT mice.

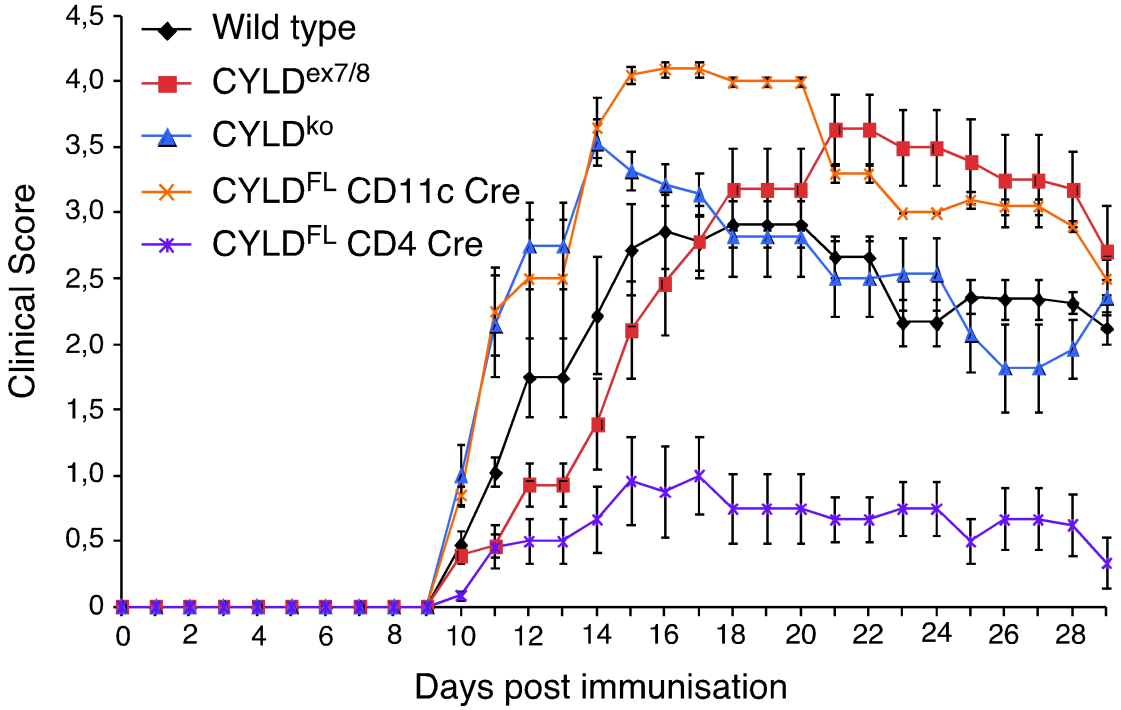

Figure 40: Increased EAE in CYLD$^{ex7/8}$ mice. EAE was actively induced by immunization of WT (black), CYLD$^{ex7/8}$ (red), CYLD^{ko} (blue), CYLD^{FL} CD11c-Cre (orange) and CYLD^{FL} CD4-Cre (purple) mice with MOGp35-55 in Complete Freund's Adjuvants. Data represent mean (± SEM) clinical scores. Shown is one representative of three individual experiments (n=7 mice/group).

Since the development and severity of disease after MOG-induced EAE induction was altered between the different genotypes, we wanted to examine the reason for the clinical outcome. Therefore, we performed histological analysis on spinal cord sections from the indicated mice 30 days after immunization (Fig. 41A). In correlation with the clinical disease scores, we found less inflammation, demyelination and infiltration of T cells and macrophages in CYLD^{FL} CD4-Cre mice compared to the other groups. Importantly, in CYLD$^{ex7/8}$ and CYLD^{FL} CD11c-Cre mice the demyelination of the spinal cord as shown by LFB staining was more prominent than in WT control mice. As shown in Figure 41B-D, a detailed analysis of demyelination and infiltration of mononuclear cells into the spinal cord illustrated, that CYLD$^{ex7/8}$ mice developed an increased severity of disease after MOG-immunization. Demyelination of the spinal cord was enhanced compared to WT mice (Fig. 41B) and more invading macrophages (Fig. 41C) as well as CD3^{+} T cells (Fig. 41D) could be detected in the

spinal cord of these mice. These data demonstrate, that overexpression of sCYLD solely in T cells protects mice from EAE pathology by impairing immune cell infiltration into the spinal cord parenchyma. Strikingly, overexpression of sCYLD in dendritic cells led to the development of severe EAE symptoms after MOG-immunization. Further, CYLD$^{ex7/8}$ mice displayed a delayed onset of disease but also showed strong signs of EAE pathology.

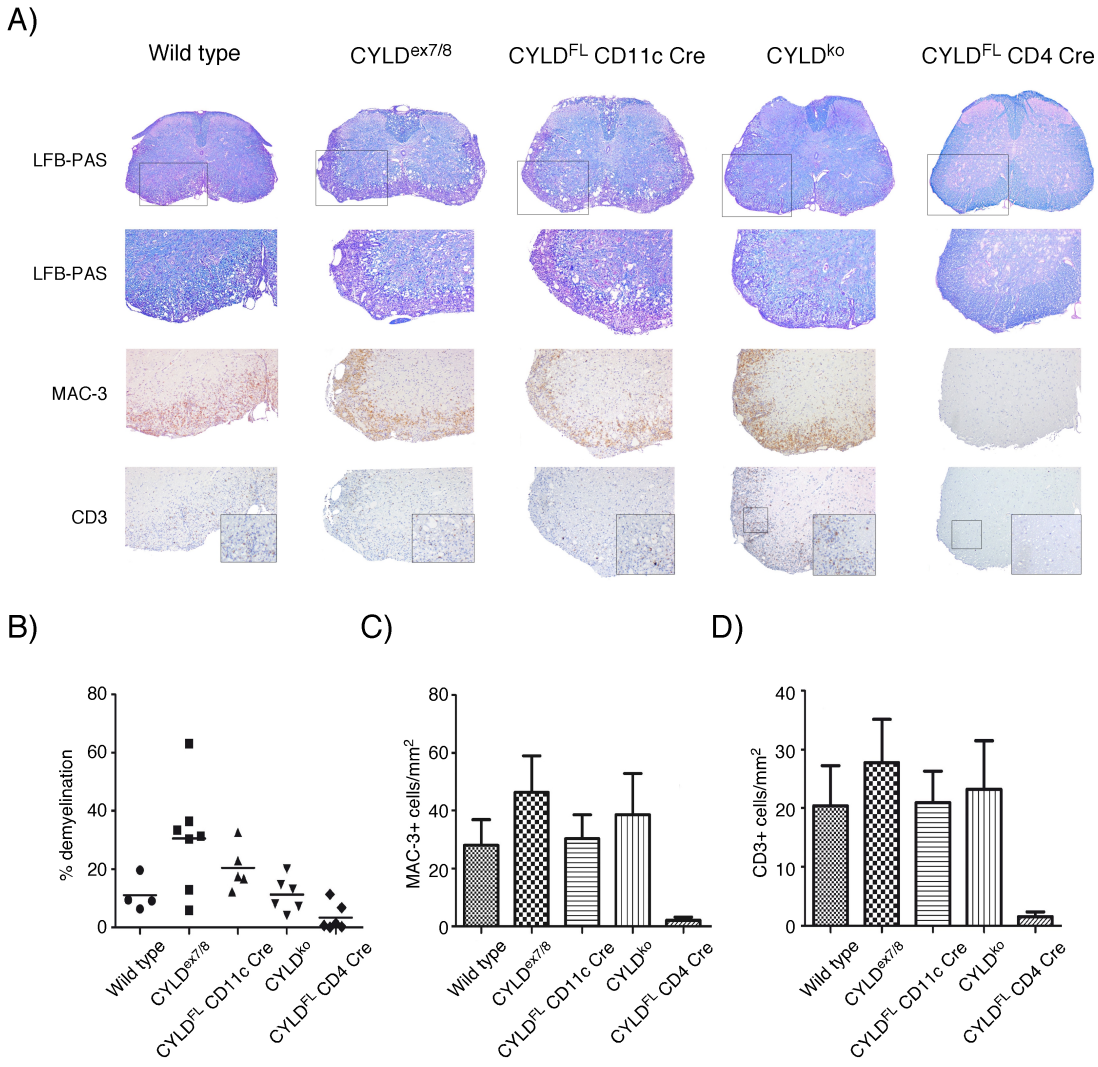

Figure 41: Enhanced mononuclear cell infiltration into the spinal cord of CYLD$^{ex7/8}$ mice. (A) Immunohistochemistry of paraffin embedded spinal cord sections from paraformaldehyd-perfused WT, CYLD$^{ex7/8}$, CYLD^{ko}, CYLD^{FL} CD11c-Cre and CYLD^{FL} CD4-Cre mice on day 30 after induction of EAE with MOGp35-55. Sections were stained with luxol fast blue-periodic acid Schiff (LFB), anti-macrophage-3 antigen (MAC-3) or anti-CD3. Shown are sections of representative mice. (B-D) Summary of experiment shown in (A), the horizontal line of the histograms represents the mean of all mice per group. Histograms display (B) the percentage of demyelination, (C) the numbers of infiltrating macrophages (MAC-3) and (D) the numbers of infiltrating T cells into the spinal cord from the indicated genotypes. Results are displayed as mean values ± SEM.

4 Discussion

CYLD is a member of the family of deubiquitiniating enzymes and was shown to be a negative regulator of the NF-κB signaling pathway (Trompouki et al. 2003) by interfering with signaling molecules TRAF2, TRAF6, NEMO as well as Bcl-3 (Massoumi, Chmielarska et al. 2007). To date, several groups have generated CYLD knockout mouse strains to investigate the function of CYLD *in vivo*, which all showed marked phenotypical differences (Zhang et al. 2006; Reiley et al. 2006; Massoumi et al. 2007). Recently, we have identified a naturally occurring splice variant of CYLD (sCYLD), which lacks exons 7 and 8 ($CYLD^{ex7/8}$) encompassing the binding sites for TRAF2 and NEMO (Hövelmeyer et al. 2007). $CYLD^{ex7/8}$ mice excessively overexpress sCYLD, while full lenght CYLD is absent. These mice exhibit enlarged spleens and peripheral lymphoid organs due to an accumulation of B cells. Further, B cells displayed enhanced survival capacity and NF-κB signaling, similary to the B cell phenotype of the $CYLD^{ko}$ mouse strain described by Jin *et al.* (Jin et al. 2007). In addition, hyperactivation accompanied with enhanced NF-κB activity of $CYLD^{ex7/8}$ bone marrow derived DCs could be observed (Srokowski, Masri et al. 2009). In this thesis, we investigated the role of sCYLD in the context of T cells using $CYLD^{ex7/8}$ mice compared to $CYLD^{ko}$ (Massoumi et al. 2007) and WT.

4.1 sCYLD positively regulates TCR signaling in thymocytes

In $CYLD^{ex7/8}$ mice we detected a strong reduction of total thymocytes when compared to control mice. Therefore, we examined the different developmental stages of T cell development and found, that $CD4^+$ and $CD8^+$ SP thymocytes and as well as peripheral T cells were drastically reduced, suggesting an essential role of sCYLD in thymocyte development. In a previous report, it was demonstrated that NF-κB has an important role in negative selection of thymocytes indicated by mice, in which the IκB super-repressor is expressed specifically by T cells (Hettmann, DiDonato et al. 1999). In these mice, DP thymocytes expressing a nondegradable form of IκBα are partially resistant to apoptosis induced by administration of CD3-specific antibodies *in vivo*. These data suggest, that NF-κB might play a role in the negative selection of thymocytes by exhibiting a pro-apoptotic function during the selection processes, possibly through upregulation of the expression of pro-apoptotic genes (Siebenlist et al. 2005). Thus, the enhanced activation of the NF-κB pathway in $CYLD^{ex7/8}$ thymocyes indicated by RT-PCR and Western Blot might explain the reduction of these cells during the transition from the DP to SP stage. When we investigating TCR signal transduction in thymocytes

by Western Blot we detected less phosphorylated Zap70 in stimulated $CYLD^{ex7/8}$ thymocytes suggesting a defect in TCR signaling. These findings are very similar to the T cell phenotype of $CYLD^{ko}$ mice described by Reiley *et al.*, where they established CYLD as a positive regulator of TCR signaling in thymocytes (Reiley, Zhang et al. 2006). They could show, that CYLD regulates a proximal step of TCR signaling in thymocytes by promoting the recruitment of active Lck to its substrate Zap70. However, $CYLD^{ko}$ mice we analyzed (Massoumi, Chmielarska et al. 2006) did not show any signs of defective T cell development, since the $CD4^+$ and $CD8^+$ SP thymocyte numbers were comparable to WT. Nevertheless, TCR signaling of those thymocytes was abrogated, since upon stimulation no active phosphorylated Zap70 could be detected. Importantly, when we analyzed the activation of Lck based on its phosphorylation, we found less phosphorylated Lck in $CYLD^{ko}$ thymocytes, contrary to the CYLD deficient mice previously published (Reiley, Zhang et al. 2006), where no difference in Lck phosphorylation between WT and CYLD deficient thymocytes could be detected. This result indicated, that sCYLD probably has a positive regulatory role in the activation of Lck, since $CYLD^{ex7/8}$ mice exclusively expressing sCYLD display no difference in Lck phosphorylation in contrast to the $CYLD^{ko}$ mice. Rao *et al.* reported, that the ubiquitination of Lck mediated by c-CBL is a negative mechanism that regulates the signaling function of Lck (Rao 2002), since K^{48}-linked ubiquitination of Lck results in its proteasomal degradation, whereas K^{63}-linked ubiquitination prevents the translocation of Lck to lipid rafts (Hawash, Kesavan et al. 2002), which provide a microenvironment for concentrating TCR signaling molecules. Hence, the translocation of Lck to lipid rafts promotes its interaction with Zap70, which was shown to be attenuated in the absence of CYLD (Reiley 2006) and promoted in the absence of CBL (Murphy 1998; Sun 2008). Generally, it is believed that K^{48}-linked ubiquitin chains mediate proteosome-dependent protein degradation, whereas K^{63}-linked ubiquitin chains mediate endocytosis and signal transduction (Galan and Haguenauer-Tsapis 1997; Wang 2001). Recently, it was shown that CYLD regulates Lck by removing both K^{63}- and K^{48}-linked polyubiquitin chains (Reiley 2006), which is in contrast to the K^{63}-specific activity of CYLD towards TRAFs and Bcl-3 (Kovalenko 2003; Trompouki, Hatzivassiliou et al. 2003; Massoumi, Chmielarska et al. 2006). Since sCYLD still habors a functional catalytic domain mediating its deubiquitinating activity, it can function as DUB and deubiquitinate Lck. These finding implicates, that sCYLD might positively regulate Lck function by removing poly-ubiquitin chains, thereby compensating the loss of FL-CYLD in $CYLD^{ex7/8}$ mice. Hence, sCYLD mediating deubiquitination of K^{48} would inhibit the proteosomal degradation of Lck, whereas removing poly-ubiquitin chains of K^{63} would promote the recruitment of active Lck to the lipid

rafts, which provide a microenvironment for concentrating TCR signaling molecules such as Zap70. Nevertheless, we observed less activated Zap70 in CYLD$^{ex7/8}$ thymocytes after TCR engagement when compared to WT. Therefore, it still remains unclear if sCYLD can completely compensate the loss of FL-CYLD by physically interacting with Lck and promoting its recruitment to Zap70 as shown for FL-CYLD.

4.2 The impact of sCYLD in the development of medullary thymic epithelial cells

Next, we crossed CYLD$^{ex7/8}$ mice onto the HY TCR transgenic background in order to analyze the selection processes of thymocyte development. In male HYtg CYLD$^{ex7/8}$ mice, we detected impaired negative selection of thymocytes leading to an increased population of DP and CD8^{+} SP thymocytes. Nevertheless, total cell numbers of thymocytes were drastically reduced compared to controls. In female HYtg CYLD$^{ex7/8}$ mice, we observed a profound effect on positive selection indicated by a 3-fold increased population of DP thymocytes in CYLD$^{ex7/8}$ and CYLD^{ko} mice compared to controls, suggesting a developmental block in the DP-SP transition of T cell development. Because we observed altered T cell development in CYLD$^{ex7/8}$ mice accompanied by an impairment of the negative as well as positive selection of thymocytes, we wanted to analyze the compartment of the thymus. In the thymus, the selection of thymocytes is mediated by thymic epithelial cells including mTECs and cTECs. mTECs are a cellular component of the thymic stroma building up the medullary compartment. They were shown to be essential in the negative selection of self-reactive thymocytes by expressing TCRs specific for certain types of self-antigens (Zhang et al. 2003; Gallegos et al. 2004; Kyewski and Derbinski 2004). In addition, it is well known, that the formation of the medullary compartment is strongly defective in mice which are deficient for positive selection (Shores, van Ewijk et al. 1991; Shores, van Ewijk et al. 1994; Nasreen, Ueno et al. 2003). Interestingly, CYLD$^{ex7/8}$ mice showed an altered thymic structure accompanied by a distortion of the cortico-medullary boundary indicated by thymic histology. By staining for UEA-1 we could demonstrate, that the number of mature mTECs was reduced. The decreased number of mTECs in CYLD$^{ex7/8}$ thymi might be responsible for the reduction of SP thymocytes, since it was shown that mTECs are essential in providing survival signals to SP thymocytes (Anderson, Lane et al. 2007). Moreover, the defect in positive selection of thymocytes in CYLD$^{ex7/8}$ mice could explain the alteration of the medullary compartment.

Another study demonstrated an important role of the LTβR signaling pathway in regulating the development of mTECs, since mice deficient in LTβR exhibit disorganized thymic medullar, reduced numbers of mTECs and develop autoimmunity (Boehm, Scheu et al. 2003). LTβR signaling in mTECs results in the activation of the noncanonical NF-κB pathway, thereby allowing the differentiation of TEC precursors into mature mTECs. Hence, mice deficient in NF-κB2 display impaired mTEC development and multiorgan infiltration of activated T cells, confirming a physiological function of NF-κB2 in the regulation of mTECs (Zhang, Wang et al. 2006). In addition, the expression and activation of RelB, a member of the noncanonical NF-κB pathway, is essential for the development of mature mTECs (Weih F. et al. 1995; Burkly et al. 1995). RelB deficient mice develop rapid multiorgan inflammation and autoimmunity, and exhibit a disrupted thymic medullary compartment (Weih F. et al. 1995; Burkly et al. 1995). Therefore, autoimmunity in these mice is promoted by the absence of mature mTECs, altered thymic architecture, defects in negative selection, or a combination of the above. Of note, in addition to the altered thymic structure and reduced mTEC number, $CYLD^{ex7/8}$ mice displayed a reduction of RelB expression in mTECs, suggesting a regulatory role of sCYLD in mTEC development. In mTECs, the reduced expression of RelB downregulates the noncanonical NF-κB pathway and thereby interfering with the maturation of mTECs, which might explain the decreased numbers of mature mTECs in $CYLD^{ex7/8}$ thymi.

4.3 $CYLD^{ex7/8}$ T cells display a hyperactivated phenotype

To investigate, if sCYLD is important in regulating T cell activation, we first examined the activation of $CYLD^{ex7/8}$ T cells *in vitro*. Upon stimulation, most of the $CYLD^{ex7/8}$ T cells died, suggesting that they might be more susceptible to activation induced cell death (AICD) compared to WT and $CYLD^{ko}$ T cells. Further, we observed in an *in vivo* cell transfer model that $CYLD^{ex7/8}$ $CD4^+$ T cells proliferated to a greater extent than WT. Moreover, upon TCR stimulation peripheral $CYLD^{ex7/8}$ T cells produced increased amounts of inflammatory cytokines such as IL-6 and IL-17A. In order to understand the molecular mechanism mediating these abnormal T cell responses, we investigated the activation of the NF-κB pathway in peripheral T cells. Importantly, the expression of noncanonical NF-κB members RelB and p100 was markedly enhanced at both protein and mRNA level, displaying a constitutive activation of this pathway even without external stimuli. These data show, that the hyperresponsive phenotype of $CYLD^{ex7/8}$ T cells might be caused by the strong upregulation of the noncanonical NF-κB pathway. Similar results such as abnormal T cell responses and constitutive NF-κB activa-

tion were obtained by Reiley *et al.* (Reiley, Jin et al. 2007) in CYLD deficient T cells. They demonstrated that CYLD negatively regulates the activation of Tak1 by removin poly-ubiquitin chains, which resulted in constitutive activation of NF-κB and JNK signaling. Therefore, it has to be examined if sCYLD still can deubiquitinate Tak1. If sCYLD cannot regulate Tak1 activation, it would explain the high activation of NF-κB signaling in $CYLD^{ex7/8}$ T cells.

4.4 sCYLD overexpression disturbs the suppressive function of regulatory T cells

In previous studies it was reported, that NF-κB signaling is implicated in the regulation of Treg development (Isomura, Palmer et al. 2009; Jana, Jailwala et al. 2009; Josefowicz and Rudensky 2009; Long, Park et al. 2009; Ruan, Kameswaran et al. 2009; Visekruna, Huber et al. 2010). Long *et al.* demonstrated, that an upregulation of NF-κB activity resulted in an increased percentage and absolute number of $Foxp3^+$ Treg cells in the thymus, whereas inhibiting NF-κB activity led to a striking reduction in the number of thymic Treg cells (Long, Park et al. 2009). Further, they could show that restoring NF-κB activity with a constitutively active IKKβ (IKKEE-Tg) transgene rescued Foxp3 expression in TAK1- or CARMA1-deficient thymocytes that otherwise showed the most dramatic impairment in Treg cell development. These results implicate an essential role of NF-κB activation in the development and regulation of Treg cells. Because of the increased activation of NF-κB signaling in $CYLD^{ex7/8}$ thymocytes and peripheral T cells, we examined Treg cells in these mice. Consistent with the involvement of NF-κB in Treg development, we detected an increased frequency of Treg cells in the thymus as well as spleen and LNs of $CYLD^{ex7/8}$ mice when compared to WT and $CYLD^{ko}$ mice. It is important to note, that most of the $Foxp3^+$ Tregs were negative for the surface expression of CD25, which plays an essential role for the development of Treg cells by facilitating the expression of Foxp3. In contrast to the $CYLD^{ko}$ mice we analyzed (Massoumi, Chmielarska et al. 2006), Lee *et al.* detected in their CYLD deficient mice also increased frequencies of Treg cells in both the thymus and LNs (Lee, Wu et al. 2010). Importantly, the Treg phenotype of these mice differs from that of $CYLD^{ex7/8}$ mice, since their CYLD deficient Treg cells do express CD25 in contrast to the Treg population in $CYLD^{ex7/8}$ mice. Moreover, the $CYLD^{ex7/8}$ Treg phenotype is comparable to the one of IKEE-Tg mice, which overexpress a constitutively active IKKβ (Long, Park et al. 2009). These mice have abnormally high levels of $Foxp3^+$ thymocytes, which do not express CD25. The phenotypical

differences of Treg cells in CYLD$^{ex7/8}$ and CYLD deficient mice (Lee, Wu et al. 2010) might be due to the activation of different NF-κB signaling pathways. In addition, overexpression of sCYLD could drive the expression of Foxp3 independently of the IL-2 signal, since it was demonstrated that young IL-2$^{-/-}$ and IL-2Rα$^{-/-}$ mice have relatively normal numbers of thymic and peripheral Foxp3^{+} T cells (D'Cruz and Klein 2005; Fontenot, Rasmussen et al. 2005), pointing to other regulatory mechanism driving the expression of Foxp3. When we investigated the suppressive capacity of CYLD$^{ex7/8}$ Treg cells by an *in vitro* suppression assay or in an *in vivo* adoptive transfer model of colitis, we found that these cells were not able to suppress as the control cells. Similar results were obtained for IKKEE-Tg Foxp3 cells, which were not suppressive when measured by an *in vitro* suppression assay (Long, Park et al. 2009). These Treg cells exhibit similar to CYLD$^{ex7/8}$ T cells constitutive NF-κB activity, which might be important in regulating the functional capacity of Treg cells. The alterations of Treg cell frequences and suppressive function in CYLD$^{ex7/8}$ mice can be also due to the distortion of the thymic structure, since it is well known that natural Foxp3^{+} Treg cells originate in the medullary compartment of the thymus (Maloy and Powrie 2001; Shevach 2002; Sakaguchi 2004). There, mTECs induce the selection of Treg cells, that encompass a wide spectrum of self-reactivity, as determined by promiscuous gene expression (Derbinksi, Schulte et al. 2001). Hence, thymus-derived Treg cells are involved in the control of various tissue-specific autoimmune diseases (Sakaguchi 2000; Seddon and Mason 2000). The interaction of Treg precursors and mTECs in the medullary compartment is essential to produce functional Foxp3^{+} Treg cells, which then enter the periphery to ensure self-tolerance. The reduced numbers of mature mTECs in CYLD$^{ex7/8}$ thymi may explain the failure of CYLD$^{ex7/8}$ Treg cells to suppress abnormal T cell responses. In summary, these results indicate that the increased NF-κB activity in CYLD$^{ex7/8}$ cells promotes the expression of Foxp3 and the Treg cell lineage differentiation in the thymus. Thus, enhanced NF-κB activity in thymocytes might play a crucial role in shifting the ratio of conventional and regulatory T cells towards the regulatory T cells. However, overexpression of sCYLD inhibits the suppressive capacity of Treg cells, in which the molecular mechanism has still to be investigated.

4.5 sCYLD drives the development of spontaneous intestinal inflammation

When we analyzed how sCYLD influences T cell development and regulation, we found that the overexpression of sCYLD drives T cells to a hyperresponsive phenotype accompanied by an increased production of inflammatory cytokines. Moreover, the number of mTECs building up the medullary thymic compartment was drastically reduced. Since an impairment of

mTEC development and therefore abolished negative selection of autoreactive T cells as well as abnormal T cell responses were shown to cause multiorgan inflammation and autoimmunity (Burkly, Hession et al. 1995; Weih, Carrasco et al. 1995), we examined $CYLD^{ex7/8}$ mice for autoimmunity. Importantly, these mice spontaneously developed a mild intestinal inflammation with larger lymphoid follicles and colonic patches, which is known to be implicated in the development of inflammation in human IBD. Of note, the $CYLD^{ko}$ mice we analyzed (Massoumi, Chmielarska et al. 2006) did not develop any signs of colitis. In contrast to that, CYLD deficient mice published by Reiley *et al.* displayed severe symptoms of spontaneous intestinal inflammation mediated by hyperactivated $CD4^+$ T cells (Reiley, Jin et al. 2007). In their studies, they establish CYLD as a specific DUB preventing spontaneous activation of the Tak1 axis of TCR signaling and thereby maintaining normal T cell responses. It has to be investigated, if sCYLD can still interact with Tak1 and inactivate it by removing ubiquitins, since $CYLD^{ex7/8}$ T cells show similar abnormal T cell responses as the $CYLD^{ko}$ published by Reiley *et al.* In another study it was demonstrated, that $CYLD^{ko}$ mice did not develop spontaneous colitis, but these mice were more sensitive to dextran sodium sulfate-induced colitis and showed a dramatic increase in the incidence of tumours in a colitis-associated cancer model (Zhang 2006). It is important to note, that in these mice the development of B cells, T cells and myeloid cells was unaffected in contrast to the $CYLD^{ko}$ mice published by Reiley *et al.* (Reiley 2006; Jin, Reiley et al. 2007). Costello *et al.* investigated the expression of *cyld* in colons of UC and CD patients (Costello, Mah et al. 2005). By microarray analysis they could show that the *cyld* gene was significantly down-regulated in both human IBD subtypes, UC and CD. Hence, the decreased expression of the *cyld* gene might display an inflammation control response that is lost or impaired in some way in IBD. Moreover, the *cyld* gene is located within the major IBD susceptibility locus IBD-1, which also contains the *nod2* gene. Nod2 is known to mediate NF-κB activation and genetic mutations in *nod2* were shown to increase the risk of human IBD development (Hugot, Chamaillard et al. 2001; Ogura, Bonen et al. 2001). In both animal models and human studies, CYLD seems to be an important regulator of IBD.

When we crossed $CYLD^{ex7/8}$ mice onto a TCR transgenic background, either 2D2tg or HYtg, these mice developed a dramatic spontaneous colitis accompanied by massive infiltration of inflammatory cells such as $CD4^+$ and $CD8^+$ T cells, macrophages, dendritic cells and neutrophils. Additionally, the expression and activation of STAT-3 was drastically upregulated, which is known to be enhanced in the colonic lamina propria of patients suffering from both

Crohn's disease and Ulcerative colitis. Moreover, we found a significant increase of inflammatory cytokines in the colon of CYLD$^{ex7/8}$ mice, which are known to drive intestinal inflammation. Of note, the cytokine IL-6, which is an important regulator of STAT-3 activation, was increased 250-fold compared to controls. Because of the hyperresponsiveness of CYLD$^{ex7/8}$ T cells, we asked if these cells were responsible for causing the intestinal inflammation. Importantly, in an adoptive transfer model of colitis we observed that CYLD$^{ex7/8}$ effector CD4^{+} T cells were not able to home to the gut and induce colitis as opposed to the control cells. In this model of colitis, naive CD4^{+} T cells are capable of inducing colitis in lymphopenic RAG1$^{-/-}$ recipients, where they start homeostatic proliferation, migrate to mLNs and get activated by DCs to produce inflammatory cytokines triggering intestinal inflammation. The time course for this model takes at least 2-3 weeks for colitis development. Since we observed already in previous experiments, that CYLD$^{ex7/8}$ T cells are hyperresponsive and highly susceptible to AICD, we conclude that the time course of this colitis model is not useable to examine the capability of CYLD$^{ex7/8}$ T cells to induce intestinal inflammation. Because we could show by histology a dramatic infiltration of CD4^{+} T cells into the lamina propria of CYLD$^{ex7/8}$ mice and found a strong upregulation of T_H1, T_H2 and T_H17 produced cytokines in the intestine, we conclude that indeed the abnormal T cell responses of CYLD$^{ex7/8}$ CD4^{+} T cells may mediate the development of intestinal inflammation. Moreover, it was demonstrated that mTECs, which are responsible for the deletion of thymocytes expressing TCRs specific for certain types of self-antigens (Zhang et al. 2003; Gallegos et al. 2004), are crucial in promoting central T cell tolerance. Indeed, RelB deficient mice, which fail to develop functional mature mTECs develop rapid multiorgan inflammation and autoimmunity, and have a disrupted thymic medullary compartment (Weih F. et al. 1995; Burkly et al. 1995). Hence, the absence of mature mTECs and the altered thymic architecture in these mice might mediate the development of autoimmunity. In CYLD$^{ex7/8}$ mice we could show, that overexpression of sCYLD negatively regulates mTEC development and differentiation resulting in a distortion of the medullary compartment in these mice. Thus, the decrease of mTECs leads to a defect in negative selection of autoreactive T cells, which probably enter the periphery and cause autoimmunity such as intestinal inflammation. Another explanation for the spontaneous development of colitis in CYLD$^{ex7/8}$ mice may be an imbalance of pro-inflammatory and regulatory T cell responses. Indeed, we could show that CYLD$^{ex7/8}$ regulatory T cells were not able to suppress an inflammatory response *in vivo* in an adoptive transfer model of colitis. The regulatory disfunction of Treg cells together with a hyperresponsive phenotype of CD4^{+} T cells may result in intestinal pathology in CYLD$^{ex7/8}$ mice.

4.6 T cell-independent colitis in RAG1$^{-/-}$ CYLD$^{ex7/8}$ mice

When we examined CYLD$^{ex7/8}$ mice for autoimmunity, we observed that these mice were spontaneously developing intestinal pathology accompanied by a massive infiltration of inflammatory cells such as T cells, DCs, neutrophils and macrophages. The hyperactivated phenotype of T cells as well as the reduced suppressive capacity of Treg cells in CYLD$^{ex7/8}$ mice might explain the colitis development. Additionally, we wanted to investigate the contribution of innate immune cells such as DCs in the development of intestinal immune pathology in CYLD$^{ex7/8}$ mice, since it was reported that sCYLD is a positive regulator of NF-κB activity and its overexpression induces a hyperactive phenotype of bone marrow derived DCs *in vitro* as well as *in vivo* (Srokowski, Masri et al. 2009). DCs are known to play an essential role in the development of intestinal inflammation. Intestinal DCs sample gut-lumen derived antigen, traffic to the mLN, where they activate T cells to proliferate and express the gut-homing integrin $\alpha_4\beta_7$ (Stagg, Kamm et al. 2002). Activated T cells migrate to the lamina propria, start to express inflammatory cytokines, which drive further recruitment of inflammatory cells. Because of the hyperactivated DC phenotype in CYLD$^{ex7/8}$ mice, we wanted to investigate the involvement of these cells in mediating intestinal inflammation. Therefore, we crossed CYLD$^{ex7/8}$ mice to the RAG1$^{-/-}$ mouse strain, which lacks T and B cells, and induced colitis by adoptively transferring conventional CD4^{+} WT cells. RAG1$^{-/-}$CYLD$^{ex7/8}$ mice turned out to be highly susceptible in the transfer colitis model suggesting an essential role of DCs in mediating spontaneous colitis in CYLD$^{ex7/8}$ mice. Indeed, DCs of RAG1$^{-/-}$CYLD$^{ex7/8}$ mice displayed a hyperactivated phenotype as shown by a strong upregulation of MHCII and CD86 surface expression. Further, these cells had a better presentation efficiency as control DCs indicated by *in vitro* co-culture experiments. The hyperactivated DC phenotype might explain the abnormal T cell activation and migration into lamina propria of the intestine. In addition, it would be interesting to examine in CYLD$^{ex7/8}$ T cells the expression of the gut-homing integrin $\alpha_4\beta_7$, which was shown to be induced by activated DCs. Moreover, when we analyzed aging RAG1$^{-/-}$CYLD$^{ex7/8}$ mice, we found that these mice were spontaneously developing a T cell-independent colitis phenotype accompanied by a dramatic infiltration of innate immune cells, such as DCs, macrophages and neutrophils. Also the expression of inflammatory cytokines important in mediating an IBD-like disease were highly upregulated. Importantly, the expression of the cytokines IL-22 and IL-6 were dramatically upregulated, which are known to be produced by DCs in response to extracellular bacteria and contribute to the pathogenesis of IBD (Shih and Targan 2009). Studies in model systems have revealed a pivotal role for the

cytokine IL-23 in the development of chronic intestinal inflammation. Of note, also IL-23 was upregulated, which is primarily secreted by activated DCs, monocytes and macrophages. IL-23 was shown to have inflammatory effects on innate immune cells and to drive T cell-independent colitis in the gut (Takatori, Kanno et al. 2009) by inducing the production of inflammatory cytokines, such as IL-1, IL-6 and TNF-α, by monocytes and macrophages (Langrish, McKenzie et al. 2004; McKenzie, Kastelein et al. 2006). Also in colons of $RAG1^{-/-}$ $CYLD^{ex7/8}$ mice we could show a significant upregulation of IL-6 and TNF-α. Consistent with this upregulation, we found elevated numbers of infiltrating neutrophils and macrophages into the colon of these mice. In order to further analyze the contribution of macrophages and DCs into the development of spontaneous T cell-independent colitis when sCYLD is overexpressed, we will cross $CYLD^{FL}$ LysM-Cre and $CYLD^{FL}$ CD11c-Cre mice onto the $RAG1^{-/-}$ background to specifically overexpress sCYLD either in macrophages or DCs in the absence of B and T cells. Hence, we will be able to analyze the involvement of innate immune cells overexpressing sCYLD, such as macrophages and DCs, to mediate T cell-independent intestinal immune pathology.

4.7 Increased production of nuclear autoantibodies in TCR transgenic $CYLD^{ex7/8}$ mice

Antibodies against nuclear self-antigens (ANA) are the most common autoantibodies observed in autoimmune conditions in mouse and human (Vinuesa, Sanz et al. 2009). The presence of tissue-specific autoantibodies strongly underscores the loss of tolerance. In three independent reports, various autoantibodies have been described in patients with IBD, showing the existence of antinuclear autoantibodies in patients with Crohn's disease and ulcerative colitis (Zauli, Crespi et al. 1985; Dalekos, Manoussakis et al. 1993; Reumaux, Mézière et al. 1995). However, the role of these autoantibodies in the pathogenesis of IBD is not yet clarified. When we crossed $CYLD^{ex7/8}$ mice onto a TCR transgenic backround, either 2D2 or HY TCR transgenic, these mice developed sever intestinal pathology similar to the pathology of human IBD. Since ANAs are found in association with many different autoimmune dieseases and could be detected in patients of IBD, we analyzed these mice for the production of ANAs. Of note, we found numerously amounts of ANAs by immunohistostaining of Hep2 cells in the sera of these mice when compared to controls. The large amounts of ANAs produced in $CYLD^{ex7/8}$ TCR transgenic mice might be pathogenic and lead to increased susceptibility to autoimmunity detected in these mice.

4.8 CYLD$^{ex7/8}$ mice are more susceptible to EAE

The human autoimmune disorder MS and its animal model EAE are known to be a CD4$^+$ T cell-mediated autoimmune disease affecting the central nervous system. Historically, the disease was for a long time considered to be a T_H1-mediated disease (Sospedra and Martin 2005), supported by a clinical trial showing that administration of the T_H1 cytokine IFNγ exacerbates MS (Panitch, Hirsch et al. 1987). In addition, it was demonstrated that EAE can be induced by the adoptive transfer of myelin-reactive T_H1 cells (Baron 1993; Kuchroo, Martin et al. 1993). Previous data in genetically modified animals began to question the T_H1 model of MS. It could be shown, that mice deficient in IFNγ are highly susceptible to EAE (Ferber 1996; Willenborg, Fordham et al. 1996), whereas overexpression of T_H1 cytokines in the CNS ameliorates EAE (Furlan 2001). Recent reports have established that IL-17-producing CD4$^+$ T cells, referred to as T_H17 cells, play a pivotal role in the autoimmune pathology of EAE (Nakae, Nambu et al. 2003; Langrish 2005). As described above, we could demonstrate, that CYLD$^{ex7/8}$ mice were more susceptible to the development of the autoimmune disease IBD. Moreover, overexpression of sCYLD drives T cells to be hyperresponsive accompanied by increased production of inflammatory cytokines such as IL-17A. Because of the pathogenic role of IL-17A in the development of EAE, we wanted to examine the susceptibilty of CYLD$^{ex7/8}$ mice to the induction of EAE. Importantly, CYLD$^{ex7/8}$ mice displayed an increased severity of EAE development with enhanced demyelination of the spinal cord and increased infiltration of macrophages and T cells into the spinal cord when compared to WT mice. Since we detected an imbalance of pro-inflammatory and regulatory T cell responses in CYLD$^{ex7/8}$ mice, we wanted to examine if the increased susceptibility to EAE in these mice might be T cell intrinsic. Thus, we analyzed the suceptibility to EAE of CYLD^{FL} CD4-Cre mice which overexpress sCYLD solely in T cells. Strikingly, these mice developed only a mild form of EAE and exhibited less infiltration of macrophages as well as T cells into the spinal cord. These data might be explained by the observations that T cells overexpressing sCYLD are highly susceptible to AICD after activation. Therefore, most of the activated T cells probably died after MOG-immunization and cannot act as inflammatory cells in the pathogenesis of EAE in CYLD^{FL} CD4-Cre mice. Nevertheless, CYLD$^{ex7/8}$ mice developed a stronger EAE than WT control mice, implicating other cell types to be responsible for the CNS inflammatory pathology in these mice.

In previous studies, it was demonstrated that DCs have a pivotal role in CNS inflammation. By using a system where MHC class II expression is exclusively restricted to CD11c$^+$ DCs,

Greter *et al.* could demonstrate that these mice were susceptible to adoptive transfer EAE, suggesting that $CD11c^+$ DCs alone are sufficient for the development of EAE (Greter, Heppner et al. 2005). Moreover, it was shown that the number of DCs is correlated with the disease severity in EAE (Whartenby, Calabresi et al. 2005). Hence, the fact that $CD11c^+$ DCs are the only cell type required for the induction of EAE and that their increased numbers correlates with increased severity of disease underlines the importance of DCs to facilitate the autoimmune pathology of EAE. Because we could demonstrate, that $CYLD^{ex7/8}$ DCs exhibit a hyperactivated phenotype and increased presentation capacity, we were interested to examine the capability of these cells to mediate the development of EAE. For this purpose, we induced EAE in $CYLD^{FL}$ CD11c-Cre mice, which overexpress sCYLD solely in DCs. Of note, these mice displayed an earlier onset of disease and developed the highest clinical score of disease than control mice. In correlation to the clinical score, sever demyelination of the spinal cord as well as a massive infiltration of T cells and macrophages could be observed. Hence, these data underline the importance of DCs in the propagation of CNS inflammation. Furthermore, the enhanced antigen presenting capacity of DCs overexpressing sCYLD might explain the severity of disease after MOG-immunization in $CYLD^{ex7/8}$ mice. In addition, several studies documented that macrophages play an essential role as effector cells in EAE (Brosnan, Bornstein et al. 1981). Brosnan *et al.* showed that macrophage depletion can delay the onset of clinical signs and reduce the severity of disease in EAE. To investigate the impact of macrophages in EAE progration in $CYLD^{ex7/8}$ mice, $CYLD^{FL}$ LysM-Cre mice, in which exclusively macrophages overexpress sCYLD, were analyzed for the development of EAE after MOG-immunization. Importantly, these mice displayed sever EAE pathogenesis when compared to control mice (unpublished data by Jouman Masri), suggesting that overexpression of sCYLD in macrophages contributes to the severity of MOG-induced EAE in $CYLD^{ex7/8}$ mice.

5 Summary

The tumour suppressor gene *cyld* is mutated in familial cylindromatosis, an autosomal-dominant condition that predisposes to multiple skin tumours. The deubiquitinase CYLD acts as a negative regulator of NF-κB signaling. To analyse the function of CYLD *in vivo* we used the $CYLD^{ex7/8}$ mice, which are characterized by loss of the full-length transcript and overexpression of a short splice variant of CYLD (sCYLD). In $CYLD^{ex7/8}$ mice the overexpression of sCYLD results in splenomegaly and lymphadenopathy. Additionally, the B cell population in spleen and lymph nodes is increased at the expense of T cells. Analysis of $CYLD^{ex7/8}$ T cells showed a significant reduction of CD4 single positive (SP) and CD8 SP T cells in the thymus and in the periphery. By investigating the impact of sCYLD in TCR signaling in thymocytes, we could demonstrate that sCYLD partially inhibited the activation of Zap70 and thereby negatively regulated TCR signaling. *In vitro* as well as *in vivo* we could show that $CD4^+$ T cells displayed a hyperactive phenotype, proliferated to a better extent than WT cells and expressed high amounts of inflammatory cytokines such as IL-6 and IL-17A. Western Blots of steady state thymocytes and peripheral $CD4^+$ T cells were performed, showing that the noncanonical pathway was highly upregulated visualized by the expression levels of RelB and p100 leading to a hyperactive phenotype of $CD4^+$ T cells. In order to investigate the contribution of sCYLD in positive and negative selection in the thymus *in vivo*, the HY-TCR transgene (HYtg) was crossed to $CYLD^{ex7/8}$ mice. The analysis of $CYLD^{ex7/8}$ HYtg males revealed an increase in $CD4^+CD8^+$ DP as well as in $CD8^+$ SP thymocytes, suggesting a less pronounced negative selection in CYLD mutant mice compared to HYtg control mice. Interestingly, the impaired negative selection in the thymus was accompanied by a strong colitis phenotype at early ages (4 weeks). Since medullary TECs (mTECs) play an important role in the late stage of T cell development by negatively selecting autoreactive thymocytes, the levels of mTECs in the medullary compartment was investigated. Of note, low numbers of mTECs were observed, combined with decreased expression levels of the mTEC markers UEA-1, keratin-5, claudin-3 and claudin-4. The reduction of mTECs in the medullary compartment could explain the inflammatory phenotype of $CD4^+$ T cells in $CYLD^{ex7/8}$ mice leading to the severe intestinal pathology observed in these mice. Taken together, these results show an important role of sCYLD in T cell development and function as well as in NF-κB signaling of T cells.

6 Zusammenfassung

Das Tumorsuppressor Gen *cyld* ist mutiert in Patienten mit familiärer Zylindromatose, was zu einer autosomal-dominant vererbten Prädisposition für multiple Tumore der Haut führt. Die Deubiquitinase CYLD ist ein negativer Regulator des NF-κB Signalweges und hemmt die Aktivierung des Transkriptionsfaktors NF-κB, welcher an Entzündungsreaktion, Immunantwort, Apoptose und Onkogenese beteiligt ist. Um die *in vivo* Funktion von CYLD zu untersuchen, wurde der Mausstamm $CYLD^{ex7/8}$ analysiert, welcher ausschließlich eine natürlich vorkommende Spleißvariante des *cyld* Gens (sCYLD) überexprimiert. Als Kontrollen dienten $CYLD^{ko}$ und WT Mäuse. In $CYLD^{ex7/8}$ Mäusen führte die Überexpression von sCYLD zu vergößerten sekundären lymphatischen Organen wie der Milz und den peripheren Lymphknoten. Dieser Phänotyp resultierte aus einer drastischen Ansammlung von B Zellen, wohingegen die Anzahl von T Zellen stark reduziert war. Des Weiteren konnte gezeigt werden, dass die Gesamtzellzahl von CD4 SP und CD8 SP T Zellen sowohl im Thymus als auch in der Milz signifikant verringert war. Um die Rolle von sCYLD im TCR Signalweg der Thymozyten zu charakterisieren wurde mittels Western Blot der Signalweg untersucht. Interessanterweise konnte gezeigt werden, dass sCYLD die Aktivierung und Phosphorylierung der Proteinkinase Zap70 herunterreguliert, und somit den TCR Signalweg in Thymozyten negativ reguliert. Des Weiteren konnte sowohl *in vitro* als auch *in vivo* demonstriert werden, dass sCYLD überexprimierende $CD4^+$ T Zellen einen hyperaktiven Phänotyp besitzen, eine erhöhte Proliferationskapazität aufweisen und vermehrt inflammatorische Zytokine wie IL-6 und IL-17A produzieren. Da bekannt ist, dass CYLD ein Inhibitor des NF-κB Signalweges ist, wurde mit Hilfe von RT PCR und Western Blot die Rolle von sCYLD in diesem Signalweg untersucht. In $CYLD^{ex7/8}$ Thymozyten und peripheren $CD4^+$ T Zellen konnte eine erhöhte Aktivität des alternativen NF-κB Signalweges nachgewiesen werden, wohingegen der klassische NF-κB Signalweg keine Veränderung im Vergleich zu den Kontrollen aufwies. Um den Einfluss von sCLYD auf die positive und negative Selektion *in vivo* im Thymus zu untersuchen, wurden $CYLD^{ex7/8}$ Mäuse mit HY TCR transgenen Mäusen verpaart. Die Analyse der HYtg $CYLD^{ex7/8}$ Männchen zeigte eine erhöhte Anzahl an $CD4^+CD8^+$ DP und $CD8^+$ SP Thymozyten, was auf einen Defekt in der negativen Selektion von Thymozyten hinweist. Interessanterweise entwickelten HYtg $CYLD^{ex7/8}$ Männchen im Alter von 4 Wochen zusätzlich eine spontane Inflammation des Darmes.

Epithelzellen der thymischen Medulla (mTECs) spielen eine essentielle Rolle in der Entwicklung zentraler Toleranz, indem sie für die Eliminierung autoreaktiver T Zellen während der

späten T Zell Entwicklung im Thymus verantwortlich sind. Untersuchungen der mTECs in $CYLD^{ex7/8}$ Mäusen zeigten eine starke Reduktion dieser Zellpopulation im Thymus. Die Reduktion der mTECs in $CYLD^{ex7/8}$ Thymi könnte den inflammatorischen Phänotyp der $CD4^+$ T Zellen erklären und somit die Entwicklung der spontanen intestinalen Pathologie.

In den experimentellen Analysen der $CYLD^{ex7/8}$ T Zellen konnte gezeigt werden, dass die Überexpression von sCLYD in T Zellen eine wichtige Rolle in deren Entwicklung und Regulierung spielt und essentiell für die Aktivierung des alternativen NF-κB Signalweges ist.

7 References

Aifantis, I., J. Buer, et al. (1997). "Essential Role of the Pre-T Cell Receptor in Allelic Exclusion of the T Cell Receptor β Locus." Immunity 7(5): 601-607.

Alt, F., N. Rosenberg, et al. (1981). "Organization and reorganization of immunoglobulin genes in A-MuLV-transformed cells: Rearrangement of heavy but not light chain genes." Cell 27(2, Part 1): 381-390.

An, J., D. Mo, et al. (2008). "Inactivation of the CYLD deubiquitinase by HPV E6 mediates hypoxia-induced NF-κB activation." Cancer Cell 14: 394-407.

Anderson, G. and E. J. Jenkinson (2001). "Lymphostromal interactions in thymic development and function." Nat Rev Immunol 1(1): 31-40.

Anderson, G., P. J. L. Lane, et al. (2007). "Generating intrathymic microenvironments to establish T-cell tolerance." Nat Rev Immunol 7(12): 954-963.

Andreotti, A. H., P. L. Schwartzberg, et al. (2010). "T-Cell Signaling Regulated by the Tec Family Kinase, Itk." Cold Spring Harbor Perspectives in Biology 2(7).

Apostolou, I. and H. von Boehmer (2004). "In Vivo Instruction of Suppressor Commitment in Naive T Cells." The Journal of Experimental Medicine 199(10): 1401-1408.

Asano, Toda, et al. (1996). "Autoimmune disease as a consequence of developmental abnormality of a T cell subpopulation." J Exp Med August 1(184(2)): 387–396.

Asseman, C., S. Mauze, et al. (1999). "An essential role for interleukin 10 in the function of regulatory T cells that inhibit intestinal inflammation." J. Exp. Med. 190: 995-1004.

Atreya, I., R. Atreya, et al. (2008). "NF-κB in inflammatory bowel disease." Journal of Internal Medicine 263(6): 591-596.

Baron, J. L., Madri, J. A., Ruddle, N. H., Hashim, G., and Janeway, C. A., Jr. (1993). "Surface expression of alpha 4 integrin by CD4 T cells is required for their entry into brain parenchyma." J Exp Med 1(177): 57-68.

Bennett, C. L. (2001). "The immune dysregulation, polyendocrinopathy, enteropathy, X-linked syndrome (IPEX) is caused by mutations of FOXP3." Nature Genet. 27: 20-21.

Bettelli, E., Pagany, M., Weiner, H.L., Linington, C., Sobel, R. A., and Kuchroo, V. K. (2003). "Myelin oligodendrocyte glycoprotein-specific T cell receptor transgenic mice develop spontaneous autoimmune optic neuritis." J Exp Med 197, 1073-1081.

Biggs, P. J., R. Wooster, et al. (1995). "Familial cylindromatosis (turban tumour syndrome) gene localised to chromosome 16q12-q13: evidence for its role as a tumour suppressor gene." Nat Genet 11(4): 441-443.

Bignell, G. R. (2000). "Identification of the familial cylindromatosis tumour-suppressor gene." Nature Genet. 25: 160-165.

Boehm, T., S. Scheu, et al. (2003). "Thymic medullary epithelial cell differentiation, thymocyte emigration, and the control of autoimmunity require lympho-epithelial cross talk via LTbetaR." J Exp Med 198: 757-769.

Brosnan, C., M. Bornstein, et al. (1981). "The effects of macrophage depletion on the clinical and pathologic expression of experimental allergic encephalomyelitis." The Journal of Immunology 126(2): 614-620.

Brummelkamp, T. R., S. M. Nijman, et al. (2003). "Loss of the cylindromatosis tumour suppressor inhibits apoptosis by activating NF-κB." Nature 424: 797-801.

Brunkow, M. E. (2001). "Disruption of a new forkhead/winged-helix protein, scurfin, results in the fatal lymphoproliferative disorder of the scurfy mouse." Nature Genet. 27: 68-73.

Burkly, L., C. Hession, et al. (1995). "Expression of relB is required for the development of thymic medulla and dendritic cells." Nature 373(6514): 531-536.

Cantor, H. and E. A. Boyse (1975). "Development and function of subclasses of T cells." Journal of the Reticuloendothelial Society 17(2): 115-118.

Cao, X. (2007). "Granzyme B and perforin are important for regulatory T cell-mediated suppression of tumor clearance." Immunity 27: 635-646.

Carvalho, A. T. P., C. C. S. Elia, et al. (2003). "Immunohistochemical Study of Intestinal Eosinophils in Inflammatory Bowel Disease." Journal of Clinical Gastroenterology 36(2): 120-125.

Caton, M.L., Smith-Raska, M.R., and Reizis, B. (2007). "Notch-RBP-J signaling controls the homeostasis of CD8- dendritic cells in the spleen." J Exp Med *204*, 1653-1664.

Chen, W. (2003). "Conversion of peripheral CD4+CD25- naive T cells to CD4+CD25+ regulatory T cells by TGF-β induction of transcription factor Foxp3." J. Exp. Med. 198: 1875-1886.

Chen, Y., V. K. Kuchroo, et al. (1994). Science: 1237-1240.

Costello, C. M., N. Mah, et al. (2005). "Dissection of the Inflammatory Bowel Disease Transcriptome Using Genome-Wide cDNA Microarrays." PLoS Med 2(8): e199.

Cuthbert, A. P., S. A. Fisher, et al. (2002). "The contribution of NOD2 gene mutations to the risk and site of disease in inflammatory bowel disease." Gastroenterology 122(4): 867-874.

D'Cruz, L. M. and L. Klein (2005). "Development and function of agonist-induced CD25+Foxp3+ regulatory T cells in the absence of interleukin 2 signaling." Nat Immunol 6(11): 1152-1159.

Dalekos, Manoussakis, et al. (1993). "Soluble interleukin-2 receptors, antineutrophil cytoplasmic antibodies, and other autoantibodies in patients with ulcerative colitis." Gut 34(5): 658-664.

De Camargo Furtado, G., D. Olivares-Villagómez, et al. (2001). "Regulatory T cells in spontaneous autoimmune encephalomyelitis." Immunological Reviews 182(1): 122-134.

Dejardin, E., N. Droin, et al. (2002). "The lymphotoxin-beta receptor induces different patterns of gene expression via two NF-kappaB pathways." Immunity 17: 525 - 535.

Derbinksi, J., A. Schulte, et al. (2001). "Promiscuous gene expression medullary thymic epithelial cells mirrors the peripheral self." Nature Immunol. 2: 1032-1039.

Desreumaux, P., E. Brandt, et al. (1997). "Distinct cytokine patterns in early and chronic ileal lesions of Crohn's disease." Gastroenterology 113(1): 118-126.

Ebers, G. C. and D. A. Dyment (1998). "Genetics of multiple sclerosis." Semin. Neurol. 18: 295-299.

Ebers, G. C., A. D. Sadovnick, et al. (1995). "A genetic basis for familial aggregation in multiple sclerosis." Nature 377(6545): 150-151.

Falk, I., J. Biro, et al. (1996). "Proliferation Kinetics Associated with T Cell Receptor-β Chain Selection of Fetal Murine Thymocytes." The Journal of Experimental Medicine 184(6): 2327-2340.

Fantini, M. C., C. Becker, et al. (2004). "Cutting Edge: TGFβ Induces a Regulatory Phenotype in CD4+CD25+ T Cells through Foxp3 Induction and Down-Regulation of Smad7." The Journal of Immunology 172(9): 5149-5153.

Fehling, H. J., A. Krotkova, et al. (1995). "Crucial role of the pre-T-cell receptor α gene in development of ap but not γδ T cells." Nature 375(6534): 795-798.

Ferber, I. A. (1996). "Mice with a disrupted IFN-γ gene are susceptible to the induction of experimental autoimmune encephalomyelitis (EAE)." J. Immunol. 156: 5-7.

Finkelstein, S. D., E. Sasatomi, et al. (2002). "Pathologic features of early inflammatory bowel disease." Gastroenterology Clinics of North America 31(1): 133-145.

Fontenot, J. D., M. A. Gavin, et al. (2003). "Foxp3 programs the development and function of CD4+CD25+ regulatory T cells." Nature Immunol. 4: 330-336.

Fontenot, J. D., J. P. Rasmussen, et al. (2005). "A function for interleukin 2 in Foxp3-expressing regulatory T cells." Nature Immunol. 6: 1142-1151.

Fujino, S., A. Andoh, et al. (2003). "Increased expression of interleukin 17 in inflammatory bowel disease." Gut 52(1): 65-70.

Furlan, R. (2001). "Intrathecal delivery of IFN-γ protects C57BL/6 mice from chronic-progressive experimental autoimmune encephalomyelitis by increasing apoptosis of central nervous system-infiltrating lymphocytes." J. Immunol. 167: 1821-1829.

Fuss, I., M. Neurath, et al. (1996). "Disparate CD4+ lamina propria (LP) lymphokine secretion profiles in inflammatory bowel disease. Crohn's disease LP cells manifest increased secretion of IFN-γ, whereas ulcerative colitis LP cells manifest increased secretion of IL-5." The Journal of Immunology 157(3): 1261-1270.

Galan, J. M. and R. Haguenauer-Tsapis (1997). "Ubiquitin Lys63 is involved in ubiquitination of a yeast plasma membrane protein." EMBO J 16(19): 5847-5854.

Gallegos, A.M., M.J. Bevan. 2004. "Central tolerance to tissue-specific antigens mediated by direct and indirect antigen presentation." J. Exp.Med. 200:1039–1049

Gao, J. (2008). "The tumor suppressor CYLD regulates microtubule dynamics and plays a role in cell migration." J. Biol. Chem. 283: 8802-8809.

Germain, R. N. (2002). "T-cell development and the CD4-CD8 lineage decision." Nature Rev. Immunol. 2: 309-322.

Ghosh, S. and M. Karin (2002). "Missing Pieces in the NF-κB Puzzle." Cell 109(2, Supplement 1): S81-S96.

Ghosh, S., M. J. May, et al. (1998). "NF-κB and Rel proteins: Evolutionarily Conserved Mediators of Immune Responses." Annual Review of Immunology 16(1): 225-260.

Gilmore, T. D. and M. Herscovitch (2000). "Inhibitors of NF-κB signaling: 785 and counting." Oncogene 25(51): 6887-6899.

Gondek, D. C., L. F. Lu, et al. (2005). "Cutting edge: contact-mediated suppression by CD4+CD25+ regulatory cells involves a granzyme B-dependent, perforin-independent mechanism." J. Immunol. 174: 1783-1786.

Greter, M., F. L. Heppner, et al. (2005). "Dendritic cells permit immune invasion of the CNS in an animal model of multiple sclerosis." Nat Med 11(3): 328-334.

Groettrup, M. and H. v. Boehmer (1993). "A role for a pre-T-cell receptor in T-cell development." Immun. Today 14(12): 610-614.

Groux, H., A. O'Garra, et al. (1997). "A CD4+T-cell subset inhibits antigen-specific T-cell responses and prevents colitis." Nature 389(6652): 737-742.

Guy, C. S. and D. A. A. Vignali (2009). "Organization of proximal signal initiation at the TCR:CD3 complex." Immunological Reviews 232(1): 7-21.

Harrington, L. E. (2005). "Interleukin 17-producing CD4+ effector T cells develop via a lineage distinct from the T helper type 1 and 2 lineages." Nature Immunol. 6: 1123-1132.

Hawash, I. Y., K. P. Kesavan, et al. (2002). "The Lck SH3 domain negatively regulates localization to lipid rafts through an interaction with c-Cbl." J. Biol. Chem. 277: 5683-5691.

Hayashi, T., J.-H. Mo, et al. (2007). "3-Hydroxyanthranilic acid inhibits PDK1 activation and suppresses experimental asthma by inducing T cell apoptosis." Proceedings of the National Academy of Sciences 104(47): 18619-18624.

Hettmann, T., J. DiDonato, et al. (1999). "An essential role for nuclear factor κB in promoting double positive thymocyte apoptosis." J Exp Med 189: 145 - 158.

Hofstetter, H. H. (2005). "Therapeutic efficacy of IL-17 neutralization in murine experimental autoimmune encephalomyelitis." Cell. Immunol. 237: 123-130.

Hori, S., T. Nomura, et al. (2003). "Control of regulatory T cell development by the transcription factor Foxp3." Science 299: 1057-1061.

Hövelmeyer, N., F. T. Wunderlich, et al. (2007). "Regulation of B cell homeostasis and activation by the tumor suppressor gene CYLD." J Exp Med 204: 2615-2627.

Hugot, J.-P., M. Chamaillard, et al. (2001). "Association of NOD2 leucine-rich repeat variants with susceptibility to Crohn's disease." Nature 411(6837): 599-603.

Imboden and Stobo (1985). "Transmembrane signalling by the T cell antigen receptor. Perturbation of the T3-antigen receptor complex generates inositol phosphates and releases calcium ions from intracellular stores." J Exp Med 161: 446-456.

Isakov and Altman (2002). "Protein kinase C in T cell activation." Annu Rev Immunol 20(761-794).

Isomura, I., S. Palmer, et al. (2009). "c-Rel is required for the development of thymic Foxp3+ CD4 regulatory T cells." The Journal of Experimental Medicine 206(13): 3001-3014.

Ivanov, I. I. (2006). "The orphan nuclear receptor RORγt directs the differentiation program of proinflammatory IL-17+ T helper cells." Cell 126: 1121-1133.

Jana, S., P. Jailwala, et al. (2009). "The role of NF-κB and Smad3 in TGF-β-mediated Foxp3 expression." European Journal of Immunology 39(9): 2571-2583.

Jin, W., W. R. Reiley, et al. (2007). "Deubiquitinating Enzyme CYLD Regulates the Peripheral Development and Naive Phenotype Maintenance of B Cells." Journal of Biological Chemistry 282(21): 15884-15893.

Josefowicz, S. Z. and A. Rudensky (2009). "Control of regulatory T cell lineage commitment and maintenance." Immunity 30: 616-625.

Kanayama, A., R. B. Seth, et al. (2004). "TAB2 and TAB3 Activate the NF-κB Pathway through Binding to Polyubiquitin Chains." Molecular Cell 15(4): 535-548.

Karin, M. and B. Ben-Neriah (2000). "Phosphorylation meets ubiquitination: the control of NF-κB activity." Annu. Rev. Immunol. 18: 621-663.

Komiyama, Y. (2006). "IL-17 plays an important role in the development of experimental autoimmune encephalomyelitis." J. Immunol. 177: 566-573.

Kovalenko, A. (2003). "The tumour suppressor CYLD negatively regulates NF-κB signalling by deubiquitination." Nature 424: 801-805.

Kretschmer, Apostolou, et al. (2005). "Inducing and expanding regulatory T cell populations by foreign antigen." Nat. Immunol. 6: 1219.

Kuchroo, V., C. Martin, et al. (1993). "Cytokines and adhesion molecules contribute to the ability of myelin proteolipid protein-specific T cell clones to mediate experimental allergic encephalomyelitis." The Journal of Immunology 151(8): 4371-4382.

Kuhn, R., J. Lohler, et al. (1993). "Interleukin-10-deficient mice develop chronic enterocolitis." Cell. 75: 263-274.

Kyewski, B. and J. Derbinski (2004). "Self-representation in the thymus: an extended view." Nature Rev. Immunol. 4: 688-698.

Lahl, K., Loddenkemper, C., Drouin, C., Freyer, J., Arnason, J., Eberl, G., Hamann, A., Wagner, H., Hueuhn, J., and Sparwasser, T. (2007). "Selective depletion of Foxp3+ regulatory T cells induces a scurfy-like disease." J Exp Med 204, 57-63.

Langrish, C. L. (2005). "IL-23 drives a pathogenic T cell population that induces autoimmune inflammation." J. Exp. Med. 201: 233-240.

Langrish, C. L., B. S. McKenzie, et al. (2004). "IL-12 and IL-23: master regulators of innate and adaptive immunity." Immunological Reviews 202(1): 96-105.

Lee, A. J., X. Wu, et al. (2010). "CARMA1 Regulation of Regulatory T Cell Development Involves Modulation of Interleukin-2 Receptor Signaling." Journal of Biological Chemistry 285(21): 15696-15703.

Lee, K.-Y., F. D'Acquisto, et al. (2005). "PDK1 Nucleates T Cell Receptor-Induced Signaling Complex for NF-κB Activation." Science 308(5718): 114-118.

Li, Q. and I. Verma (2002). "NF-κB regulation in the immune system." Nat Rev Immunol 2: 725 - 734.

Li, S. S. (2005). "Specificity and versatility of SH3 and other proline-recognition domains: structural basis and implications for cellular signal transduction." Biochem J 390: 641-653.

Long, M., S.-G. Park, et al. (2009). "Nuclear Factor-κB Modulates Regulatory T Cell Development by Directly Regulating Expression of Foxp3 Transcription Factor." Immunity 31(6): 921-931.

Maloy, K. J. and F. Powrie (2001). "Regulatory T cells in the control of immune pathology." Nat. Immunol. 2: 816-822.

Mangan, P. R. (2006). "Transforming growth factor-β induces development of the TH17 lineage." Nature 441: 231-234.

Massoumi, R., K. Chmielarska, et al. (2006). "CYLD inhibits tumor cell proliferation by blocking Bcl-3-dependent NF-κB signaling." Cell 125: 665-677.

McKenzie, B. S., R. A. Kastelein, et al. (2006). "Understanding the IL-23-IL-17 immune pathway." Trends in Immunology 27(1): 17-23.

Mellor, A. L. and D. H. Munn (2004). "IDO expression by dendritic cells: tolerance and tryptophan catabolism." Nature Rev. Immunol. 4: 762-774.

Molina, T. J. (1992). "Profound block in thymocyte development in mice lacking p56lck." Nature 357: 161-164.

Mombaerts, P., A. R. Clarke, et al. (1992). "Mutations in T-cell antigen receptor genes α and β block thymocyte development at different stages." Nature 360(6401): 225-231.

Monteleone, G., L. Biancone, et al. (1997). "Interleukin 12 is expressed and actively released by Crohn's disease intestinal lamina propria mononuclear cells." Gastroenterology 112(4): 1169-1178.

Mosmann, T. R. and R. L. Coffman (1989). "TH1 and TH2 Cells: Different Patterns of Lymphokine Secretion Lead to Different Functional Properties." Annual Review of Immunology 7(1): 145-173.

Mudter, J. and Neurath M.F. (2007). "Il-6 signaling in inflammatory bowel disease: Pathophysiological role and clinical relevance." Inflammatory Bowel Disease 13(8): 1016-1023.

Mullis and Faloona (1987). "Specific synthesis of DNA in vitro via a polymerase-catalyzed chain reaction." Methods Enzymol 155: 335-350.

Murphy, M. A. (1998). "Tissue hyperplasia and enhanced T-cell signalling via ZAP-70 in c-Cbl-deficient mice." Mol. Cell. Biol. 18: 4872-4882.

Nakae, S., A. Nambu, et al. (2003). "Suppression of immune induction of collagen-induced arthritis in IL-17-deficient mice." J. Immunol. 171: 6173-6177.

Nasreen, M., T. Ueno, et al. (2003). "In vivo treatment of class II MHC-deficient mice with anti-TCR antibody restores the generation of circulating CD4 T cells and optimal architecture of thymic medulla." J. Immunol. 171: 3394-3400.

Ogura, Y., D. K. Bonen, et al. (2001). "A frameshift mutation in NOD2 associated with susceptibility to Crohn's disease." Nature 411(6837): 603-606.

Pahl, H. (1999). "Activators and target genes of Rel/NF-κB transcription factors." Oncogene 18: 6853 - 6866.

Panitch, H. S., R. L. Hirsch, et al. (1987). "Treatment of multiple sclerosis with gamma interferon." Neurology 37(7): 1097.

Park, H. (2005). "A distinct lineage of CD4 T cells regulates tissue inflammation by producing interleukin 17." Nature Immunol. 6: 1133-1141.

Pearse, M., P. Gallagher, et al. (1988). "Molecular characterization of T-cell antigen receptor expression by subsets of CD4- CD8- murine thymocytes." Proceedings of the National Academy of Sciences of the United States of America 85(16): 6082-6086.

Pearse, M., L. Wu, et al. (1989). "A murine early thymocyte developmental sequence is marked by transient expression of the interleukin 2 receptor." Proceedings of the National Academy of Sciences of the United States of America 86(5): 1614-1618.

Rao, N. (2002). "Negative regulation of Lck by Cbl ubiquitin ligase." Proc. Natl Acad. Sci. USA 99: 3794-3799.

Read, S., V. Malmstrom, et al. (2000). "Cytotoxic T lymphocyte-associated antigen 4 plays an essential role in the function of CD25+ CD4+ regulatory cells that control intestinal inflammation." J. Exp. Med. 192: 295-302.

Read, S., V. Malmström, et al. (2000). "Cytotoxic T Lymphocyte-Associated Antigen 4 Plays an Essential Role in the Function of CD25+CD4+ Regulatory Cells That Control Intestinal Inflammation." The Journal of Experimental Medicine 192(2): 295-302.

Regamey, A., D. Hohl, et al. (2003). "The Tumor Suppressor CYLD Interacts with TRIP and Regulates Negatively Nuclear Factor κB Activation by Tumor Necrosis Factor." The Journal of Experimental Medicine 198(12): 1959-1964.

Reiley, W., M. Zhang, et al. (2005). "Regulation of the Deubiquitinating Enzyme CYLD by IκB Kinase Gamma-Dependent Phosphorylation." Mol. Cell. Biol. 25(10): 3886-3895.

Reiley, W. W. (2006). "Regulation of T cell development by the deubiquitinating enzyme CYLD." Nature Immunol. 7: 411-417.

Reiley, W. W., W. Jin, et al. (2007). "Deubiquitinating enzyme CYLD negatively regulates the ubiquitin-dependent kinase Tak1 and prevents abnormal T cell responses." The Journal of Experimental Medicine 204(6): 1475-1485.

Reiley, W. W., M. Zhang, et al. (2006). "Regulation of T cell development by the deubiquitinating enzyme CYLD." Nat Immunol 7: 411-417.

Reumaux, D., C. Mézière, et al. (1995). "Distinct Production of Autoantibodies to Nuclear Components in Ulcerative Colitis and in Crohn's Disease." Clinical Immunology and Immunopathology 77(3): 349-357.

Rivers, T. M., D. H. Sprunt, et al. (1933). "Observations on attempts to produce acute disseminated encephalomyelitis in monkeys." J. Exp. Med. 58: 39-53.

Roose, J. P., M. Mollenauer, et al. (2005). "A Diacylglycerol-Protein Kinase C-RasGRP1 Pathway Directs Ras Activation upon Antigen Receptor Stimulation of T Cells." Mol. Cell. Biol. 25(11): 4426-4441.

Ruan, Q., V. Kameswaran, et al. (2009). "Development of Foxp3+ Regulatory T Cells Is Driven by the c-Rel Enhanceosome." Immunity 31(6): 932-940.

Rudensky, A. (2005). "Foxp3 and dominant tolerance." Philos. Trans. R. Soc. Lond. B. Biol. Sci. 360: 1645-1646.

Saiki, R., S. Scharf, et al. (1985). "Enzymatic amplification of β-globin genomic sequences and restriction site analysis for diagnosis of sickle cell anemia." Science 230(4732): 1350-1354.

Saito, K., T. Kigawa, et al. (2004). "The CAP-Gly domain of CYLD associates with the proline-rich sequence in NEMO/IKKγ." Structure 12: 1719-1728.

Sakaguchi, S. (2000). "Regulatory T cells: key controllers of immunologic self tolerance." Cell 101: 455-458.

Sakaguchi, S. (2004). "Naturally arising CD4+ regulatory T cells for immunologic self-tolerance and negative control of immune responses." Annu. Rev. Immunol. 22: 531-562.

Sakaguchi, S., N. Sakaguchi, et al. (1995). "Immunologic self-tolerance maintained by activated T cells expressing IL-2 receptor α-chains (CD25). Breakdown of a single mechanism of self-tolerance causes various autoimmune diseases." J. Immunol. 155: 1151-1164.

Salomon, B., D. J. Lenschow, et al. (2000). "B7/CD28 Costimulation Is Essential for the Homeostasis of the CD4+CD25+ Immunoregulatory T Cells that Control Autoimmune Diabetes." Immunity 12(4): 431-440.

Sambrook (1989). "Molecular cloning." A laboratory manual (2nd edition).

Seddon, B. and D. Mason (2000). "The third function of the thymus." Immunol. Today 21: 95-99.

Senftleben, U., Y. Cao, et al. (2001). "Activation by IKKα of a second, evolutionary conserved, NF-κB signaling pathway." Science 293: 1495-1499.

Shevach, E. M. (2002). "CD4+CD25+ suppressor T cells: more questions than answers." Nat. Rev. Immunol. 2: 389-400.

Shih, D. and S. Targan (2009). "Insights into IBD pathogenesis." Current Gastroenterology Reports 11(6): 473-480.

Shores, E. W., W. van Ewijk, et al. (1991). "Disorganization and restoration of thymic medullary epithelial cells in T cell receptor-negative scid mice: evidence that receptor-bearing lymphocytes influence maturation of the thymic microenvironment." Eur. J. Immunol. 21: 1657-1661.

Shores, E. W., W. van Ewijk, et al. (1994). "Maturation of medullary thymic epithelium requires thymocytes expressing fully assembled CD3-TCR complexes." Int. Immunol. 6: 1393-1402.

Silver (1995). "Mouse Genetics: concepts and practice."

Smith-Garvin, Koretzky, et al. (2009). "T cell activation." Annu Rev Immunol 27: 591-619.

Sojka, D. K., Y.-H. Huang, et al. (2008). "Mechanisms of regulatory T-cell suppression – a diverse arsenal for a moving target." Immunology 124(1): 13-22.

Sommers, C. L., L. E. Samelson, et al. (2004). "LAT: a T lymphocyte adapter protein that couples the antigen receptor to downstream signaling pathways." BioEssays 26(1): 61-67.

Sospedra, M. and R. Martin (2005). "Immunology of multiple sclerosis." Annual Review of Immunology 23(1): 683-747.

Srokowski, C. C., J. Masri, et al. (2009). "Naturally occurring short splice variant of CYLD positively regulates dendritic cell function." Blood 113(23): 5891-5895.

Stagg, A. J., M. A. Kamm, et al. (2002). "Intestinal dendritic cells increase T cell expression of α4β7 integrin." European Journal of Immunology 32(5): 1445-1454.

Starr, T. K., S. C. Jameson, et al. (2003). "Positive and negative selection of T cells." Annu. Rev. Immunol. 21: 139-176.

Steinman, L. (1996). "Multiple sclerosis: a coordinated immunological attack against myelin in the central nervous system." Cell 85: 299-302.

Steinman, L. (2007). "A brief history of TH17, the first major revision in the TH1/TH2 hypothesis of T cell-mediated tissue damage." Nat Med 13(2): 139-145.

Stromnes, I. M., L. M. Cerretti, et al. (2008). "Differential regulation of central nervous system autoimmunity by TH1 and TH17 cells." Nat. Med. 14: 337-342.

Sun, L., L. Deng, et al. (2004). "The TRAF6 ubiquitin ligase and TAK1 kinase mediate IKK activation by BCL10 and MALT1 in T lymphocytes." Mol. Cell 14: 289-301.

Sun, S. C. (2008). "Deubiquitylation and regulation of the immune response." Nat Rev Immunol 8: 501-511.

Sun, S. C. (2009). "CYLD: a tumor suppressor deubiquitinase regulating NF-κB activation and diverse biological processes." Cell Death Differ 17(1): 25-34.

Szabo, S. J., S. T. Kim, et al. (2000). "A Novel Transcription Factor, T-bet, Directs Th1 Lineage Commitment." Cell 100(6): 655-669.

Takatori, H., Y. Kanno, et al. (2009). "Lymphoid tissue inducer-like cells are an innate source of IL-17 and IL-22." The Journal of Experimental Medicine 206(1): 35-41.

Tang, Q. and J. A. Bluestone (2008). "The Foxp3+ regulatory T cell: a jack of all trades, master of regulation." Nature Immunol. 9: 239-244.

Taub, D. D. and D. L. Longo (2005). "Insights into thymic aging and regeneration." Immunological Reviews 205(1): 72-93.

Thompson, C. and F. Powrie (2004). "Regulatory T cells." Current Opinion in Pharmacology 4(4): 408-414.

Trompouki, E., E. Hatzivassiliou, et al. (2003). "CYLD is a deubiquitinating enzyme that negatively regulates NF-κB activation by TNFR family members." Nature 424: 793-796.

Tsukada, Y., T. Nakamura, et al. (2002). "Cytokine profile in colonic mucosa of ulcerative colitis correlates with disease activity and response to granulocytapheresis." The American Journal of Gastroenterology 97(11): 2820-2828.

Tzartos, J. S. (2008). "Interleukin-17 production in central nervous system-infiltrating T cells and glial cells is associated with active disease in multiple sclerosis." Am. J. Pathol. 172: 146-155.

Uematsu,Y., Ryser,S., Dembic,Z., Borgulya,P., Krimpenfort,P., Berns,A., von Boehmer,H., and Steinmetz,M. (1988). "In transgenic mice the introduced functional T cell receptor β gene prevents expression of endogenous b genes." Cell *52*, 831-841.

Vallabhapurapu, S. and M. Karin (2009). "Regulation and function of NF-κB transcription factors in the immune system." Annu Rev Immunol 27: 693-733.

Vieira, P. L., J. R. Christensen, et al. (2004). "IL-10-Secreting Regulatory T Cells Do Not Express Foxp3 but Have Comparable Regulatory Function to Naturally Occurring CD4+CD25+ Regulatory T Cells." The Journal of Immunology 172(10): 5986-5993.

Vignali, D. A. A., L. W. Collison, et al. (2008). "How regulatory T cells work." Nat Rev Immunol 8(7): 523-532.

Vinuesa, C. G., I. Sanz, et al. (2009). "Dysregulation of germinal centres in autoimmune disease." Nat Rev Immunol 9(12): 845-857.

Visekruna, A., M. Huber, et al. (2010). "c-Rel is crucial for the induction of Foxp3+ regulatory CD4+ T cells but not TH17 cells." European Journal of Immunology 40(3): 671-676.

Wang, C. (2001). "TAK1 is a ubiquitin-dependent kinase of MKK and IKK." Nature 412: 346-351.

Wang, H., T. A. Kadlecek, et al. (2010). "ZAP-70: An Essential Kinase in T-cell Signaling." Cold Spring Harbor Perspectives in Biology 2(5).

Warren, S. and S. C. Sommers (1954). "Pathology of regional ileitis and ulcerative colitis." Journal of the American Medical Association 154(3): 189-193.

Weih, F. and J. Caamano (2003). "Regulation of secondary lymphoid organ development by the nuclear factor-κB signal transduction pathway." Immunol Rev 195: 91-105.

Weih, F., D. Carrasco, et al. (1995). "Multiorgan inflammation and hematopoietic abnormalities in mice with a targeted disruption of RelB, a member of the NF-κB/Rel family." Cell 80(2): 331-340.

Weiner, H. L. (2001). "Induction and mechanism of action of transforming growth factor-β-secreting Th3 regulatory cells." Immunological Reviews 182(1): 207-214.

Wekerle, H., K. Kojima, et al. (1994). "Animal models." Ann. Neurol. 36: S47-S53.

Whartenby, K. A., P. A. Calabresi, et al. (2005). "Inhibition of FLT3 signaling targets DCs to ameliorate autoimmune disease." Proceedings of the National Academy of Sciences of the United States of America 102(46): 16741-16746.

Wildin, R. S. (2001). "X-linked neonatal diabetes mellitus, enteropathy and endocrinopathy syndrome is the human equivalent of mouse scurfy." Nature Genet. 27: 18-20.

Willenborg, D., S. Fordham, et al. (1996). "IFN-γ plays a critical down-regulatory role in the induction and effector phase of MOG-induced encephalomyelitis." J. Immunol. 157: 3223-3227.

Wilson, A., W. Held, et al. (1994). "Two waves of recombinase gene expression in developing thymocytes." J Exp Med 179(4): 1355-1360.

Wolfer, A., Bakker, T., Wilson, A., Nicolas, M., Ioannidis, V., Littman, D.R., Lee, P.P., Wilson, C.B., Held, W., MacDonald, H.R., et al (2001). "Inactivation of Notch 1 in immature thymocytes does not perturb CD4 or CD8 T cells development." Nat Immunol 2, 235-241.

Xiao, G., E. W. Harhaj, et al. (2001). "NF-κB-inducing kinase regulates the processing of NF-κB2 p100." Mol Cell 7: 401-409.

Y. Sawa, N. O., K. Adachi, K. Higuchi, T. Matsumoto and T. Arakawa (2003). "Comprehensive analysis of intestinal cytokine messenger RNA profile by real-time quantitative polymerase chain reaction in patients with inflammatory bowel disease." Int J Mol Med 11(2): 175–179.

Yednock, T. A. (1992). "Prevention of experimental autoimmune encephalomyelitis by antibodies against α4β1 integrin." Nature 356: 63-66.

Zarnegar, B. J., Y. Wang, et al. (2008). "Noncanonical NF-κB activation requires coordinated assembly of a regulatory complex of the adaptors cIAP1, cIAP2, TRAF2 and TRAF3 and the kinase NIK." Nat Immunol 9: 1371-1378.

Zauli, Crespi, et al. (1985). "Antibodies to the cytoskeleton components and other autoantibodies in inflammatory bowel disease." Digestion 32: 140-144.

Zhang, B., Z. Wang, et al. (2006). "NF-κB2 is required for the control of autoimmunity by regulating the development of medullary thymic epithelial cells." J Biol Chem 281: 38617 - 38624.

Zhang, J. (2006). "Impaired regulation of NF-κB and increased susceptibility to colitis-associated tumorigenesis in CYLD-deficient mice." J. Clin. Invest. 116: 3042-3049.

Zheng, W.-p. and R. A. Flavell (1997). "The Transcription Factor GATA-3 Is Necessary and Sufficient for Th2 Cytokine Gene Expression in CD4 T Cells." Cell 89(4): 587-596.

8 Acknowledgements

9 Versicherung

10 Lebenslauf

Publikationen:

Reissig S., Hövelmeyer N., Weih D., Weigmann B., Nikolaev A., Kalt B., Wunderlich F. T., Weih F**.,** Neurath M. F. and Waisman A. A short splice variant of the tumor suppressor gene CYLD negatively regulates the development of autoimmune gut inflammation. (submitted)

Hövelmeyer* N, Reissig* S, Xuan NT, Adams-Quack P, Lukas D, Nikolaev A, Schlüter D, Waisman A. A20 deficiency in B cells enhances B-cell proliferation and results in the development of autoantibodies. Eur J Immunol. 2011 Mar;41(3):595-601

*Equal contribution

Bros M, Dexheimer N, Besche V, Masri J, Trojandt S, Hövelmeyer N, Reissig S, Massoumi R, Grabbe S, Waisman A, Reske-Kunz AB. Mutated cylindromatosis gene affects the functional state of dendritic cells. Eur J Immunol. 2010 Oct;40(10):2848-57